# Durham E-Theses

## *Enzyme activity in bicontinuous microemulsions*

### STEUDLE, ANNE,KATHARINA

**How to cite:**

**Use policy**

# Enzyme activity in bicontinuous microemulsions

Anne Katharina Steudle

A thesis submitted for the degree of Doctor of Philosophy

at the University of Durham

Chemistry Department, Durham University

2015

# Table of Contents

# Abstract

The thesis deals with enzymatic catalysis in bicontinuous microemulsions, which consist of a dynamic network of oil and water domains separated by a monolayer of surfactant molecules, i.e. the interfacial layer. Hence, a microemulsion with the composition buffer – $n$-octane – nonionic surfactant was tested as a reaction medium for enzyme-catalysed reactions with the emphasis on the conversion of hydrophobic substrates, which are difficult to convert in aqueous buffer solutions. The first part of the thesis focuses on the activity of the lipase B from *Candida antarctica* (CalB) in bicontinuous microemulsions. First, the optimum reaction conditions determined by temperature, pH and ionic strength were evaluated. Second, it was found that CalB concentrations which showed fast adsorption at an oil-water interface also displayed fast reaction rates. Additionally, no saturation was found for substrate concentrations up to 40 mM of $p$-nitrophenyl laurate, which according to Michaelis-Menten suggests a $K_m \gg 40$ mM. Third, the composition of the interfacial layer had a distinct influence on CalB activity, e.g. the presence of sugar surfactants ($\beta$-$C_{10}G_1$) or phospholipids (DOPC) enhanced or decreased CalB activity, respectively. The second part of the thesis describes the activity of the squalene-hopene cyclase from *Alicyclobacillus acidocaldarius* (Aac SHC) converting its natural substrate squalene in bicontinuous microemulsions. The Aac SHC activity studies revealed a linear dependence on enzyme concentration and a hyperbolic curve for the substrate concentration, with a saturation of Aac SHC at substrate concentrations above 20 mM. The composition of the interfacial layer was found to have neither a significant influence on the activity nor on the conformation of Aac SHC. In summary, good turnover rates were achieved for interfacially-active enzymes (CalB) due to enhanced enzyme-substrate contact at the interfacial layer. For water-soluble enzymes (Aac SHC), a distinctly enhanced selectivity was discovered, although no faster reaction rate was found. The main difference in the catalytic turnover was explained by the adsorption of CalB at the interfacial layer, whereas Aac SHC stays in the aqueous phase of the microemulsion. To conclude, bicontinuous microemulsions were suitable for enzymatic catalysis and are thus interesting in terms of reaction medium engineering to optimise biocatalytic processes.

# i.    List of Figures

6

# ii. List of Tables

# iii.  List of Schemes

# iv.    List of Abbreviations

<u>Numbers</u>

| | |
|---|---|
| 1 | one-phase region |
| $\overline{2}$ | two-phase region, w/o-microemulsion with co-existing water excess phase |
| $\underline{2}$ | two-phase region, o/w-microemulsion with co-existing oil excess phase |
| 3 | three-phase region |

<u>Abbreviations and Variables</u>

| | |
|---|---|
| $A$ | absorbance |
| A | water |
| a | water-rich phase |
| Aac SHC | squalene-hopene cyclase from *Alicyclobacillus acidocaldarius* |
| AOT | anionic surfactant dioctyl sulfosuccinate sodium salt |
| B | oil |
| b | oil-rich phase |
| $c$ | concentration |
| C | surfactant |
| c | surfactant-rich phase |
| $c_1$ | $= 1/R_1$ |
| $c_2$ | $= 1/R_2$ |
| CalB | lipase B from *Candida antarctica* |
| CD | circular dichroism |
| $C_iE_j$ | nonionic alkyl polyethylene glycol ether with $i$ carbon atoms in the hydrophobic chain and $j$ ethylene groups in the hydrophilic head group |
| cmc | critical micelle concentration |
| $C_mG_n$ | sugar surfactant with $m$ carbon atoms in the hydrophobic chain and $n$ sugar units in the hydrophilic head group |

16

| | |
|---|---|
| cp$_\alpha$ | upper critical point |
| cp$_\beta$ | lower critical point |
| $c_{Substrate}$ | concentration of the substrate |
| $c_{CalB}$ | concentration of the substrate |
| $d$ | path length of the cuvette |
| DOPC | phospholipid 1,2-dioleoyl-sn-glycero-3-phosphocholine |
| E | enzyme |
| E* | enzyme adsorbed at the interfacial layer |
| $E_a$ | activation energy |
| EC number | enzyme commission number |
| ECN | effective carbon number |
| ee | enantiomeric excess |
| $E_L$ | left handed circularly polarised light |
| EPR | electron paramagnetic resonance |
| $E_R$ | right handed circularly polarised light |
| FID | flame ionisation detector |
| $g$ | acceleration due to gravity |
| GC | gas chromatography |
| $H$ | mean curvature |
| $h$ | Planck constant $6.626 \times 10^{-34}$ J s |
| $I$ | transmitted intensity of light beam |
| $i$ | number of carbon atoms in the hydrophobic chain |
| $I_0$ | incident intensity of a light beam |
| $j$ | number of ethylene groups in the hydrophilic head group |
| $k$ | rate constant |
| $K^\ddagger$ | equilibrium constant |
| $k_2$ | second order rate constant |
| K$_a$ | acid dissociation constant |
| $k_B$ | Boltzmann constant $1.38 \times 10^{-23}$ J K$^{-1}$ |
| $k_{cat}$ | catalytic turnover number |
| $K_m$ | Michaelis-Menten constant |
| $k_{off}$ | rate constant for desorption of the interfacial layer |

17

| | |
|---|---|
| $k_{on}$ | rate constant for adsorption at the interfacial layer |
| $m_A$ | mass of aqueous phase |
| $m_B$ | mass of oil phase |
| $m_C$ | mass of surfactant |
| $m_{co\text{-}surfactant}$ | mass of co-surfactant |
| $m_{H2O}$ | mass of water in the aqueous phase of a microemulsion |
| $m_{NaCl}$ | mass of NaCl in the aqueous phase of a microemulsion |
| $m_{surfactant}$ | mass of surfactant |
| NMR | nuclear magnetic resonance |
| o/w | oil in water |
| P | product |
| P* | product adsorbed at the interfacial layer |
| PDB | protein data bank |
| $pK_a$ | logarithmic constant ( $= -\log_{10} K_a$ ) |
| $R$ | gas constant 8.314 J K$^{-1}$ mol$^{-1}$ |
| $R_1$ | principal curvature |
| $R_2$ | principal curvature |
| RF | relative response factor |
| S | substrate |
| S* | substrate adsorbed at the interfacial layer |
| $T$ | temperature |
| $\tilde{T}$ | temperature at the $X$-point of a microemulsion |
| $t$ | time |
| $T_l$ | lowest temperature at which a three-phase region is formed |
| $T_u$ | highest temperature at which a three-phase region is formed |
| $V_A$ | volume of aqueous phase |
| $V_B$ | volume of oil |
| w/o | water in oil |
| $X$-point | defined by $\tilde{T}$ and $\tilde{\gamma}$ it is the point where a minimum of surfactant is required to form a one-phase microemulsion |
| $z$ | vertical height of the drop |
| $\Delta^{\ddagger}G$ | energy of activation |

| | |
|---|---|
| $\Delta^{\ddagger}H$ | enthalpy of activation |
| $\Delta^{\ddagger}S$ | entropy of activation |
| $\Delta A$ | differential absorbance |
| $\Delta P_0$ | pressure difference in a reference plane |
| $\Delta_r G_0$ | Gibbs energy |
| $\beta\text{-}C_{10}G_1$ | sugar surfactant $n$-decyl-β-D-glucopyranoside |

Greek letters

| | |
|---|---|
| $\alpha$ | mass fraction of the oil in the total mass of oil and aqueous phase |
| $\delta$ | mass fraction of co-surfactant in the total mass of surfactants |
| $\varepsilon$ | mass fraction of salt in the aqueous phase of a microemulsion |
| $\varepsilon$ | molar absorptivity |
| $\phi$ | oil to water ratio |
| $\gamma$ | surfactant mass fraction |
| $\tilde{\gamma}$ | surfactant mass fraction at the $X$-point of a microemulsion |
| $\gamma_0$ | lowest surfactant mass fraction at which a three-phase region is formed |
| $\gamma_{Reaction}$ | surfactant mass fraction in the reaction mixture |
| $\kappa$ | transmission coefficient |
| $\lambda$ | wavelength |
| $\lambda_{isosbestic}$ | isosbestic wavelength |
| $\lambda_{max}$ | wavelength of maximum absorption |
| $\Delta\rho$ | density difference |
| $\theta$ | ellipticity |
| $\theta_m$ | molar ellipticity |
| $\sigma_{ab}$ | interfacial tension between the phases a and b |
| $\sigma_{ac}$ | interfacial tension between the phases a and c |
| $\sigma_{bc}$ | interfacial tension between the phases b and c |

# v. Statement of Copyright

# vi.  Acknowledgements

# 1 Motivation

## 1.1 Biocatalysis

Green chemistry is the term for a nowadays widely spread concept of making production processes in chemical industry more environmentally friendly and economically competitive.[Anastas 2009] A "green" process is meant, amongst others, to reduce waste and side-products, provide good atom economy, avoid toxic substances, employ more renewable materials and save energy by working at mild temperatures and ambient pressures.[Poliakoff 2002] One possibility to fulfil these requirements is the use of non-toxic and biodegradable biocatalysts, which are already successfully applied in numerous processes in industry.[Ran 2008] By way of an example, the use of biocatalysts implies no need for protecting groups, less side-products due to their high substrate specificity and mild reaction conditions.[Clouthier 2012] Additionally the remarkable high stereo- and regioselectivity of biocatalysts[Schmid 2001] allows targeting complex molecules with many stereocenters that may not be accessible by conventional organic synthesis. Hence, the overall benefit from biocatalysis can be described in two ways. First it replaces classic chemical processes with environmentally friendly biotechnological processes. Second it opens up new reaction pathways for products which so far could not be synthesised by conventional synthetic chemistry.[Drepper 2006]

Possible biocatalysts can be either whole cells or isolated and purified enzymes.[Pollard 2007] Whole cells are favoured for multi-step reactions that involve many enzymes and cofactors, which can be recovered in a living cell.[León 1998] An additional positive effect is that the enzymes are in their natural environment and therefore inactivation due to isolation can be avoided or at least be reduced.[Duetz 2001] For instance, the production of β-lactam antibiotics like penicillin and cephalosporin, which are made by fermentation, is a successful application of whole cell catalysis.[Elander 2003] On the other hand, isolated and purified enzymes are easier to handle and no side-products are generated during the reactions.[Goldberg 2007] They have been successfully applied in

hydrolytic reactions, reduction and oxidative reactions or carbon-carbon bond forming reactions and represent a versatile tool in organic synthesis.[Clouthier 2012]

A crucial step when designing a biocatalytic process is the selection of the biocatalytic pathway. The repertoire in available biocatalysts and possible reactions has enlarged significantly, since not only wild type enzymes are employed, but huge mutant libraries are created.[Davids 2013] For instance, the advances in computer simulations allow predicting regions and even single amino acids that are important for the desired application, e.g. for the enantioselectivity of the enzyme. This knowledge can then be used for rational protein design and consequently leads to the mutant with the desired properties.[Rotticci 2001] Another approach is random mutagenesis, which means that lots of mutants are generated and tested in high-throughput screenings where biocatalysts with desired properties are rapidly identified. The best candidates will undergo a second round of random mutagenesis and this procedure is repeated until an optimised biocatalyst is found.[Bornscheuer 2002]

Once a suitable biocatalyst is found, the stability of the biocatalyst in the chosen reaction medium should be targeted. For example, a technique to improve the stability of enzymes and facilitate their reuse is immobilisation.[Mateo 2007] Several methods have been developed to immobilize enzymes, i.e. entrapment or encapsulation, adsorption on solid supports, cross-linking and covalent coupling.[Adlercreutz 2013] Each of them has advantages and disadvantages, and for each application the immobilisation technique should be carefully chosen. By way of an example, entrapment and encapsulation procedures protect enzymes successfully from the environment, but suffer from mass transfer limitations.[Tischer 1999] Adsorption on solid supports provides good stability but is mainly used in organic solvents as loss of volumetric and specific activity occurs in aqueous environment due to leaching of enzyme into the aqueous phase.[Kim 2006] One can also cross-link enzymes with the help of bifunctional cross-linkers. Best results are obtained when cross-linking enzyme crystals, so that the enzymes are in close proximity to each other.[Brady 2009] Covalent binding to a carrier attaches the enzyme tightly, and thus no leaching of enzyme is possible, but one should keep in mind that the enzyme is now chemically modified. Often the enzymes are immobilised by covalently linking the amino

groups to the carrier. However, one has to ensure that the active site of the enzyme is not modified, to avoid loss of activity.[Hanefeld 2009] For even more simplified separation of the catalyst from the reaction mixture, immobilisation on magnetic nanoparticles has also been reported.[Bornscheuer 2003] Once a suitable biocatalyst has been found for the selected reaction and both stability and activity of the biocatalyst are satisfactory, the recovery and purification of the product must be addressed.

## 1.2  Non-Conventional Reaction Media

In typical enzymatic reactions, substrates are usually hydrophobic and oil-soluble whereas enzymes are preferably dissolved in a hydrophilic environment. *In vivo*, cells provide the optimum environment to provide contact between the biocatalyst and the appropriate substrate. However, in an aqueous buffer solution, good contact between a poorly water-soluble substrate and the dissolved enzyme can only be achieved *via* rigorous mixing or addition of detergents.[Acharya 2002] In both cases one often faces low product concentration and sometimes reduced enzyme activity due to the additives needed for solubilising the substrate. Hence, several non-conventional reaction media have been investigated to improve enzyme performance and thus the efficiency of the process. For instance, organic solvents, ionic liquids, microemulsions, supercritical fluids, two-phase systems or aqueous-organic mixtures have been investigated.[Illanes 2012] In the following only organic solvents and microemulsions will be described.

Especially hydrophobic organic solvents have proved to have surprisingly good properties for enzyme catalysis.[Klibanov 2001] Even if enzyme activity is sometimes lower than in aqueous environment, organic solvents have the advantage that reactions can be carried out in dry conditions. This enables the inversion of many naturally catalysed reactions, thus significantly enlarging the synthetic potential of the biocatalysts. Additionally, different selectivity compared to that observed in aqueous solutions has been found, and even steering of the enantioselectivity by the choice of the organic solvent is possible.[Carrea 2000] By way of an example, the asymmetric hydrolysis of dihydropyridine carboxylates catalysed by *Pseudomonas*

*sp.* lipase gives the (S)-enantiomer when conducted in diisopropylether and the (R)-enantiomer when conducted in cyclohexane.[Hirose 1992] Several models have been developed to explain this phenomenon, which are (1) the enzyme conformation changes upon solvent polarity and thus changing the selectivity due to the altered molecular enzyme-substrate recognition, (2) the selectivity depends on the solubilisation of the substrate in the solvent and (3) the solvent molecules could bind at the active site of the enzyme and could lead to the preferred formation of one of the enantiomers. However it should be mentioned that none of these theories could reliably predict the selectivity of enzymes. It is likely that the selectivity of enzymes is steered by more than one mechanism.[Carrea 2000]

Another interesting feature is the "molecular memory" of enzymes, which means that in the organic solvent they retain the conformation in which they have been lyophilised.[Klibanov 2001] This implies the importance of a careful preparation, i.e. the choice of buffer and its pH, prior to its lyophilisation to ensure an active enzyme conformation in the organic solvent. A possible explanation for this "molecular memory" is that in the organic solvent not enough water molecules exist to ensure conformational flexibility and the resulting rigidity of the enzymes explains the unchanged conformation.

Microemulsions are thermodynamically stable, optically isotropic mixtures of at least three components.[Kahlweit 1985] They consist of a water domain, an oil domain and an interfacial layer composed of surfactant molecules which separates oil and water domains. From all possible microstructures, scientists have mainly studied water-in-oil (w/o-) droplet microemulsions for biocatalytic purposes.[Carvalho 2000] In this system, the biocatalysts can be located either in the water droplets' core - if hydrophilic - or adsorbed at the interfacial layer - if interfacially-active. The substrate is dissolved in the hydrophobic continuous oil phase, or, more precisely, in the organic solvent. It should be noted that the partitioning of substrates between oil and water phase can play an important role for the reaction rate and should be studied prior to the analysis of the reaction kinetics;[Bru 1990] it cannot merely be assumed that the substrate resides solely in the hydrophobic phase. Apart from the possibility to dissolve substrate and enzyme in a macroscopic homogeneous mixture, the large oil-water interface is

another feature from which interfacially-active enzymes like lipases can benefit.[Stamatis 1999] However, interfacially inactive enzymes like α-chymotrypsin,[Ruckenstein 1990] trypsin[Avramiotis 1996] or cutinase[Papadimitriou 1997] have also been employed successfully in w/o-microemulsions. The water droplet size was identified as a key parameter for the enzymatic activity, which shows a bell-shaped dependency from the water content.[Stamatis 1999] Although there is no complete agreement on this theory, the maximum of enzyme activity seems to occur often at the point where the size of the water droplet equals the size of the enzyme molecule. The possibility of changing the water content is the reason for the fact that both hydrolytic and synthetic reactions can be realised in w/o-microemulsions and thus greatly enhances the application range of this reaction medium.[Orlich 2001]

Bicontinuous microemulsions, distinct from w/o-microemulsions, have no droplet structure but a sponge-like structure with continuous oil and water domains, which are separated by the interfacial layer.[Stubenrauch 2009] As is the case with w/o-microemulsions, the reactants will partition - depending on their polarity - between the oil phase, the water phase and the interfacial layer. The reaction is assumed to occur at the interfacial layer where enzyme and substrate can get in contact. As the bicontinuous microstructure provides a huge continuous interfacial layer,[Strey 1994] enzyme and substrate contacts may be improved which, in turn, leads to higher reaction rates compared to w/o-microemulsions.

A few investigations have been already made in bicontinuously-structured microemulsions and they showed that these systems are suitable reaction media for biocatalysis. For instance, Larsson *et al*. investigated the oxidation of racemic 3-methyl-cyclohexanone by horse-liver alcohol dehydrogenase in different microstructures, going from an o/w-microemulsion to a w/o-microemulsion via a bicontinuous microemulsion. They found a decrease of the reaction rate with increasing oil volume fraction $\phi$. However, they could show qualitatively and quantitatively that the reason for this decreased activity is the partitioning of the substrate from the oil to the aqueous phase, thus lowering the substrate availability rather than decreasing the enzyme activity itself.[Larsson 1991] Additionally, they described how enzyme reuse and product recovery from a bicontinuous

microemulsion can be addressed.[Larsson 1990] Another study of Skagerlind *et al.* was performed with lipases in w/o- and bicontinuous microemulsions. In this study they compared microemulsions containing the nonionic surfactant pentaethylene glycol monododecyl ether ($C_{12}E_5$) with microemulsions containing the anionic surfactant dioctyl sulfosuccinate sodium salt (AOT). No significant influence of the microstructure could be detected, but very low hydrolysis rates were found for the nonionic surfactant which were explained by esterification of the surfactant.[Skagerlind 1992] A slightly different approach of using bicontinuous microemulsion for enzymatic reactions was followed by Vaze *et al.* They used metallo-proteins immobilised on electrode surfaces which were optimised for the use in bicontinuous microemulsions.[Vaze 2004] They obtained better stability and higher turnover number for epoxidation in bicontinuous microemulsions, which, in their opinion, could be used for many proteins. The higher turnover number in bicontinuous microemulsion than in o/w-microemulsions and micelles is supposed to be due to the more efficient mass transport in the oil phase. More recently, Sathishkumar *et al.* used an esterase in a bicontinuous microemulsion to hydrolyse (R,S)-ketoprofen ethyl ester.[Sathishkumar 2010] They found a much faster reaction rate as reported before in biphasic systems, which shows the superiority of the bicontinuous microemulsion as reaction medium. However, the enzyme displayed low selectivity, so that both enantiomers were formed. Also ω-transaminases have been used successfully in bicontinuous microemulsions.[Laupheimer 2011] In this study, it was shown that more hydrophobic substrates were more effectively converted in a bicontinuous microemulsion than in a aqueous solution. However, for less hydrophobic substrates the conversion was lower than in aqueous solutions. Consequently, it shows that bicontinuous microemulsions are an especially interesting reaction medium for hydrophobic substrates which can be dissolved in the oil phase of the microemulsion. Enzyme activity combined with scattering techniques were presented by Wellert *et al.* in order to characterise the properties and activity of DFPase in bicontinuous microemulsions prepared with sugar surfactants.[Wellert 2011] They discovered that the enzyme did not influence the bicontinuous microstructure, nor was influencing the properties of the interfacial layer of the microemulsion. The slightly decreased enzyme activity was again explained with the physical transport of the substrate

which has to partition from the oil phase to the aqueous phase, via the interfacial film. Thus, they showed that bicontinuous microemulsions made from sugar surfactants can be a mild reaction medium for enzymatic decontamination of toxic organophosphates. The advantage is the good solubility of these toxic compounds in the oil phase of the microemulsion.

In a nutshell, the studies clearly demonstrate the complexity of the reaction medium due to the numerous possible interactions between the components of the system and the enzyme. Hence, a systematic study to investigate the key parameters which influence enzymatic activity in bicontinuous microemulsions is needed to understand in more detail the potential and limits of this system. With organic solvents being the perfect reaction medium for synthetic reactions and w/o-microemulsions being suitable for both synthetic and hydrolytic reactions, bicontinuous microemulsions should be the perfect medium for hydrolytic reactions due to their large water content.[Sathishkumar 2008]

## 1.3  Task Description

The main aim of this work was to study the activity of two different enzymes in a non-conventional reaction medium. The non-conventional reaction medium of choice was a bicontinuous microemulsion because of its bipolarity and huge interfacial area. In the present case the system consisting of buffer – $n$-octane – alkyl polyethylene glycol ether ($C_iE_j$) and equal volumes of water and oil was used. The buffer can dissolve the enzyme at the appropriate pH and ensure sufficient ionic strength for the enzyme stability. The oil phase consisting of $n$-octane can dissolve a wide range of hydrophobic substrates which are interesting for enzymatic catalysis, but not water-soluble and therefore unsuitable for conventional enzymatic reactions in aqueous media. Nonionic $C_iE_j$ surfactants are available in a large range of homologues, with systematically increasing or decreasing amphiphilicity and hydrophilicity, without changing the overall nature of the surfactant. Additionally, co-surfactants can be added to the microemulsion to change the properties of the interfacial layer. For this purpose, the hydrophilic sugar surfactant $n$-decyl-β-D-glucopyranoside ($β$-$C_{10}G_1$)

and the hydrophobic phospholipid 1,2-dioleoyl-sn-glycero-3-phosphocholine (DOPC) were used.

Two reactions were studied. Task I was dealing with a lipase-catalysed hydrolysis reaction, where the interfacially-active enzyme could benefit from the large interfacial layer. The focus were hydrolytic reactions due to the large water content of the bicontinuous microemulsion that should favour the hydrolytic reaction against the esterification reaction. Applications for this type of reaction are the kinetic resolution of racemic mixtures[1] to generate small, optically pure molecules like chiral amines[Breuer 2004] and the direct asymmetric synthesis of drugs, for example profens, which are among the most important non-steroidal anti-inflammatory drugs.[Kourist 2011] The lipase activity was studied by following the conversion of $p$-nitrophenyl esters to $p$-nitrophenol and fatty acid (see Scheme 1.1).
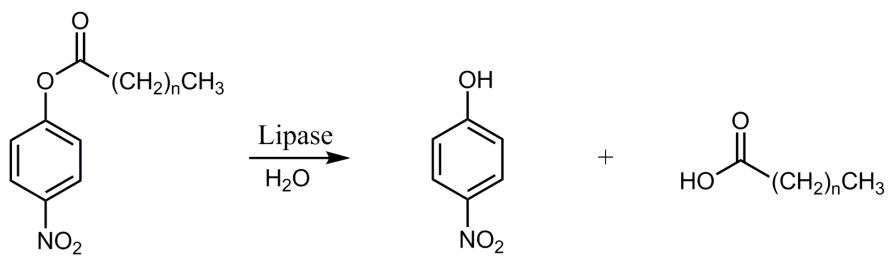


$n = 14$: $p$-nitrophenyl palmitate          $p$-nitrophenol          $n = 14$: palmitic acid
$n = 10$: $p$-nitrophenyl laurate                                        $n = 10$: lauric acid
$n = \phantom{0}6$: $p$-nitrophenyl caprylate                          $n = \phantom{0}6$: caprylic acid

**Scheme 1.1**: The hydrolysis of the $p$-nitrophenyl esters with different chain lengths leads to $p$-nitrophenol and the respective fatty acid. The reaction is catalysed by lipases.

This assay is typically used to determine lipase activities in both aqueous reaction media[Winkler 1979; Zhang 2003] and w/o-microemulsions.[Das 2003] The reaction rate was

---

[1] The kinetic resolution of an acetamide was studied in a bicontinuous microemulsion, as described in Section 7.2, although it will not be in the focus of this thesis.

determined photometrically by monitoring the *p*-nitrophenol concentration at the isosbestic wavelength as a function of time. The aim of this study was to learn which parameters influence the lipase activity in bicontinuous microemulsions. The lipase B from *Candida antarctica* (CalB) was chosen because of its high stereoselectivity,[Anderson 1998] its well-known crystal structure and reaction mechanism.[Uppenberg 1995; Uppenberg 1994]

The study comprised first basic investigations on phase behaviour and partitioning of the additives in a well-characterised microemulsion consisting of buffer – *n*-octane – pentaethylene glycol monodecyl ether ($C_{10}E_5$). The phase behaviour of CalB containing microemulsions, as well as their microstructure, was studied intensely in a previous work, combined with investigations on the conformation of CalB in bicontinuous microemulsions.[Subinya 2014a] The next step was the determination of optimal pH, temperature and ionic strength for CalB activity in microemulsions. Finally, the influence of the properties of the interfacial layer of the microemulsion on the CalB activity was tested by adding co-surfactants to the mixture.

Task II dealt with squalene-hopene cyclases. In contrast to lipases, cyclases have not yet been applied in microemulsions and have just been recently discovered as general Brønsted acid catalysts that widened considerably their possible application range. The question was whether cyclases were still active in presence of organic solvents and surfactants, and whether their conformation was disturbed or not. The squalene-hopene cyclase from *Alicyclobacillus acidocaldarius* (Aac SHC) was used to convert squalene to the products hopene and hopanol (see Scheme 1.2).



Squalene          Hopene          Hopanol
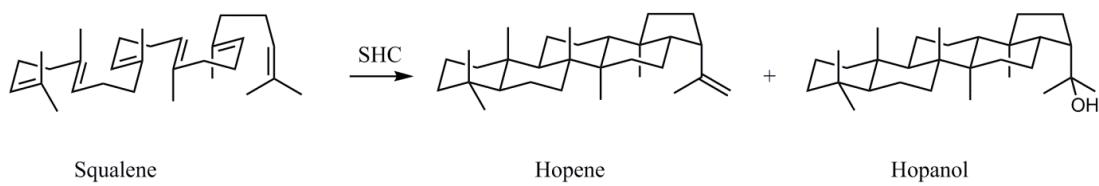
**Scheme 1.2**: Conversion of squalene to hopene and hopanol. The reaction is catalysed by squalene-hopene cyclases.

The study focused first on the influence of enzyme and substrate concentration and the reaction rate obtained for one enzyme and substrate concentration. Second, the influence of the composition of the interfacial layer on the Aac SHC activity was studied, as well as the conformation of Aac SHC in the respective microemulsions. Third, *n*-octane was replaced by squalene, to investigate the influence of an organic solvent as oil phase of the microemulsion. Finally, the temperature dependence of Aac SHC activity was tested by formulating microemulsions with different phase inversion temperatures. The aim of this part of the thesis was to show that bicontinuous microemulsions could act as reaction medium not only for lipases but for enzymatic catalysis in general.

# 2 Theoretical Background

This section is an overview of the concepts and theories on which this work is based. The first part deals with microemulsions and those properties which are important for the present study, i.e. the phase behaviour, the microstructure and the interfacial tension. The influence of additional components - so-called additives - on the microemulsion's properties is also described. The second part is about enzymes and reaction kinetics. More specifically, enzyme kinetics are explained and a short overview is given about how to interpret kinetics in heterogeneous systems. The conformation of enzymes as well as techniques to study the conformation are described. The two enzymes used in this work are described in detail as well as their use in catalysis and their reaction mechanism.

## 2.1 Microemulsions

Microemulsions are thermodynamically stable, optical isotropic mixtures of at least three components like water, oil and surfactant.[Stubenrauch 2009] The surfactant is an amphiphilic molecule, which has at least one hydrophilic head group and at least one hydrophobic chain and separates the oil from the water domain. Note that throughout this thesis, only nonionic surfactants are used and thus only properties of nonionic surfactants are described. The fact that the surfactant molecules form an interfacial layer between oil and water, the result are "ultra-low" interfacial tensions between the oil and the aqueous phase, which can reach values down to $10^{-5}$ mN m$^{-1}$.[Strey 1994] In these ternary mixtures, several microstructures can be formed depending on the composition of the mixture and the temperature. In the following, the phase behaviour, the microstructure, the interfacial tension and the influence of additives will be explained.

### 2.1.1 Phase Behaviour

To describe the phase behaviour of a ternary mixture, four independent thermodynamic variables are necessary. These are temperature, pressure and two composition variables. If one considers the low influence of pressure on the phase

behaviour of liquid mixtures and the fact that the pressure is held constant throughout this work (1 atm) this variable can be neglected.[Kahlweit 1988] Thus the phase behaviour can be presented with the remaining three variables in a phase prism, where the ordinate represents the temperature and a Gibbs triangle forms the basis. The sides of the phase prism represent the binary systems' phase diagrams, namely water-oil, water-surfactant and oil-surfactant.[Strey 1994] The water-oil system displays a miscibility gap which extends nearly over the whole temperature range from 0-100 °C. The other two binary systems water-surfactant and oil-surfactant are shown in Figure 2.1.
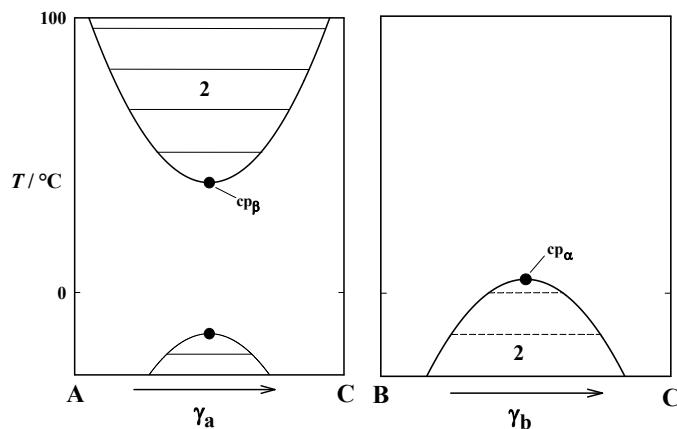


**Figure 2.1**: Binary systems of water (A)–surfactant (C) and oil (B)–surfactant (C). Marked are the lower critical point $cp_\beta$ of the upper miscibility gap between A and C and the upper critical point $cp_\alpha$ of the lower miscibility gap between B and C (taken from [Sottmann 2005]).

The water-surfactant system is the most complex one as above the critical micelle concentration (cmc) of the surfactant, association colloids and liquid crystalline phases are formed. However, for clarity reasons, these are omitted in the diagram. Additionally, the miscibility gap below the melting point is not relevant for us, as we work in a temperature range of 0-100 °C. Important is thus the upper miscibility gap which has a lower critical point $cp_\beta$. From this we can conclude that surfactant and water are only miscible at lower temperatures.[Kahlweit 1985] Certainly, the nature of the components can influence the miscibility: the more hydrophilic a surfactant, the more soluble it is in water and the smaller is the miscibility gap. The result is a higher $cp_\beta$. Additionally, additives to the water phase influence the miscibility gap as

will be explained in Section 2.1.4. The oil-surfactant system displays only one lower miscibility gap in the relevant temperature range. It has an upper critical point $cp_\alpha$.[Kahlweit 1985] From this we deduce that oil and surfactant are only miscible at elevated temperatures. Furthermore, the more hydrophobic the surfactant is the better its solubility in the oil resulting in a lower $cp_\alpha$. Again, additives in the oil phase or the polarity of the oil influence the position of the miscibility gap (see Section 2.1.4).

Going back to the phase prism of ternary mixtures, it is now important to introduce the two parameters describing the composition of such a mixture.

i)      The mass fraction of the surfactant in the total mixture is given by

$$\gamma = \frac{m_C}{m_A + m_B + m_C},$$
[2.1]

ii)      the oil to water ratio is either given by the mass fraction of the oil in the mixture of oil and aqueous phase

$$\alpha = \frac{m_B}{m_B + m_A},$$
[2.2]

iii)      or by the corresponding volume fraction

$$\phi = \frac{V_B}{V_B + V_A}.$$
[2.3]

In practice, a two-dimensional plot is always easier to work with than a three-dimensional plot. We can realise this by keeping the oil to water ratio constant at $\phi = 0.5$ and thus reduce once more the variables. The phase behaviour can now be described as a function of temperature $T$ and surfactant mass fraction $\gamma$. In other words, this is a vertical cut through the phase prism, a so called $T$-$\gamma$ cut.[Strey 1994] Figure 2.2 shows a schematic view of such a phase diagram, with the Kahlweit nomenclature[Kahlweit 1988] indicating the number of phases present.
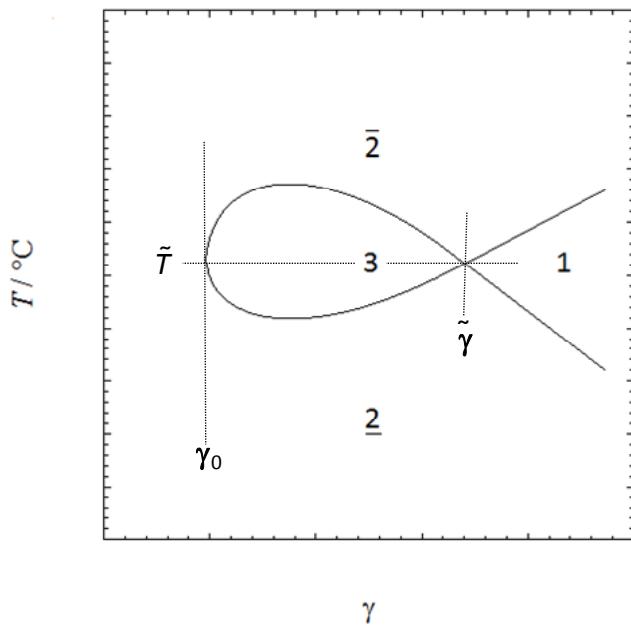
**Figure 2.2**: Characteristic phase behaviour for a ternary mixture with equal volumes of water and oil ($\phi = 0.5$). At surfactant mass fractions between $\gamma_0$ and $\tilde{\gamma}$ and the phase inversion temperature $\tilde{T}$, a three-phase system exists, until the one-phase system is formed at $\gamma > \tilde{\gamma}$. Above and below the three-phase and one-phase region, droplet microemulsions are in equilibrium with an oil or water excess phase, so that a two-phase system is generated. The bar indicates if the microemulsion is the upper or the lower phase.

At very low surfactant mass fractions ($\gamma < \gamma_0$) water and oil exist as two separate phases. The surfactant molecules are adsorbed at the macroscopic interface and are dissolved according to their monomeric solubility in the oil phase and the water phase, respectively. When the surfactant mass fraction is $\gamma > \gamma_0$ and the system is at its phase inversion temperature $\tilde{T}$ a third, surfactant-rich phase is formed. The bottom phase is still the water phase with monomerically dissolved surfactant and the oil phase with monomerically dissolved surfactant remains on top. In between the two phases, a small bicontinuous microemulsion phase has been formed which is the phase in which most of the surfactant is present. Increasing further the surfactant mass fraction $\gamma$, still at the phase inversion temperature $\tilde{T}$, the middle-phase microemulsion grows and the excess phases shrink. The lowest temperature at which a three-phase region is formed is called $T_l$, the highest temperature at which there is still a three-phase region present is called $T_u$. Finally, at the surfactant mass fraction $\tilde{\gamma}$ the excess phases are completely solubilised in the middle-phase microemulsion and

a one-phase bicontinuous microemulsion is created. At even higher surfactant mass fraction, lytropic liquid crystalline phases can occur. As indicated in the schematic drawing, at temperatures below and above the three-phase region (3) and the one-phase region (1), two-phase systems occur. They consist of a microemulsion phase and an excess phase, where the bar indicates whether the microemulsion, i.e. the surfactant-rich phase, is the upper or the lower phase. The intersection where the three-phase and the one-phase system merge, defined by $\tilde{T}$ and $\tilde{\gamma}$, is called the $X$-point. Working with the same oil and water phase, one can use the $X$-point to compare the efficiency of surfactants.[Sottmann 2009]

A widely used class of nonionic surfactants are alkyl polyethylene glycol ethers $C_iE_j$. The hydrophobic part consists of an alkyl chain ($C_i$) where $i$ denotes the number of carbon atoms. The hydrophilic part consists of ethylene glycol groups ($E_j$) where $j$ indicates how many of these groups form the head group of the surfactant. For instance, Scheme 2.1 shows $n$-decyl pentaethylene glycol ether ($C_{10}E_5$) a surfactant which is often used in this study.
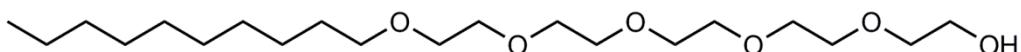


**Scheme 2.1**: The molecular structure of $n$-decyl pentaethylene glycol ether ($C_{10}E_5$).

The advantage of these surfactants is that the hydrophilicity can be easily increased by adding ethylene glycol groups and the hydrophobicity by extending the alkyl chain. Figure 2.3 shows the influence of the alkyl chain length and the number of ethylene glycol groups on the efficiency and phase inversion temperature $\tilde{T}$ of the microemulsions.

Plotted are the $X$-points of the respective microemulsions. From the regular pattern for the system consisting of $H_2O$ − $n$-octane − $C_iE_j$ it can be seen that by increasing the alkyl chain length of the surfactant $i$ at constant $j$, both temperature and surfactant mass fraction of the $X$-point decrease. By increasing the number of ethylene groups $j$ at constant $i$, the temperature of the $X$-point raises distinctly and the system looses efficiency.[Burauer 1999] In summary, a variety of systems can be formed with surfactants

of similar molecular structure at a desired temperature and surfactant mass fraction. However, in most cases, the aim is to create efficient systems with low surfactant concentrations to reduce costs, minimise possible interactions and facilitate handling of the samples.
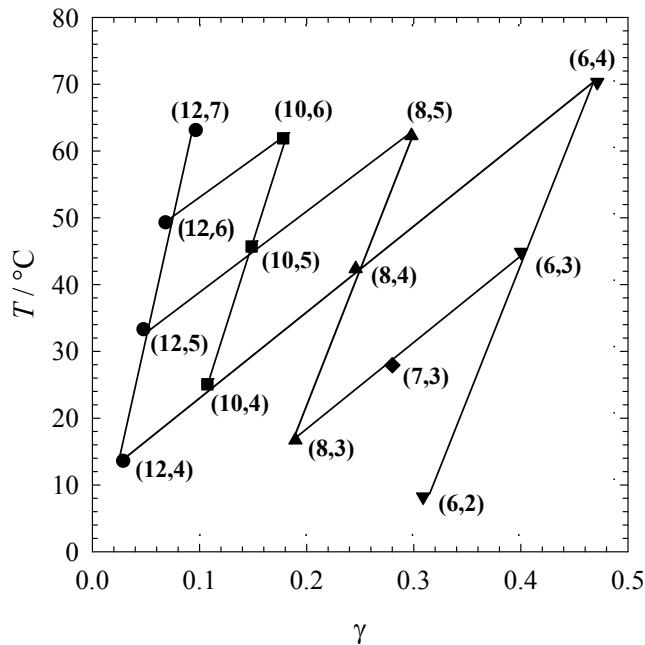


**Figure 2.3**: The influence of hydrophobic chain length (*i*) and hydrophilic head group size (*j*) on the *X*-point of a microemulsion consisting of $H_2O$ – *n*-octane – $C_iE_j$. The water to oil ratio is $\phi = 0.5$ (figure taken from[Burauer 1999], modified).

## 2.1.2 Microstructure

The possibly most interesting feature of microemulsions is their ability to form different microstructures. Due to their amphiphilicity the surfactant molecules reside at the water-oil interface where they create a topologically ordered interfacial film. The microstructure of a microemulsion depends on the nature and properties of this interfacial film, or more exactly on its local curvature. The two principal radii $R_1$ and $R_2$ define the principal curvatures $c_1 = 1/R_1$ and $c_2 = 1/R_2$. With the principal curvatures, the mean curvature of the interfacial film is defined by

$$H = \frac{1}{2}(c_1 + c_2). \qquad\qquad [2.4]$$

The curvature $H$ is defined as being positive for a surfactant film bent around the oil phase and as negative for being bent around the aqueous phase.[Strey 1994] Figure 2.4 shows three possible structures, the oil-in-water (o/w) microemulsion, the bicontinuous microemulsion and the water-in-oil (w/o) microemulsion.



T / °C
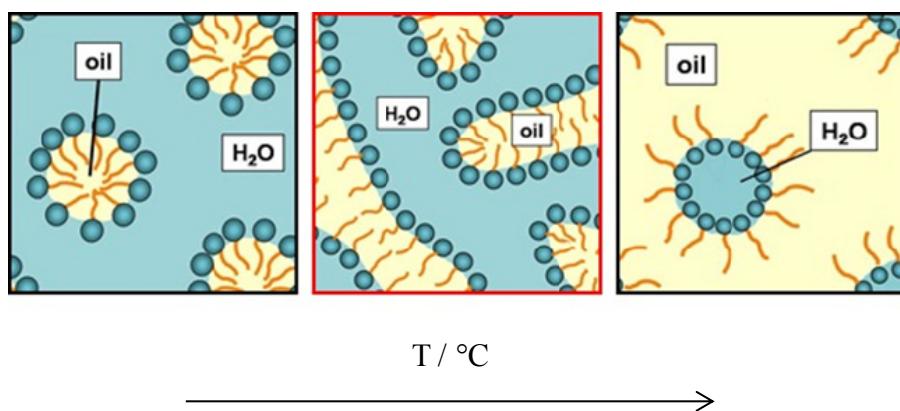
**Figure 2.4**: Microemulsions with different microstructures. At low temperatures the interfacial film is bended around the oil droplets in a continuous water phase, $H > 0$. At the phase inversion temperature $\tilde{T}$ a bicontinuous microemulsion is formed, $H = 0$. At higher temperatures the interfacial film is bended around the water droplets in a continuous oil phase, $H < 0$ (drawn by Dr. Sandra Engelskirchen).

In the o/w microemulsion with a mean curvature of the interfacial film of $H > 0$ the hydrophilic head groups of the surfactant are well hydrated and the hydrophobic chains point into the oil droplet. At elevated temperatures, the head group is smaller due to dehydration. At the same time, the hydrophobic chains can adapt more chain conformations and oil molecules penetrate increasingly in between the hydrophobic alkyl chain of the surfactant resulting in a mean curvature of $H < 0$ and thus in the formation of a w/o microemulsion. The transition between these two droplet structures goes via a bicontinuous microstructure, which has a locally planar interfacial film with $H = 0$. This bicontinuous microemulsion occurs at the phase inversion temperature $\tilde{T}$. Note that the mean curvature is not only influenced by the

temperature but also by the salt content and the composition of the interfacial film, which change the curvature and thus the microstructure of a microemulsion.

Several methods were applied to prove and quantify these structures experimentally. It is possible to visualise the freeze-dried microstructure by transmission electron microscopy, from which detailed local information about the microstructure can be obtained.[Kumar 1999] For more statistical properties and quantitative information about length scales and correlation lengths in microemulsions, scattering methods have been proven very useful. Especially small angle neutron scattering (SANS) and small angle X-ray scattering (SAXS) are appropriate due to the characteristic length scales of microemulsions which are between $5 - 100$ nm.[Gradzielski 2008; Magid 1988] Also pulsed field gradient nuclear magnetic resonance (PFG-NMR) is widely used to study the connectivity of and transitions between the different microstructures.[Lindman 1981; Olsson 1986] Measuring the diffusion coefficients of several components of the system allows one to distinguish droplet from bicontinuous structures. Last but not least, conductivity can be used to distinguish between water-continuous and water-discontinuous structures because the conductivity drops several orders of magnitudes when going from o/w-microemulsions to w/o-microemulsions.[Lagourette 1979]

## 2.1.3 Interfacial Tension

Another unique property of microemulsions is the low interfacial tension which can be measured between the macroscopic phases of a microemulsion and an excess phase ($\underline{2}$ and $\bar{\underline{2}}$) or between two excess phases (3). When the microemulsion is in equilibrium with two excess phases, ultra low values of down to $10^{-5}$ mN m$^{-1}$ may occur between the two excess phases.

To measure such low interfacial tensions, a spinning drop tensiometer can be used. The measuring principal is the analysis of the shape of a droplet, which is rotating (spinning). For this purpose, the droplet is dispersed in a second phase, i.e. the matrix phase which has a higher density than the droplet. The two phases are enclosed in a cylindrical glass tube, which rotates about its horizontal axis. The speed of this rotation can be chosen freely or, in other words, the force which is shaping the

interface can be varied, in contrast to pendant drop tensiometers, where the shape of the drop is defined by gravity. At low velocities the droplet will still have the shape of a spherical droplet, but at higher velocities, the droplet will stretch and finally resemble a cylindrical shape with rounded ends. Additionally, at sufficiently high velocities, the influence of gravity becomes negligible and the shape of the droplet can be calculated from Vonnegut's equation

$$\sigma = \frac{\Delta\rho\omega^2 r_0^3}{4} .$$

[2.5]

where $r_0$ is the radius of the cylindrical part, $\omega$ the angular velocity and $\rho$ the density.[Seifert 1992]

A schematic view of the interfacial tension curves in a microemulsion is shown in Figure 2.5. The correlation between the ultra low interfacial tension and the formation of a three-phase region can be explained by considering the microemulsion's phase behaviour.

At temperatures below $T_l$ an o/w-microemulsion (a) is formed in equilibrium with an oil excess phase (b). The interfacial tension that can be measured between these two macroscopic phases is called $\sigma_{ab}$. Once the lower temperature $T_l$ is reached, a third phase evolves, so that now three different interfacial tensions exists. The interfacial tension $\sigma_{ac}$ can be measured between the water excess phase (a) and the microemulsion middle-phase (c), as well as the interfacial tension $\sigma_{bc}$ between the oil excess phase (b) and the microemulsion middle-phase (c). Additionally, when the microemulsion middle-phase is removed until only a lens is still floating between the two excess phases, the interfacial tension $\sigma_{ab}$ can be measured between the two excess phases. At temperatures above $T_u$, a w/o-microemulsion (b) is formed which is in equilibrium with a water excess phase (a), so that again the interfacial tension $\sigma_{ab}$ can be measured between the macroscopic phases.
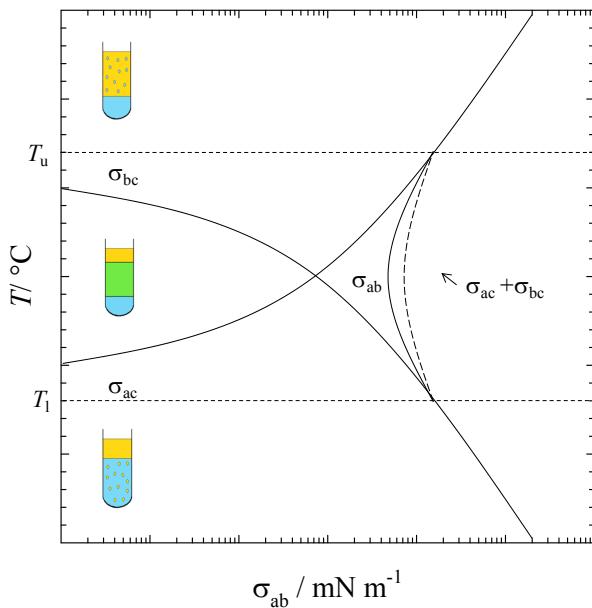
**Figure 2.5**: Schematic description of the interfacial tension $\sigma_{ab}$. The interfacial tension $\sigma_{ab}$ can be described as the sum of the interfacial tensions $\sigma_{ac}$ and $\sigma_{bc}$. The interfacial tension $\sigma_{ac}$ starts at zero, as in the o/w-microemulsion the surfactant is mainly dissolved in the water phase, and the water-rich and the surfactant-rich phase is the same. Once the third phase is formed, the interfacial tension $\sigma_{ac}$ increases, as now, two separate phases are formed, a surfactant-rich phase (c) and a water-rich phase (a). Due to the reverse behaviour of the interfacial tension $\sigma_{bc}$ at higher temperatures, the interfacial tension $\sigma_{ab}$ runs through a minimum in the three-phase region (redrawn from [Stubenrauch 2009]).

This knowledge allows us to draw the qualitative shape of the interfacial tension curves. The interfacial tension $\sigma_{ac}$ starts at zero, when (a) and (c) are identical, as the water-rich and the surfactant-rich phase are one phase, namely the o/w-microemulsion, but once the third phase is formed and thus the interface between the water-rich (a) and the surfactant-rich (c) phases is created, it increases monotonically with the temperature. Vice versa, the interfacial tension $\sigma_{bc}$ equals first the interfacial tension $\sigma_{ab}$, as the surfactant rich phase in this case would be the o/w-microemulsion (a) so that (a) is equal to (c). The interfacial tension decreases until at $T_u$ the third phase vanishes and the surfactant and the oil-rich phase merge into the w/o-microemulsion phase, meaning that the interface between oil-rich (b) and surfactant-rich (c) phase disappears and thus results in an interfacial tension $\sigma_{bc}$ of zero. Due to this opposite behaviour of the two interfacial tension curves, one obtains a minimum when considering the sum of $\sigma_{ac}$ and $\sigma_{bc}$. As $\sigma_{ab}$ is defined as the sum of $\sigma_{ac}$ and $\sigma_{bc}$,

$\sigma_{ab}$ has to pass through a minimum at the phase inversion temperature $\tilde{T}$. Figure 2.6 shows the relationship between the molecular structure of the surfactant and the position of the minimum of the interfacial tension.
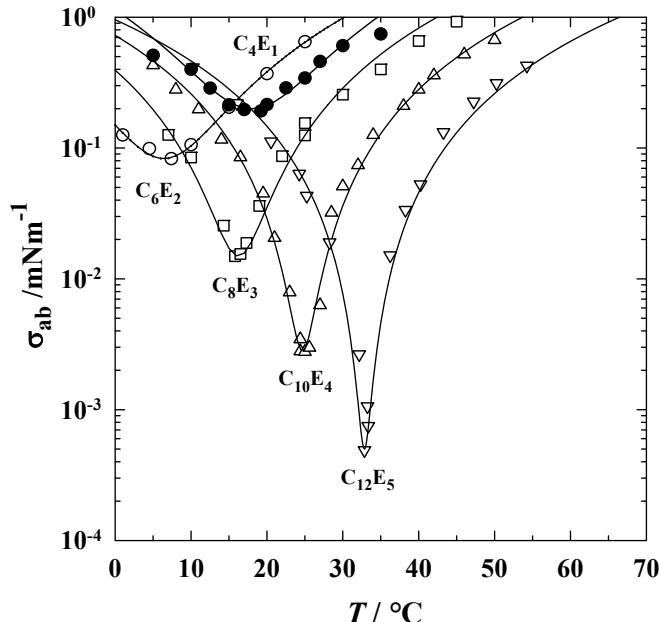


**Figure 2.6**: Interfacial tension curves plotted against the temperature. Each curve shows a minimum at the respective phase inversion temperature $\tilde{T}$ of the system. The microemulsions are formulated with increasingly efficient surfactants, namely $C_4E_1$, $C_6E_2$, $C_8E_3$, $C_{10}E_4$ and $C_{12}E_5$. Remarkable is the strong decrease of interfacial tension with increasing efficiency of the surfactant. The water to oil ratio is $\phi = 0.5$, with $H_2O$ and *n*-octane as water and oil phase, respectively. (taken from [Sottmann 2005]).

With increasing both the hydrophobic chain *i* and the number of ethylene glycol units *j* of a $C_iE_j$ surfactant, the interfacial tension values decrease, which means that for more efficient surfactants, lower interfacial tension values are observed than for less efficient ones (for efficiency compare with Figure 2.3). Additionally, one can note that the curves sharpen with increasing efficiency of the systems. For each system the minimum is always found at the phase inversion temperature of the respective system, as expected.

## 2.1.4 Additives

Microemulsions offer great possibilities to solubilise components of different polarity. However, one should note that nearly all additives added to a microemulsion influence its phase behaviour. Therefore two cases should be distinguished: (1) additives can be a reactant needed for a special application or chemical reaction in the microemulsion or (2) additives can act as fine tuning parameters to adjust the phase inversion temperature, the efficiency or other properties of the microemulsion. In the following, possible additives to aqueous and oil phases will be discussed as well as additives acting as co-surfactants.

The probably most common additive to the aqueous phase is NaCl, where the mass fraction of NaCl in the total mass of the aqueous phase is defined as

$$\varepsilon = \frac{m_{NaCl}}{m_{NaCl} + m_{H_2O}}.$$
[2.6]

As a lyotropic salt, it decreases the solubility of the surfactant in water and thus enlarges the upper miscibility gap in the binary water-surfactant system (see Figure 2.1). Consequently, the critical point $cp_\beta$ is lowered. One should note that the described effect is more pronounced for less amphiphilic surfactants.[Kahlweit 1988] In the ternary mixture, the addition of NaCl results in a lower phase inversion temperature $\tilde{T}$. Additives other than salt can also decrease the lower critical point $cp_\beta$, an example of which is the lipase B from *Candida antarctica* investigated in this work (see Figure 2.7 (left)). In the resulting phase behaviour of lipase-containing microemulsions (not shown here) the phase inversion temperatures $\tilde{T}$ are decreased accordingly.
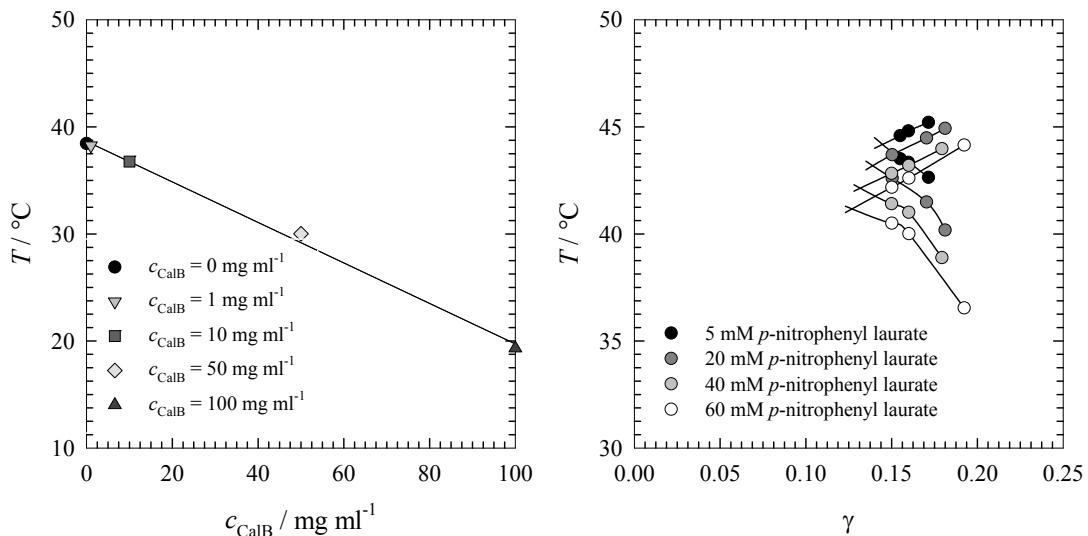
**Figure 2.7**: (left) The influence of increasing CalB concentration on the upper miscibility gap of the binary system buffer/4 wt% NaCl/CalB – $C_{10}E_5$. The temperature of the lower critical point $cp_\beta$ decreases with increasing CalB concentration indicating that CalB decreases the solubility of $C_{10}E_5$ in a buffer solution containing 4 wt% NaCl and a surfactant concentration of $\gamma = 0.15$ (taken from [Steudle 2011]). (right) Phase diagrams of microemulsions consisting of buffer – $n$-octane/$p$-nitrophenyl laurate – $C_{10}E_5$. The higher the concentration of the substrate $p$-nitrophenyl laurate, the lower the phase inversion temperature $\tilde{T}$ due to shrinkage of the miscibility gap in the binary system $n$-octane – $C_{10}E_5$. The substrate acts thus as co-oil, rendering the oil phase more hydrophilic.

Additives to the oil phase of the microemulsion are called "co-oil", although they are very often both co-oil and co-surfactant. Typical co-oils are polar or cyclic oils which are located in the oil phase of the microemulsion and do not adsorb at the interfacial layer.[Burauer 2000] The co-oil leads to a less hydrophobic oil phase so that the solubility of the surfactant is increased. Therefore the lower miscibility gap shrinks and the upper critical point $cp_\alpha$ drops. The resulting phase inversion temperature $\tilde{T}$ of the ternary mixture is again shifted to lower temperatures.[Kahlweit 1991] The same effect is observed when no additives, but oils of different polarity are compared. The less hydrophobic the oil phase, the lower is the phase inversion temperature $\tilde{T}$ because of the shrinking of the miscibility gap. Many additives other than alcohols can act as co-oils. One example is the substrates used in this work, which are oil soluble and thus act as co-oils as illustrated in Figure 2.7 (right). The shift to lower phase inversion temperatures of the microemulsion with increasing substrate concentrations reflects the shrinkage of the miscibility gap since the oil phase becomes less hydrophobic.

Longer chained alcohols or other amphiphilic compounds which adsorb at the interfacial layer can act as co-surfactants. They influence the efficiency of the system and the phase inversion temperature. The addition of a co-surfactant, which is more hydrophobic than the main surfactant, leads to a lower phase inversion temperature $\tilde{T}$, while less hydrophobic co-surfactants lead to higher phase inversion temperatures.[Kahlweit 1990] In this work, two co-surfactants will be investigated, namely the sugar surfactant $n$-decyl-β-D-glucopyranoside (β-$C_{10}G_1$) and the phospholipid 1,2-dioleoyl-sn-glycero-3-phosphocholine (DOPC). Their molecular structure is illustrated in Scheme 2.2.
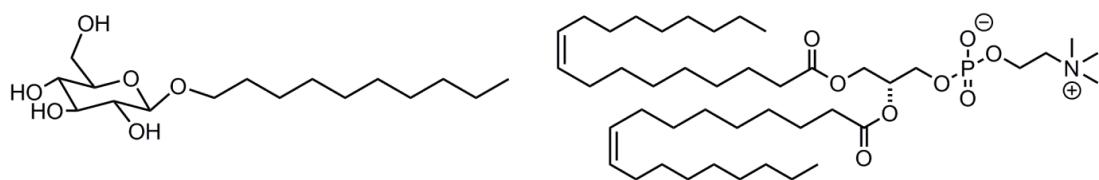


**Scheme 2.2**: Shown is the molecular structure of the sugar surfactant β-$C_{10}G_1$ (left) and of the phopholipid DOPC (right).

The amount of co-surfactant is given by the mass fraction of the co-surfactant in the surfactant mixture, i.e.

$$\delta = \frac{m_{\text{co-surfactant}}}{m_{\text{co-surfactant}} + m_{\text{surfactant}}} \qquad [2.7]$$

Sugar surfactants are nonionic surfactants which are biodegradable and non-toxic. They are a promising alternative especially in food, cosmetic or pharmaceutical industry, where non-toxic formulations are indispensable. In addition, they are made from renewable materials, an important feature for conducting green chemistry.[von Rybinski 1998] Alkyl polyglucosides are abbreviated as $C_mG_n$, with $m$ defining the number of carbon atoms in the hydrophobic chain, and $n$ the number of glucose units in the head group. The α and β nomenclature is used to distinguish the configuration at the anomeric carbon atom of the glucose unit. There are many possible linkages

between the sugar head group and the hydrophobic chain. Moreover, the surfactants can possess several head groups and two or more chains.[Stubenrauch 2001]

The head groups of these sugar surfactants are hydrated due to the hydroxyl groups of the glucose units which form hydrogen bonds with the surrounding $H_2O$ molecules. In contrast to alkyl polyethylene glycol ethers, this hydration is very strong and thus hardly depends on the temperature. In other words, the temperature cannot be used as a tuning parameter for the phase behaviour. The phase behaviour of sugar surfactants was investigated in detail by Kaler et. al.[Ryan 2001] They identified the formation of a growing channel in the three-phase region, where the three-phase region expands towards higher temperatures, when adding sugar surfactant to a microemulsion prepared with water – $n$-octane – $C_iE_j$ from $\delta = 0$ to $\delta = 0.5$. This behaviour is attributed to the fact that the sugar surfactants - in contrast to alkyl polyethylene glycol ethers - are immiscible with $n$-octane, even at elevated temperatures.[Ryan 1997] They showed that this channel is indeed not formed when choosing oils of higher polarity in which sugar surfactants are soluble at elevated temperatures. Even microemulsions containing only sugar surfactants as amphiphilic compounds could be formulated, with a phase behaviour similar to that of alkyl polyethylene glycol ethers if polar oils are used.[Ryan 2001] In the work at hand, in order to keep $n$-octane as the oil phase in the microemulsions, the sugar surfactant was mixed with an alkyl polyethylene glycol ether. As can be seen in Figure 2.8 (left), adding sugar surfactant to a microemulsion consisting of water – $n$-octane – $C_{10}E_5$ leads to increasing phase inversion temperatures as expected for a hydrophilic co-surfactant.

Phospholipids are the main components of cell membranes. In nature as well as in aqueous environment a lipid bilayer is formed, in which the hydrophobic chains point to the inside of the bilayer and the hydrophilic head groups point towards the outside. Phospholipids are strongly amphiphilic and are very efficient co-surfactants, but they are not able to form stable microemulsion alone due to their hydrophobicity. However, the formation of microemulsions with a phospholipid, e.g. lecithin, and a co-surfactant, e.g. a short chained alcohol, is well-known and commonly used for different applications.[Shinoda 1991] In this study, DOPC will be used as co-surfactant in a

microemulsion consisting of water – $n$-octane – $C_{10}E_5$. Figure 2.8 (right) shows the respective phase diagrams.
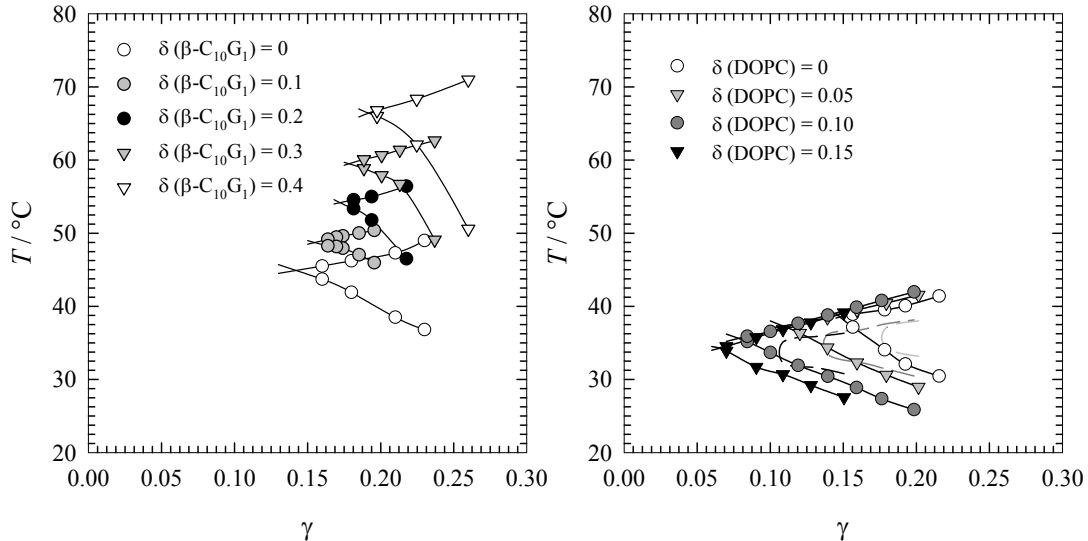


**Figure 2.8**: (left) Increasing phase inversion temperatures $\tilde{T}$ for microemulsions prepared with water – $n$-octane – $C_{10}E_5$/β-$C_{10}G_1$ with increasing amount of β-$C_{10}G_1$ from δ = 0 to δ = 0.4 (taken from[Steudle 2011]). (right) Decreasing phase inversion temperatures $\tilde{T}$ for microemulsions prepared with water/4 wt% NaCl – $n$-octane – $C_{10}E_5$/DOPC with increasing amount of DOPC from δ = 0 to δ = 0.15 (taken from[Subinya 2014a]).

The shift to lower phase inversion temperatures $\tilde{T}$ are expected due to the increasing hydrophobicity of the surfactant mixture and the strong amphiphilic character of the DOPC explains the significant shift towards more efficient microemulsions, even though the amount of the co-surfactant is very low.

## 2.2  Enzymes and Kinetics

The first part of this section deals with reaction kinetics, with a special focus on enzyme kinetics and reaction kinetics in heterogeneous systems. The second part gives an overview about the general structure of enzymes and how to investigate it. In addition, the two enzymes used in this work, namely the lipase B from *Candida antarctica* and the squalene-hopene cyclase from *Alicyclobacillus acidocaldarius*, are described.

## 2.2.1 Reaction Kinetics

Reaction kinetics describe how rapidly reactants are consumed and products are formed. They give information about how the reaction rate is influenced when reaction conditions are changed or a catalyst is present. Thus, reaction kinetics are an important tool to analyse and understand reactions. Many methods can be used to determine reaction rates. A widely used method is spectrophotometry, but also conductivity, light emission, titration, mass spectrometry, gas chromatography or magnetic resonance (EPR, NMR) can be used to carry out kinetic measurements. In the following, only spectrophotometry and gas chromatography will be explained in more detail, as these two methods were used in this thesis.[Atkins 2005]

With spectrophotometry, the concentration of one or more absorbing species in the sample can be easily determined from the absorbance using the Beer-Lambert law

$$\log \frac{I_0}{I} = \varepsilon\, c\, d \,, \qquad\qquad [2.8]$$

where $I_0$ denotes the incident intensity, $I$ the transmitted intensity, $\varepsilon$ the molar absorptivity, $c$ the concentration and $d$ the path length of the cuvette. The absorbance is defined as follows

$$A = \log \frac{I_0}{I} \,. \qquad\qquad [2.9]$$

The concentration is therefore directly proportional to the measured absorbance of the sample, so that the concentration of the species can be determined at any point of the reaction if the absorbance is recorded during the reaction. In case that several components are present and absorb at the same wavelength, the absorbances are additive and it holds

$$A = d \cdot \sum_i \varepsilon_i c_i \, .$$

[2.10]

Spectrophotometry is a non-invasive method which is an advantage as the measurements can take place *in situ*. However, for substances that do not absorb in the UV/Vis range, other analytic methods, e.g. gas chromatography, must be used to record the progress of the reaction. In this case, the sample must be completely volatile and it is injected in a stream of a carrier gas, usually hydrogen, where it is nearly instantly evaporated. The sample is then transported by the carrier gas, i.e. the mobile phase, over a thin and long column, i.e. the stationary phase. The column is situated in an oven, so that all the compounds stay in the gas phase. Moreover, the column is coated with a liquid or a solid phase which, depending on its polarity and the polarity of the compounds, leads to a separation.

At the end of the column, the mobile phase is analysed by a detector. A widely used one is the flame ionisation detector (FID). The sample gas passes through a flame and the formed ions are collected in a biased electrode. The current produced from the ions is proportional to the number of ions that are collected by the electrode. Organic compounds create ions in a characteristic way. The carbon-carbon bonds are broken ("cracking") and the hydrogen atoms are removed ("stripping"). The carbons are then converted in an oxomethylium ion ($CHO^+$) that quickly separates into a proton and CO. Thus, the FID can be seen as a carbon counter. To address the lower response of more complex compounds, the effective carbon number (ECN) concept was developed, which helps to quantitatively analyse the obtained data.[Faiola 2012] The procedure based on the ECN concept is explained in Section 6.9.

**Michaelis-Menten Kinetics**

The experimental determination of the reaction rate allows possible rate laws of the reaction to be postulated. In the case of enzymatic reactions, Michaelis-Menten

kinetics are widely used to describe the reaction mechanism and its kinetics.[Atkins 2005] It is assumed that enzyme [E] and substrate [S] form an enzyme-substrate complex [ES] before the product [P] is formed, i.e.

$$[E]+[S] \; \underset{k_{-1}}{\overset{k_1}{\rightleftharpoons}} \; [ES] \; \xrightarrow{k_{cat}} \; [E]+[P] \qquad\qquad [2.11]$$
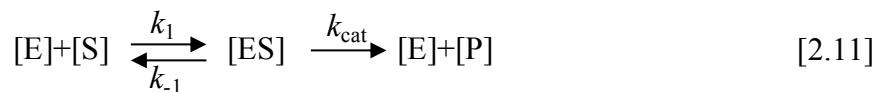
The formation of the enzyme-substrate complex is reversible and described by the rate constants $k_1$ and $k_{-1}$. The formation of the product from the enzyme-substrate complex is described by the rate constant $k_{cat}$ which is also called the turnover number and where the back reaction is assumed to be negligible.

Scheme 2.3 describes qualitatively the reaction rate as function of the substrate concentration. At low substrate concentrations, i.e. $[S] \ll K_m$, the reaction rate increases linearly with increasing substrate concentration. At higher substrate concentrations the reaction rate slows down and a hyperbolic curve is obtained at the maximum reaction rate $v_{max}$, which accounts for the case that all enzymes are bound to a substrate molecule. The Michaelis-Menten parameter $K_m$ is reached at half $v_{max}$ and describes the enzyme's affinity for the substrate. The lower the $K_m$ values are, the faster the maximum reaction rate $v_{max}$ is reached and thus the higher is the enzyme's affinity for the substrate.

The reaction rate can be expressed by

$$v = \frac{d[P]}{dt} = \frac{k_{cat}[E][S]}{[S]+K_m} = \frac{v_{max}[S]}{[S]+K_m}, \qquad\qquad [2.12]$$

with $K_m$ being defined as

$$K_m = \frac{k_{-1} + k_{cat}}{k_1} \; .$$ [2.13]
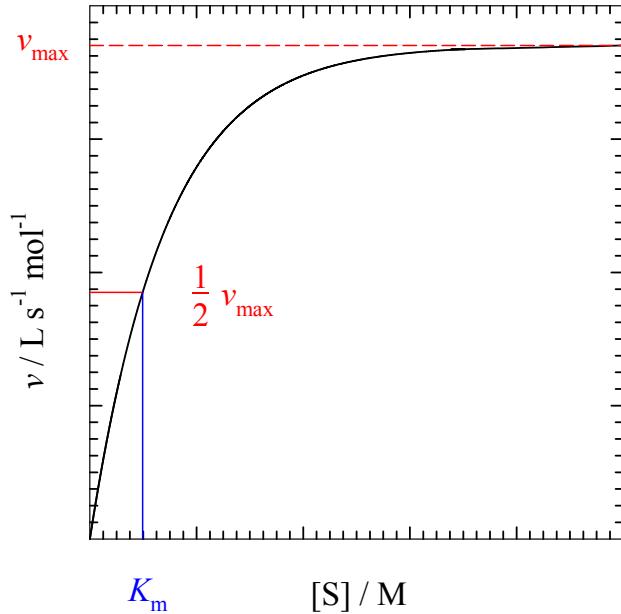


**Scheme 2.3**: Schematic drawing of influence of the substrate concentration [S] on the reaction rate $v$. Indicated are the parameters $K_m$ describing the enzyme's affinity for the substrate and the maximum reaction rate, $v_{max}$.

When the substrate concentration is small compared to $K_m$, i.e. $[S] \ll K_m$, then the reaction rate is a linear function of the substrate concentration, since equation [2.12] can be written as

$$v = \frac{k_{cat}[E][S]}{K_m} \; .$$ [2.14]

If now, we define a second order rate constant $k_2 = k_{cat}/K_m$, we can write a second order rate law for the reaction, namely

$$v = k_2 [\text{E}][\text{S}] . \qquad\qquad [2.15]$$

The second order rate constant $k_2$ has the units L s$^{-1}$ mol$^{-1}$, however, note that in the thesis at hand the enzyme concentration is given in mg mL$^{-1}$ and thus the resulting unit is L s$^{-1}$ g$^{-1}$.

At the other extreme, when [S]>>$K_m$, then equation [2.12] shows that the maximum reaction rate $v_{max}$ is obtained, as shown in Scheme 2.3.

**Temperature Dependence of the Rate Constant**

The temperature dependence of rate constants can be used to determine the activation energy of the examined reaction. Most reaction rates increase with temperature. However, for enzymatic reactions, an increase of the temperature can cause conformational changes that might decrease the enzyme activity and thus the reaction rate. In this case, the data must be looked at very carefully.

Arrhenius was the first to propose a relationship between the temperature and the rate constant in 1889, which showed that an increase of the temperature by 10 °C approximately doubles the reaction rate. The Arrhenius equation is

$$k = A \cdot e^{-\frac{E_a}{RT}} , \qquad\qquad [2.16]$$

so that plotting ln $k$ against $1/T$ gives the activation energy $E_a$ and the pre-exponential factor $A$. If the slope is very steep, the temperature has a very strong influence on the reaction rate and the activation energy is high. On the other hand, if the slope is approximately flat the activation energy is low.[Atkins 2005]

In 1935, Eyring presented the transition state theory, which is applicable in the gas phase and in solution.[Eyring 1935] This theory describes the approach of two reactants which leads to an increase of their potential energy until a maximum (the transition

state) is reached. In this region a so called "activated complex" is formed, which either gives the product or separates back into the reactants. It is important to note that such an "activated complex" should not be confused with reaction intermediates that can be isolated and studied; reaction intermediates are at local, but not global potential energy minima whereas activated complexes are at potential energy maxima. If we say that the activated complex $C^{\ddagger}$ is formed from reactants A and B ($A+B \rightleftharpoons C^{\ddagger}$) we can write for its equilibrium constant $K^{\ddagger} = [C^{\ddagger}]/[A][B]$. The Eyring equation is then given as

$$k = \kappa \frac{k_B T}{h} K^{\ddagger} \quad , \qquad\qquad [2.17]$$

where $k$ is the rate constant, $\kappa$ is the transmission coefficient (to take into account that not every activated complex forms a product) which is usually assumed to be one, $k_B$ is the Boltzmann constant, and $h$ is the Planck constant. The calculation of $K^{\ddagger}$ from this equation is not trivial, thus it is easier to use the thermodynamic parameters and discuss the reactions with their empirical values. We know that the equilibrium constant $K$ is related with the Gibbs energy $\Delta_r G^0$

$$-RT \ln K = \Delta_r G^0 \qquad\qquad [2.18]$$

so that we can also relate the equilibrium constant $K^{\ddagger}$ of the activated complex with the activation Gibbs energy $\Delta^{\ddagger}G$

$$-RT \ln K^{\ddagger} = \Delta G^{\ddagger} \Rightarrow K^{\ddagger} = e^{-\frac{\Delta^{\ddagger}G}{RT}} \; . \qquad\qquad [2.19]$$

If we now insert the expression for $K^{\ddagger}$ from equation [2.19] into the Eyring equation [2.17] we can write

$$k = \frac{k_B T}{h} e^{-\frac{\Delta^\ddagger G}{RT}} \, , \qquad\qquad [2.20]$$

and consequently replace the activation Gibbs energy $\Delta^\ddagger G$ with the activation enthalpy $\Delta^\ddagger H$ and the activation entropy $^\ddagger S$ ($\Delta^\ddagger G = \Delta^\ddagger H - T\Delta^\ddagger S$)

$$k = \frac{k_B T}{h} \cdot e^{\frac{\Delta^\ddagger S}{R}} \cdot e^{-\frac{\Delta^\ddagger H}{RT}} \, . \qquad\qquad [2.21]$$

To compare the activation energy $E_a$ with the enthalpy of activation $\Delta^\ddagger H$ we have to take the logarithm of equations [2.16] and [2.21] and differentiate with respect to temperature. Thus we obtain from equation [2.16]

$$\frac{\partial \ln k}{\partial T} = \frac{\partial \ln A}{\partial T} - \frac{\partial}{\partial T}\left(\frac{E_a}{RT}\right) = \frac{E_a}{RT^2} \, , \qquad\qquad [2.22]$$

and from equation [2.21] we obtain the expression

$$\frac{\partial \ln k}{\partial T} = \frac{\partial}{\partial T}\left(\frac{\ln k_B}{h}\right) + \frac{\partial \ln T}{\partial T} + \frac{\partial}{\partial T}\left(\frac{\Delta^\ddagger S}{R}\right) - \frac{\partial}{\partial T}\left(\frac{\Delta^\ddagger H}{RT}\right) = \frac{RT + \Delta^\ddagger H}{RT^2} \, . \qquad [2.23]$$

Comparing equations [2.22] and [2.23], the resulting definition of $E_a$ for reactions in solutions is then

$$E_a = RT + \Delta^\ddagger H \, . \qquad\qquad [2.24]$$

## Kinetics in Heterogeneous Systems

The analysis of enzymatic reactions with the Michalis-Menten theory has the advantage that the data collection is fast and the data analysis simple. However, this is only true for homogeneous aqueous solutions in which both enzyme and substrate are well dissolved. Considering the situation in a living cell, with the cytosol as an aqueous region which is crowded with macromolecules and other solutes and surrounded by a lipid bilayer, it is very clear that the difference to a diluted buffer solution is large.[Asaad 2003] In the cell, the enzyme must function with substrate accessibility, distribution, orientation, partitioning and exchange. This implies that the challenge is to define and characterise the steady-state conditions for the variables of the elementary events that make up the catalytic turnover. The partitioning of the substrate as well as the enzyme binding equilibria determine the kinetic path and influence the turnover rate.[Berg 2003] The use of multiphase systems has thus the advantage of better mimicking a living cell compared to a simple buffer solution. However, with multiphase systems, it is difficult to determine exactly the concentration, and possible diffusion limits for substrate or enzyme are not known precisely.

By way of an example, for interfacial enzymes the binding to the interface precedes the binding of the substrate. Furthermore, the density of the substrate molecules at the interface controls the substrate concentration dependence of the interfacial turnover cycle. Also the residence time of the enzyme determines the processivity of the successive turnover cycles. Finally, the substrate replenishment rate in the microenvironment of the bound enzyme has to considered, too.[Berg 2003] This shows the complexity of the interpretation of enzyme kinetics in heterogeneous systems, but one should keep in mind that this is the biophysical reality.

There have been many attempts to solve this problem with w/o-microemulsions both theoretically and experimentally to find the "true" kinetic parameters in such multiphase systems.[Bru 1990; Verhaert 1989] Two models have evolved one of which takes into account the total volume of the w/o-microemulsion to express the kinetic parameters. The other one, which is called the pseudophase model, refers only to the

volume of the water droplets to describe the enzymatic activity.[Verhaert 1989] For the pseudophase model, knowledge about the partitioning of both enzyme and substrate in the different phases is crucial. By way of an example, the substrate can be solely dissolved in the oil phase, it can be adsorbed at the interfacial layer or it can be partitioned between the oil and the aqueous phase, depending on its polarity.[Bru 1990] Thus, the partition coefficient of the substrate is important for the interpretation of the kinetics.

## 2.2.2 Enzymes

**Structure of Enzymes**

Enzymes are proteins which have essential functions in nearly all biological processes. They are very versatile and their function is strongly related to their structure. The wide range of different proteins is built from only 20 different amino acids as basic components. Amino acids possess a central carbon atom, to which an amino group, a carboxylic acid group, a hydrogen atom and a specific side chain is linked. The side chain differentiates the 20 amino acids. The side chain can be polar, non-polar or charged, can contain hydroxyl or thiol groups and thus determines the properties of the amino acid as well as the reactivity. The simplest amino acid which has a hydrogen atom as side chain (glycine) is the only amino acid that is achiral, all other amino acids are chiral. For building the proteins, interestingly, solely the L-isomer is used. At physiological pH, amino acids are zwitterionic molecules, as the amino group is protonated ($NH_3^+$) and the carboxylic group is deprotonated ($COO^-$). To describe the structure of proteins, one distinguishes between the primary, secondary, tertiary and quaternary structure of proteins.

The primary structure simply describes the sequence of amino acids that built a linear polymer, the so-called polypeptide. The carboxyl group of one amino acid binds to the amino group of the other amino acid and so on. This connection is named "peptide bond" and is kinetically stable against hydrolysis although not thermodynamically favoured. The polypeptide chain has a backbone made of repeating peptide bonds from which the side chains of the amino acids evolve. The

polypeptide backbone has remarkable capacities to form hydrogen bonds as it possesses both hydrogen donors and hydrogen acceptors. In general, proteins contain between 50 to 2000 amino acids, which form the peptide chain.[Berg 2007]

The secondary structure describes the spatial orientation of the peptide backbone. The polypeptide chain can fold into regular structures such as the α-helix, the β-sheet, the β-turn or random coil structures. An α-helix has a rodlike structure with a tightly coiled backbone in the inner part of the rod and the side chains pointing outward. The hydrogen bonds are formed characteristically between the carbonyl group of the first residue and the amide group of the fifth residue in the chain. This results in a compact structure where adjacent amino acids have a distance of 1.5 Å and where the radius of the rod is 2.3 Å (excluding side chains). Seen from the top, the α-helix forms a right-handed screw (left handed helices are very rare). As the amide groups of the backbone are already involved in intrachain hydrogen bonds, interactions of the helix with other peptide domains can only occur via its side chains. The α-helix is the preferred structure in non-polar solvents, but also amphiphilic helices exist, where one face of the helix is polar and the other one non-polar. The non-polar residues can interact with adjacent helices or with a membrane interface. A schematic view of an α-helix can be seen as the red parts in Figure 2.9.

The β-sheet structure is another periodic structure and is build from at least two polypeptide chains which are called β-strands. They form an extended structure with adjacent amino acids having a distance of 3.5 Å to each other and the side chains point in opposite directions. In a β-sheet two or more β-strands are linked via hydrogen bonds in a parallel or anti-parallel fashion. The main function of β-sheets is the stabilisation of proteins and protein complexes. An example of a parallel β-sheet (arrows point in the same direction) can be seen in yellow in the crystal structure of CalB in Figure 2.9.

A β-turn allows a protein to fold back on itself. For this purpose, the carbonyl group of residue *i* forms a hydrogen bond with the amino group of residue *i*+3. [Pelton 2000] An example is shown in Figure 2.9 in blue, on the outside of the protein. The absence of

any regular structure can be summarised as "random coil" structures, which are shown in green in Figure 2.9.
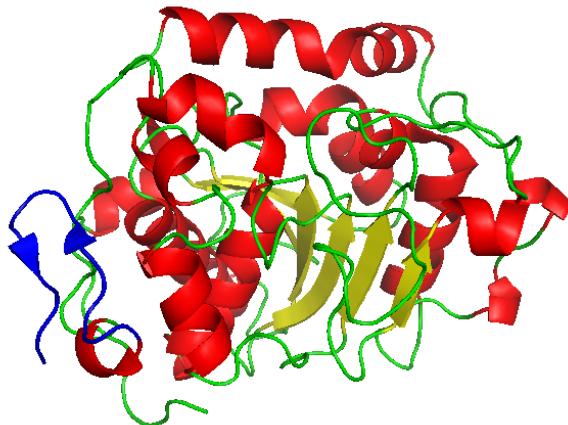


**Figure 2.9**: Crystal structure of the lipase B from *Candida antarctica* (PDB code: 1TCA,[Uppenberg 1994] resolution 1.55 Å) in the so-called "ribbon" representation. To see are many α-helices in red as well as a parallel β-sheet in yellow. One β-turn (blue) is also to distinguish on the outside of the protein.

The overall course of the peptide chain, the arrangement of the different secondary structures in a complex folding, is named the tertiary structure. Usually the protein is folded with very little space inside. In an aqueous environment, the non-polar residues are mainly hidden in the inner of the protein, while charged residues are located more on the surface of the protein. If the protein is part of a multi-subunit structure, then the spatial arrangement of these subunits is described by the quaternary structure. The simplest multi-subunit structure would be a dimer.[Berg 2007] An example for this would be the squalene-hopene cyclase, which crystal structure is shown in Section 2.2.4.

**Techniques to Determine the Structure of Enzymes**

To examine the structure of an enzyme, X-ray crystallography and nuclear magnetic resonance spectroscopy (NMR) have been proven extremely powerful. With X-ray crystallography the exact structure of an enzyme can be determined. The tertiary, secondary and sometimes even the primary structure can be resolved, where the ultimate resolution is determined by the degree of perfection of the crystal, which

leads typically to a resolution of about 2 Å for enzymes.[Berg 2007] When no crystals can be produced or additional information about the structure in solution is desired, two-dimensional NMR spectroscopy is a powerful tool to investigate the range of enzyme conformations adopted in solution. Due to the experimental observation of a large number of molecules in solution, the calculated structures represent a family of possible structures. However, the complexity of two-dimensional NMR spectra leads to the limitation that only enzymes up to 40 kDa can be analysed.[Berg 2007] The two techniques of X-ray crystallography and NMR were also combined successfully, e.g. in screening for drug discovery.[Jhoti 2007]

If there is no need for full characterisation of the enzyme, also spectroscopic methods, i.e. circular dichroism (CD) or fluorescence spectroscopy can be used to gain information about protein structures. The advantage of spectroscopic methods is their fast and easy application. By way of an example, the enzyme's folding properties and secondary structures can be investigated by CD spectroscopy. Especially changes of the enzyme's structure e.g. in different conditions or at different temperatures can be followed. Circular dichroism is the property of some materials, to absorb left and right handed circularly polarised light to a different extend. Circularly polarised light is created by superposition of two plane polarised waves that meet out of phase. The phase difference is 90° but amplitude and wavelength are the same. The planes of the two waves must be perpendicular to each other. Circularly polarised light can rotate either clockwise ($E_R$) or counter-clockwise ($E_L$) and is thus called right-handed or left-handed. However, CD can only be observed at wavelengths where the material absorbs light. The CD intensity can be thus reported as the differential absorbance of left and right circularly polarised light and can be written as

$$\Delta A = A_L - A_R .$$ [2.25]

Accordingly, the molar absorptivity ε can be used, which is expressed as

$$\Delta\varepsilon = \varepsilon_L - \varepsilon_R = \frac{\Delta A}{cd},$$

[2.26]

with $c$ being the molar concentration and $d$ the cuvette path length. However, in most cases, either for historical reasons or to avoid confusion with absorption spectroscopy, the ellipticity $\theta$ is plotted to present CD spectra. Ellipticity is given in degrees, where linear polarised light has 0°, left circularly polarised light +45° and right circularly polarised light -45°.[Kobayashi 2012] To convert the differential absorbance into ellipticity $\theta$ it holds that

$$\Delta A = \theta / 32.982 .$$

[2.27]

Due to the very small differences of ellipticity observed, $\theta$ is often given in mdeg, so that the denominator would become 32982, accordingly. The molar ellipticity $[\theta]_M$ can be calculated via

$$[\theta]_M = \frac{100\theta}{cd}$$

[2.28]

and has the unit deg cm$^2$ dmol$^{-1}$. Consequently, the molar absorptivity $\varepsilon$ and the ellipticity values can be converted into each other by

$$\Delta\varepsilon = [\theta]_M / 32982 .$$

[2.29]

The different regular secondary structures that occur in proteins give characteristic spectra as can be seen in Figure 2.10. The absorbance in this region (190-240 nm) is mainly due to the peptide bonds.[Kelly 2005]
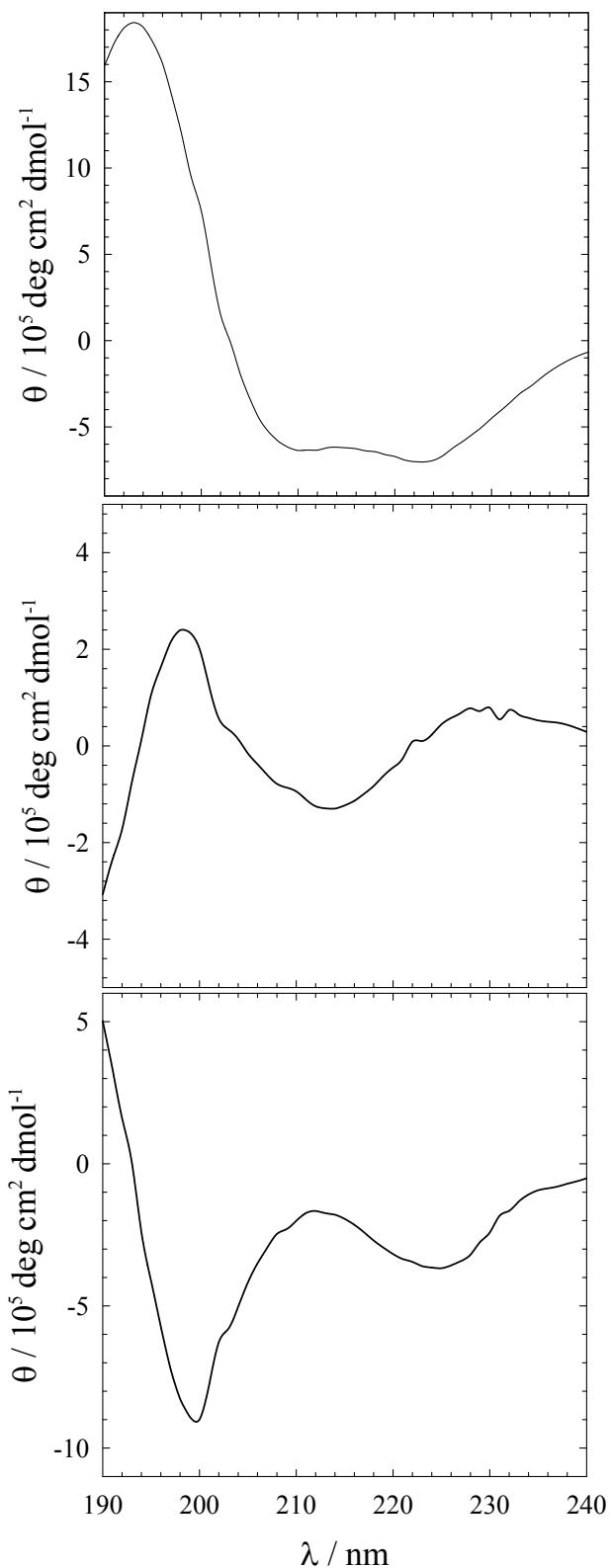
**Figure 2.10**: Characteristic CD spectra of three different model polypeptides containing α-helical structure (top), β-sheet structure (middle) or random coil structures (bottom). The spectra were provided by Prof. T. Jurkowski.

The α-helix structure is dominant in many proteins, with a typical negative peak which shows two bands at wavelengths of 222 nm and 208 nm. The peak at 222 nm can be assigned to the $n \rightarrow \pi^*$ transition, whereas the peak at 208 nm can be assigned to the $\pi \rightarrow \pi^*$ transition. Also a positive band at 192 nm is assigned for the $\pi \rightarrow \pi^*$ transition.

For the β-sheet structure an exact analysis is difficult as the structure is less defined and random coil structures give similar spectra. Usually, a negative peak is observed at around 215 nm which is due to the peptide $n \rightarrow \pi^*$ transition and a positive peak at around 195 nm as well as a negative peak at 175 nm which both correspond to a $\pi \rightarrow \pi^*$ transition. The β-turn structures can vary, as different conformations are available, namely eight different types have been identified. Some resemble a β-sheet, some resemble an α-helix, but the determination of a typical CD spectrum of β-turns is difficult. Note that for the determination of the proportion of the β-turn structure, infrared (IR) spectroscopy has proven more useful.[Kobayashi 2012]

The quantitative analysis of CD spectra is difficult for various reasons. Just like absorption spectra, CD spectra depend on the microenvironment of the residues. In addition, there are usually more structures in a protein than the well-known α-helix, β-sheet and β-turn. Single amino acids can also disturb the measurements because especially tyrosine, tryptophan and phenylalanine absorb strongly at wavelengths above 250 nm. However, CD is a useful technique to discover changes in the enzyme structure when observed in different experimental conditions,[Hammes 2005] e.g. different reaction media or microemulsions of different composition.

## 2.2.3  Lipases

Lipases are very versatile biocatalysts and are thus widely used in industry and research.[Gotor-Fernández 2006a; Jaeger 1999; Reis 2009; Soumanou 2013; Tan 2010] Under certain conditions, lipases catalyse transesterification reactions,[Santaniello 1993] Michael additions[Torre 2004] or ring-opening polymerisation reactions.[Córdova 1998] In fine chemical production, the formation of small chiral molecules, which are mostly used as

building blocks for the pharmaceutical industry, is probably one of the most important applications of lipases.[Breuer 2004] However, lipases are also useful biocatalysts for the asymmetric total synthesis of pharmaceutical products. A prominent example is Pregabalin, the active ingredient in a chronic pain relief drug, which is synthesised by introducing the main stereocenter by a lipase-catalysed kinetic resolution.[Martinez 2008] In addition, also for the production of nutritional products, like cocoa butter equivalent or margarine, where the products have to meet nutritional standards, the high selectivity of lipases is appreciated. Even for the production of bulk chemicals, lipases are widely employed, for example in washing powder to split and remove strains at low temperatures.[Hasan 2013] Moreover, the transesterification of triglycerides and alcohols to glycerol and biodiesel (fatty acid acyl esters), which is the most common way to produce biodiesel, can be catalysed by lipases.[Abbaszaadeh 2012] These examples show that lipases are already widely implemented in industrial processes due to their great selectivity in the production of fine chemicals as well as their robust and cheap application in bulk chemicals. Hence, being a widely used biocatalyst, lipases help to establish green chemistry in industry.[Biermann 2011]

To classify enzymes, the Enzyme Commission (EC) numbers were introduced to describe enzymes by the reaction they catalyse. Lipases have the Enzyme Commission number 3.1.1.3, as they belong to the class of hydrolases (EC 3), which act on ester bonds (3.1), more specifically on carboxylic ester bonds (EC 3.1.1), namely triacylglycerol lipases (EC 3.1.1.3). *In vivo*, they hydrolyse triglycerides at an oil-water interface[Reis 2009] and for this purpose possess a "lid", which opens in contact with a hydrophobic phase, e.g. the triglyceride, and covers the active site when no substrate is present.[Verger 1997] This phenomenon is called interfacial activation. In nature, lipases are responsible for food and fat degradation. The main function of the human pancreatic lipase is to digest dietary triglycerides. It hydrolyses the primary ester bonds of tri- and diglycerides, giving the less lipophilic products, fatty acids and 2-monoglycerides, the possibility to pass the intestinal barrier. Thus, the lipase acts in a hydrophilic environment, where the hydrophobic substrate forms a small oil droplet to protect itself from the hydrophilic environment.

In comparison, most lipase shows low activity towards monomerically solubilised substrates.[Jaeger 2002]

Although the sequences of lipases from different organisms can vary significantly, there are many similar features in the structures of lipases. The three-dimensional structure of most of the lipases has an amphiphilic peptide loop, which covers the active site during inactivity like a lid. When adsorbed at an oil-water interface, this lid undergoes a conformational change, opening the active site for the substrate. There is now a large hydrophobic surface around the active site, allowing the hydrophobic substrate to bind. The lid of the lipase can have different sizes. As regards the lipase B from *Candida antarctica*, only a small α-helix is moved during interfacial activation. Consequently, the conformational changes in the enzyme are very small.[Gruber 2012] Many lipases show a common architecture of predominantly parallel β strands surrounded by an α-helix. Since many hydrolases show the same pattern, they belong to the so called "α/β-hydrolase fold" family. In the active site of lipases, a catalytic triad composed of serine, histidine and aspartate can be found, which are involved in the catalytic mechanism of the hydrolysis. In some lipases, aspartate is replaced by glutamate. The reaction mechanism is shown in Scheme 2.4.

First, a carboxylate ester binds in the active site, where its carboxyl carbon atom is attacked by the nucleophilic hydroxyl group of the serine residue, which is activated by hydrogen bonds from the histidine and aspartate residues. Second, the resulting tetrahedral intermediate with the negatively charged oxyanion is stabilized in the characteristic "oxyanion hole". Third, the alcohol and the acylated enzyme are formed. Finally, the hydrolysis of the acylated enzyme gives the second product as a carboxylic acid and the enzyme in its original state, ready for the next catalytic cycle.[Schmid 1998]
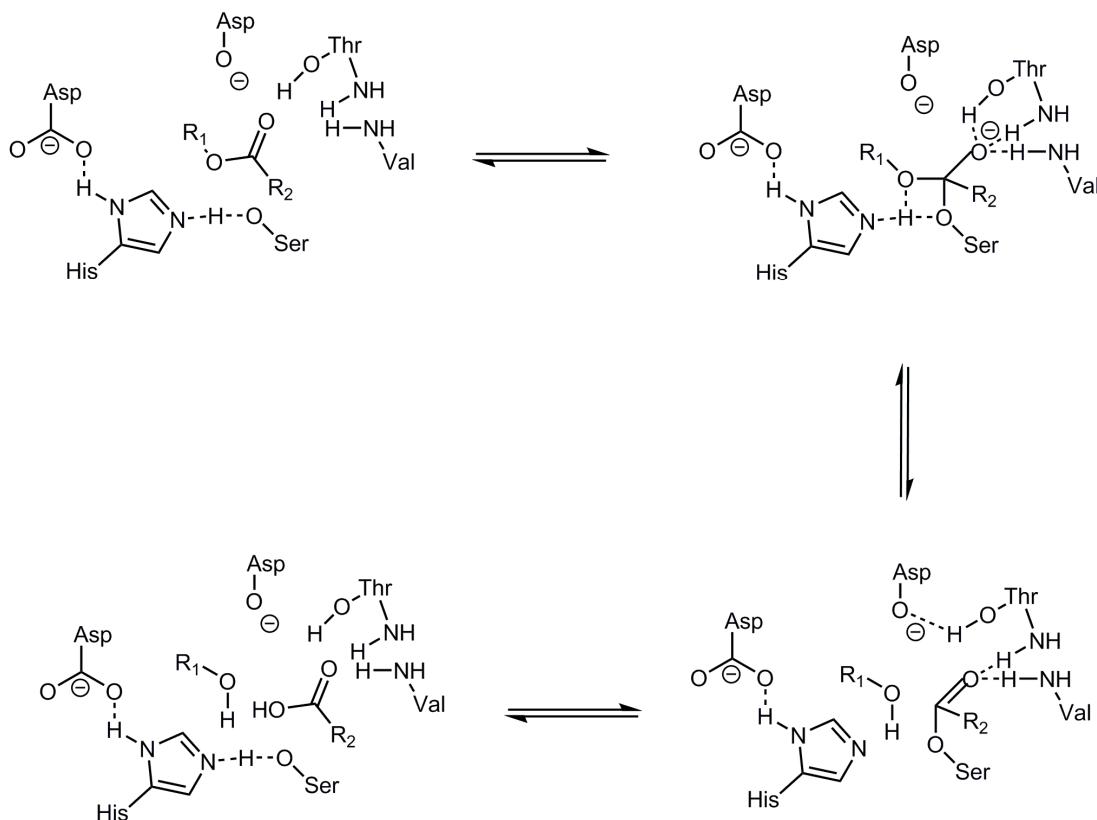
**Scheme 2.4**: Reaction mechanism of a lipase catalysed hydrolysis of a carboxylate ester into carboxylic acid and alcohol. The nucleophilic serine residue is activated by a hydrogen bond from histidine and aspartate residues. The tetrahedral intermediate is stabilized through an oxyanion hole, leading to the alcohol and the acylated enzyme. Hydrolysis of the enzyme gives the second product, the carboxylic acid.

In the work at hand, the lipase B from *Candida antarctica* (CalB) was chosen due to its conformational stability, its high stereoselectivity and its stability towards a wide range of temperatures and pH values. The lipase is expressed by the yeast *Candida antarctica* and is obtained in two different isoforms, A and B. The CalB is constituted of 317 amino acids and has a molecular mass of 33 kD.[Gotor-Fernández 2006b] The access to the active site is rather restricted, which can be the reason for the high stereoselectivity of this lipase.[Uppenberg 1994] It has been shown previously that mainly three residues are responsible for anchoring the CalB at an hydrophobic interface, which can be seen in Figure 2.11 (blue).

65
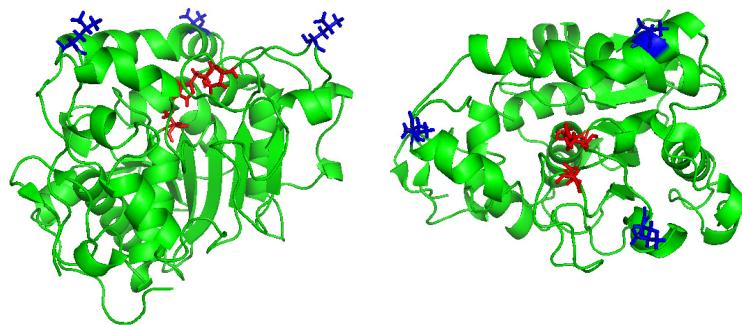
**Figure 2.11**: Crystal structure of CalB (PDB code: 1TCA,[Uppenberg 1994] resolution 1.55 Å) in the so-called "ribbon" representation. Seen in side view (left) and in top view (right), the active centre (red sticks) is surrounded by the residues Leu 147, Leu 219 and Val 272 (blue) which are responsible for anchoring the protein at an hydrophobic interface.[Gruber 2012] In the side view (left) one can see the three blue residues at the top form a plane which is then adsorbed at the oil-water interface.

The three residues surround the active site shown as red sticks (in Figure 2.11 (right)) and are coordinated in a plane (see in Figure 2.11 (left)). Upon binding on a substrate interface, it has been shown that there is a movement of an α-helix of 7.5 Å, compared to the crystal structure.[Gruber 2012] The movement of the α-helix, although being rather small, shows that even in the absence of a typical "lid", the binding process on an interface is well defined and thus necessary for the catalytic activity of the lipase.

## 2.2.4  Cyclases

Terpenoid cyclases catalyse some of the most complex reactions, namely the formation of cyclic terpenes from linear terpenes. The products are obtained in an astonishing precision with regards to both structure and stereochemistry.[Wendt 2005] To achieve these highly complex products from quite simple and flexible polyisoprenoid substrates, the active site is assumed to be a template which steers the reaction towards the desired product. The reaction starts upon formation of a highly reactive carbocation. Depending on their substrate size, cyclases are divided in groups. The ones converting monoterpenes (terpenes with 10 carbon atoms in their polyisoprene backbone $C_{10}$) are called monoterpene cyclases, the ones converting sesquiterpenes

(terpenes with 15 carbon atoms in their polyisoprene backbone $C_{15}$) are called sesquiterpene cyclases and consequently diterpene cyclases convert $C_{20}$ backbones, sesterterpene cyclases convert $C_{25}$ backbones and triterpene cyclases are converting terpenes with 30 carbon atoms in their polyisoprene backbone ($C_{30}$). To form the first carbocation two different approaches are used. Mono- and sesquiterpene cyclases use a metal-triggered departure of a pyrophosphate leaving group to form the carbocation, while triterpene cyclases use a protonation of the epoxide ring or a carbon-carbon double bond to create the carbocation.[Christianson 2006] For di- and sesterterpene cyclases, both pathways exist. Probably these different mechanisms are due to different level of reactivity of the substrates, for the shorter substrates, the formation of the carbocation requires more energy as the resulting carbocation is less stable then the ones formed from longer substrates due to more effective conjugation. Hence, cyclases can be divided in two groups, the class I cyclases for which the initiation step is ionization dependent and the class II cyclases for which the initiation step is protonation dependent.[Hammer 2013]

Interestingly, triterpene cyclases (class II cyclases) were recently found to act as general Brønsted acid catalysts and thus to be able to convert substrates with different functional groups including substrates that require pyrophosphate activation ($C_{10}$-$C_{20}$) in nature. By way of an example, the squalene-hopene cyclase from *Alicyclobacillus acidocaldarius* (Aac SHC), a triterpene cyclase whose crystal structure is well-known,[Siedenburg 2012; Wendt 1997] converts homofarnesol to ambroxan, a fragrance. The further evaluation of SHCs revealed the conversion of a wide range of substrates containing different types of terminal nucleophiles. From shortened and functionalised substrates cyclic ethers, lactones, and enol ethers were obtained, which demonstrates the ability of SHCs to catalyse a broad variety of cyclisation reactions with excellent stereoselectivities.[Hammer 2013; Seitz 2013] Another achievement in expanding the toolbox was a successful Friedel-Crafts alkylation catalysed by SHCs.[Hammer 2012] In summary, not only truncated squalene analogs ($C_{15}$-$C_{25}$) can be converted by triterpene cyclases, but also many alternative nucleophiles are accepted, so that this class of enzymes is highly promising for the use in organic synthesis.

The structure of squalene-hopene cyclase from *Alicyclobacillus acidocaldarius* was resolved in 1997 with a resolution of 2.9 Å. It is classified as isomerase (EC 5), more specifically as intramolecular transferase (EC 5.4), which transfers "other groups" (EC 5.4.99) and is named squalene-hopene cyclases with a resulting Enzyme Commission number of EC 5.4.99.17. The structure is shown in Figure 2.12.
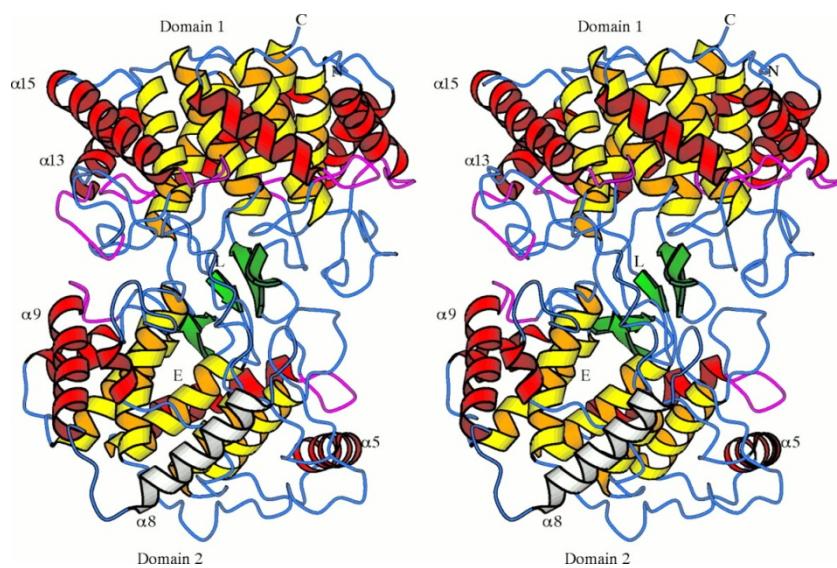


**Figure 2.12**: Structure of the squalene-hopene cyclase. The active site is near the β-sheet structures in green, the white α-helix anchors the enzyme in the membrane. The two α, α-barrel domains are shown in yellow and red (internal and external, respectively). The glutamine-tryptophan motifs are shown in purple, linking the α-helices of the α, α-barrel.

It was found as a dimeric enzyme, where each subunit consists of 631 amino acids and has a molecular weight of 72 kDa. Each subunit is organised in two domains that contain a 1200 Å$^3$ large cavity in between them. The domains form α, α-barrels of two concentric rings of parallel α-helices. Noticeable is the common motif of glutamine-tryptophan units that connect all outer helices and thus stabilise the whole protein. The large central cavity is the active site of the enzyme, which can be entered by a non-polar channel. The entrance of this non-polar channel is surrounded by a mobile and non-polar plateau, which is encircled by a ring of positively charged residues. This leads most probably to a non-polar plateau being plunged in the non-polar centre of a membrane, where the positively charged ring forms salt bridges with displaced phospholipid and sulfolipid head groups. This model characterise a monotopic membrane protein, i.e. a protein that penetrates but does not completely

68

pass through the bacterial membrane. Thus, the substrate squalene can diffuse from the inner of the membrane into the active site of the enzyme.[Wendt 1997]

*In vivo*, squalene-hopene cyclases catalyse the formation of hopanol and hopene from squalene, where five ring structures, 13 carbon-carbon bonds and nine stereocenters are formed.[Siedenburg 2012] Scheme 2.5 illustrates the reaction mechanism. It is assumed that squalene is already in a fixed conformation that facilitates the conversion to hopene. The reaction involves several carbocationic intermediates, where the first step is the protonation of squalene at C3 by base 1 ($B_1$), and the last step deprotonation at C29 catalysed by base 2 ($B_2$).
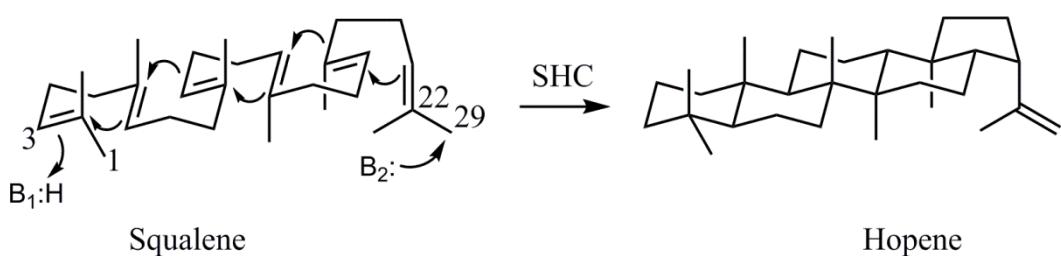


**Scheme 2.5**: The reaction mechanism of the SHC-catalysed conversion of squalene to hopene.

The enzyme catalysed squalene hopene conversion is one of the most complex enzymatic one-step reactions and not yet chemically feasible.[Siedenburg 2011] Hopanoids can adjust the properties of bacterial membranes as they are able to stabilise the lipid layers and to make them more rigid.[Ourisson 1987] They therefore have the same tasks as sterols in eukaryotic membranes, namely to inhibit gel phase formation and to order the lipids.[Sáenz 2012] More generally, in nature terpenoids are important for signalling, defense and communication, whereas in the chemical industry they can be used as chiral building blocks or as anti-cancer or anti-malaria drugs.[Seitz 2013]

In summary, this section showed that microemulsions have specific properties, which can be useful for enzymatic catalysis. They feature a large interfacial area as well as ultra-low interfacial tensions, which could facilitate the contact between a hydrophilic enzyme and a hydrophobic substrate. Additionally, many additives are tolerated in microemulsions and thus enzyme, substrate and any other required

additives for the reaction can be solubilised in the microemulsion, regardless of their polarity. A brief overview of reaction kinetics was given in the second half, together with some basics of enzyme structures and how to investigate the conformation of enzymes. Finally, the enzymes used in this work, namely the lipase B from *Candida antarctica* (CalB) and the squalene-hopene cyclase from *Alicyclobacillus acidocaldarius* (Aac SHC) were described in detail. Knowing the likely reaction mechanism, as well as the enzymes' natural environments, we can now start investigating enzymatic catalysis in the complex reaction media of bicontinuous microemulsions.

# 3 Activity of CalB in Bicontinuous Microemulsions

Enzyme catalysed biotransformations offer great potential due to high substrate specificity and high enantioselectivity as observed e.g for lipases.[Schmid 1998] As lipases convert *in vivo* substrates at an oil-water interface, in this study a bicontinuous microemulsion is investigated as a reaction medium. For the biocatalyst, the lipase B from *Candida antarctica* (CalB) was chosen, which is known to be a robust enzyme with high stereoselectivity and which is thus widely used in industry.[Anderson 1998] In the study at hand, the hydrolysis of *p*-nitrophenyl palmitate, -laurate and -caprylate (see Scheme 1.1) yielding the respective fatty acid and *p*-nitrophenol as products was used as a model reaction to investigate the CalB activity in the bicontinuous microemulsion. In the first part of this chapter the phase behaviour of microemulsions containing the reactants, as well as the partitioning of the reactants between the phases, is addressed. Special focus was set on clarifying the behaviour of *p*-nitrophenol in the microemulsion and the effect of the reaction media on the spectral properties of *p*-nitrophenol. The second part of the chapter deals with the influence of temperature, pH, ionic strength, substrate polarity and substrate concentration on the CalB activity, which needed to be studied to determine the optimum conditions. Interfacial tension measurements of diluted CalB solutions were carried out and correlated with the performed activity measurements. Also the impact of the composition of the interfacial film on the CalB activity was measured using two different co-surfactants, namely the phospholipid 1,2-dioleoyl-sn-glycero-3-phosphocholine (DOPC) and the sugar surfactant *n*-decyl-$\beta$-D-glucopyranoside ($\beta$-$C_{10}G_1$). Finally, the kinetics were analysed in terms of the Eyring theory by calculating the enthalpy, entropy and free energy of activation for each system.

## 3.1 Phase Behaviour of Microemulsions

The phase behaviour of microemulsions prepared with equal volumes of oil and water ($\phi = 0.5$) can be measured as function of the temperature $T$ and the surfactant mass fraction $\gamma$ (see Section 2.1). It is absolutely necessary to study the influence of substrate, product, and enzyme on the phase behaviour prior to the reaction. This

knowledge then allows one counteracting and thus preventing any changes of the phase behaviour, i.e. of the microstructure, during the reaction. The influence of CalB on the phase behaviour of the microemulsion system $H_2O$/NaCl (CalB) – *n*-octane – $C_{10}E_5$ was published previously by us and revealed that an increase of CalB concentration in the microemulsion system shifts the phase inversion temperature $\tilde{T}$ to lower values and on the other hand, $\tilde{\gamma}$ passes a minimum with increasing CalB concentration.[Subinya 2014b] The phase behaviour of the CalB containing microemulsions combined with the partitioning studies revealed that 80-90% of the CalB molecules are located at the interfacial layer while the rest is located in the microemulsions' water domain.[Subinya 2014b]

In the following, the influence of one substrate and two products on the phase behaviour of microemulsions containing buffer/4 wt% NaCl (*p*-nitrophenol) – *n*-octane (*p*-nitrophenyl palmitate/palmitic acid) – $C_{10}E_5$ is presented. By way of an example, the influence of *p*-nitrophenyl palmitate, *p*-nitrophenol and palmitic acid is shown in Figure 3.1.
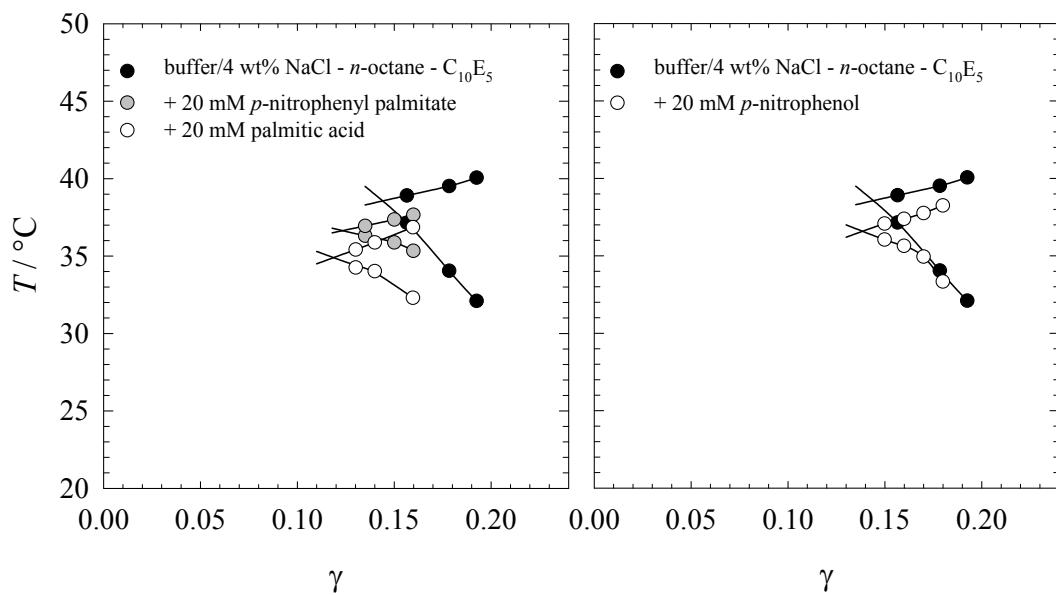


**Figure 3.1:** Phase diagrams near the *X*-point of microemulsions consisting of buffer/4 wt% NaCl – *n*-octane – $C_{10}E_5$ as a function of *T* and $\gamma$. Influence of the oil soluble additives *p*-nitrophenyl palmitate and palmitic acid (left) as well as of the water soluble additive *p*-nitrophenol (right). The oil to water ratio was kept constant at $\phi$ = 0.5 (figure taken from [Steudle 2015])

All additives were dissolved in the aqueous or in the oil phase of the microemulsion at a concentration of 20 mM. The oil soluble additives *p*-nitrophenyl palmitate and palmitic acid were found to shift the *X*-point of the microemulsion to lower phase inversion temperatures $\tilde{T}$ and lower surfactant mass fractions $\tilde{\gamma}$. This effect of polar oil additives on the phase behaviour is well-known and hence was expected.[Burauer 1999] The water soluble additive *p*-nitrophenol showed no effect on the efficiency of the microemulsions (i.e. on $\tilde{\gamma}$), while the phase inversion temperature $\tilde{T}$ decreased. In order to avoid changes in the microemulsions' composition during the reaction, the surfactant mass fraction and temperature was chosen such that the one-phase region is not left during the reaction. In other words, the reaction rate was determined from the first 20 minutes of the reaction to minimise the influence of the products on the phase behaviour. Additionally, by choosing a surfactant mass fraction which was high enough to overlap the one-phase regions of substrate-containing and CalB-containing microemulsions, changes of the phase behaviour during the reaction could be prevented. Whether the one-phase region was indeed not left was checked visually after each measurement.

**Partitioning of Substrates**

For a better understanding of the reaction kinetics of the CalB, the location of the substrates in the microemulsion was investigated. The aim was to facilitate the hydrolysis of a hydrophobic carboxylate ester, which was located in the oil domain of the microemulsion and could then be converted by CalB at the interfacial layer. To prove that the substrates were only located in the microemulsion's oil domain, samples were prepared in the three-phase region. The advantage of using a three-phase system is the fact that the compositions of oil and water excess phases can be approximated to be the same as the respective domains in the middle-phase microemulsion, which has a bicontinuous microstructure, because each component must have the same chemical potential at equilibrium. Therefore, a three-phase system was prepared and each of the phases was analysed by UV/Vis spectroscopy. The three-phase system was prepared with buffer/4 wt% NaCl – *n*-octane/5 mM substrate – $C_{10}E_5$ with a surfactant mass fraction of $\gamma = 0.08$.
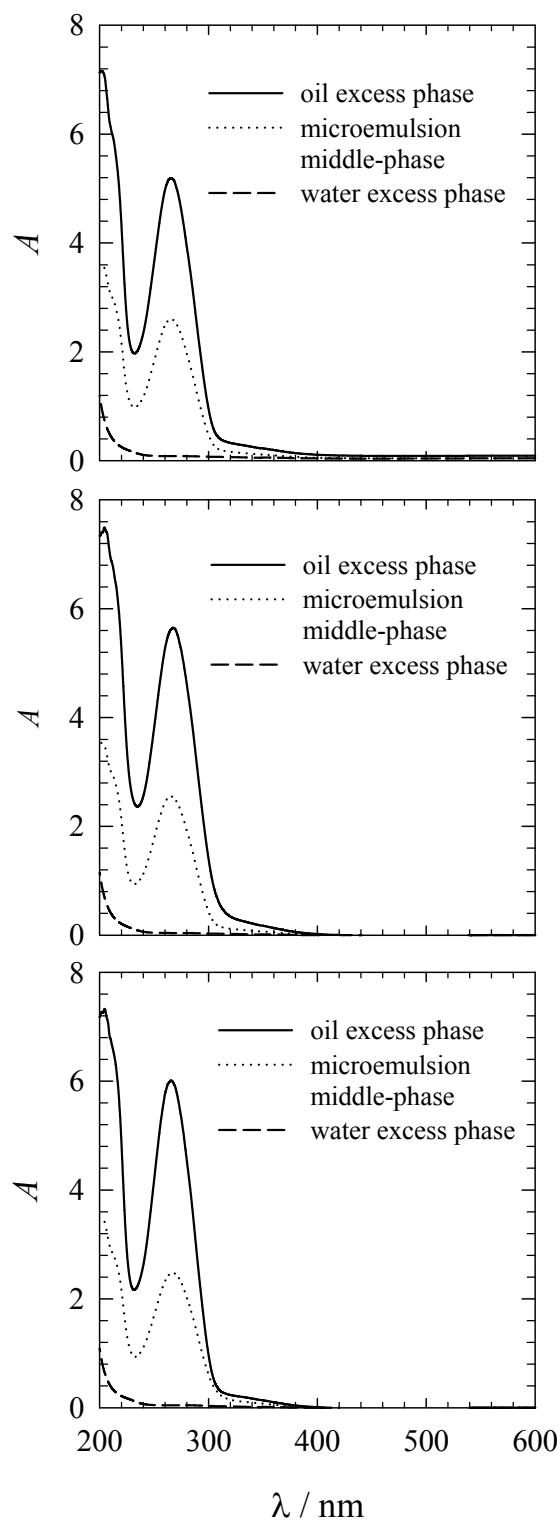
**Figure 3.2**: UV/Vis spectra of the individual phases of three-phase systems prepared at $\gamma$ = 0.08 and $\phi$ = 0.5. The samples consisted of buffer/4 wt% NaCl – $n$-octane/substrate – $C_{10}E_5$ and contained 5 mM $p$-nitrophenyl caprylate (top), 5 mM $p$-nitrophenyl laurate (middle) and 5 mM $p$-nitrophenyl palmitate (bottom) in the oil phase (figure taken from [Steudle 2015], modified).

Figure 3.2 shows the spectra of *p*-nitrophenyl caprylate, *p*-nitrophenyl laurate and *p*-nitrophenyl palmitate in the oil excess phase, the microemulsion middle-phase and the water excess phase. The oil excess phase shows in all cases the highest absorbance, and it thus can be concluded that the substrates are mainly dissolved in the oil domain. The water excess phase did not show any absorbance indicating negligible amounts of substrate in the water domain of the microemulsion. The microemulsion phase showed about half the absorbance of the oil excess phase because the volume fraction of oil is only 50 % ($\phi = 0.5$). Additionally, the wavelength of the maximum absorbance remained at 267 nm for all spectra which is the same as observed for the stock solutions of the substrates (substrate in *n*-octane), indicating that the polarity of the environment did not change. To conclude, the substrates are mostly located in the oil phase of the microemulsion.

**Acid-Base Behaviour of *p*-Nitrophenol**

To understand the behaviour of the weak acid *p*-nitrophenol in the microemulsion, first the location of the *p*-nitrophenol was determined in the same way as described above for the substrates. A three-phase system with the composition buffer/4 wt% NaCl/2 mM *p*-nitrophenol – *n*-octane – $C_{10}E_5$ was prepared at $\gamma = 0.08$ and pH 7 and was then equilibrated at the phase inversion temperature. The separated phases were analysed by UV/Vis spectroscopy and the resulting spectra are shown in Figure 3.3 (left). Comparing the three spectra one can see that only the microemulsion middle-phase shows a distinct peak, which appears at 314 nm. Both water and oil excess phase do not absorb in the relevant region, thus there are negligible amounts of *p*-nitrophenol in these two phases. Hence, the *p*-nitrophenol is located at the interfacial layer of the microemulsion. It is noteworthy that only *p*-nitrophenol (absorbing at 314 nm) and no *p*-nitrophenolate (absorbing at around 400 nm) is present in the sample. In aqueous solutions at pH 7, the majority of *p*-nitrophenol is deprotonated and thus absorbs at around 400 nm as *p*-nitrophenolate. To conclude, the *p*-nitrophenol is located at the interfacial layer of the microemulsion and is not deprotonated at all, which is contrary to the situation in the bulk aqueous solution at pH 7. Fernandez et al. investigated in detail the behaviour of chromophores at interfaces. They found that essentially two components are responsible for the

observed changes between the behaviour in the aqueous phase and the micelles, namely (1) an electrostatic potential contribution (a shift of "local pH") and (2) a pKa shift in which the nature of the interface has to be considered.[Fernandez 1977]

To further study and quantify the different behaviour of *p*-nitrophenol in aqueous solutions and the microemulsion, the dissociation constant (pKa) of *p*-nitrophenol was measured in aqueous buffer solution and in a three-phase system. The pKa can be used to classify acids according to their acidity. The pKa value indicates, at which pH value exactly the same amount of non-dissociated and dissociated species is present. Stronger acids have therefore smaller pKa values than weaker acids. Apart from the acidity of the molecule, the pKa value can also depend on the environment of the molecule, which can influence its tendency to dissociate by stabilising one or the other species. For this purpose, *p*-nitrophenol solutions in buffer solutions of pH 4-9 were prepared and their UV/Vis spectra measured. Then, these solutions were used to prepare the three-phase systems that were equilibrated and the phases separated. The spectra of the middle-phase microemulsions were measured and all of them were overlapping at the isosbestic point. This is important as it indicates that the concentration of *p*-nitrophenol is not changing at any pH value and thus the *p*-nitrophenol is located at the interfacial layer of the microemulsions at all pH values. To calculate the pKa of *p*-nitrophenol in this system, the absorbance values at $\lambda_{max}$ of the *p*-nitrophenolate (392 nm) were taken at the different pH values and the data were fitted to the equation

$$A_{obs} = \frac{A_{min} \cdot 10^{-pH} + K_a \cdot A_{max}}{10^{-pH} + K_a},$$ [3.1]

from which the pKa can be easily calculated as the negative common logarithm of $K_a$. The same was done for *p*-nitrophenol in buffer solution and in buffer solutions + 4 wt% NaCl. The data points, as well as the fitted curves, are shown in Figure 3.3 (right). For the buffer solution, a pKa value of 7.2 was obtained at 37 °C which is in line with literature values, the addition of 4 wt% NaCl slightly decreases the pKa to 7.1 and for the microemulsion a significant increase of the pKa to 8.2 was observed. Comparing the data of *p*-nitrophenol with the corresponding pKa values, one can

readily say in a qualitative way that the lower the *p*-nitrophenolate peak at pH 7, the more the $pK_a$ is shifted to higher values.
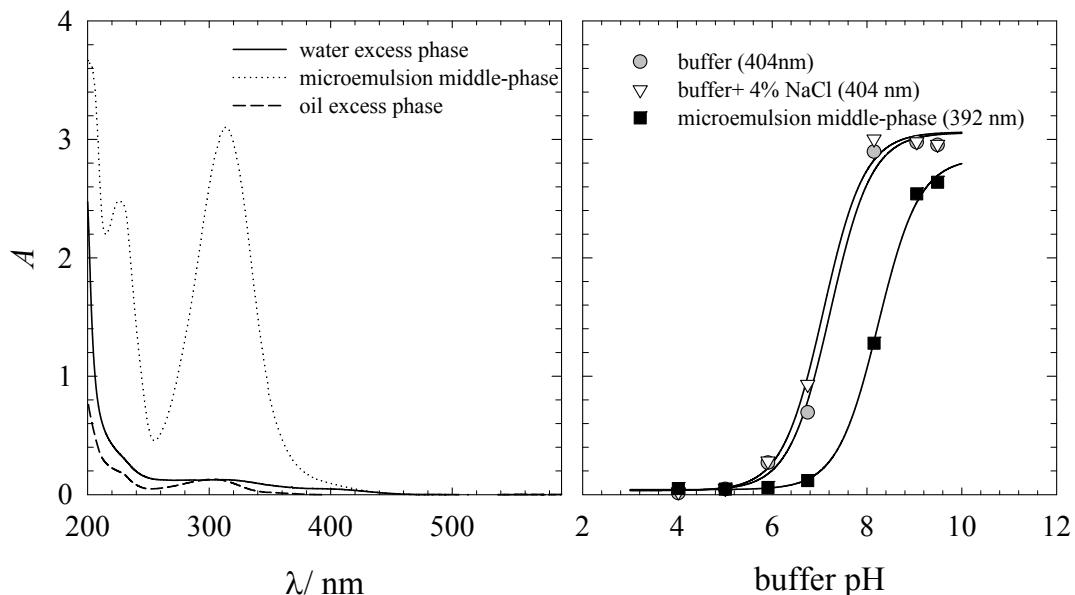


**Figure 3.3**: (left) UV/Vis spectra of the individual phases of a three-phase system containing *p*-nitrophenol at pH 7. The samples consisted of buffer/4 wt% NaCl/2 mM *p*-nitrophenol – *n*-octane – $C_{10}E_5$ and were prepared at $\gamma = 0.08$ and $\phi = 0.5$. (right) Absorbance at $\lambda_{max}$ of *p*-nitrophenolate dissolved in buffer, buffer + 4 wt% NaCl and middle-phase microemulsions against the pH. The points are fitted to equation [3.1] to give the $pK_a$ of *p*-nitrophenol in the different systems. Note that in the middle-phase microemulsions, *p*-nitrophenolate absorbtion is only observed at buffer pH values greater than 7.

As mentioned previously, two components can be the reason for this $pK_a$ shift, either local pH changes near the interfacial layer of the microemulsion where *p*-nitrophenol is located or an influence of the nature of the interface leading to the $pK_a$ shift. In the literature, a similar phenomenon observed in w/o-microemulsions was explained by the presence of *p*-nitrophenol near the interfacial layer - as observed in our system - and the higher hydrogen bond donor capacities from the highly structured hydration shell of the surfactant monolayer.[Oldfield 1990] The presence of the numerous hydrogen bonds between water molecules and surfactant molecules could hinder the deprotonation of *p*-nitrophenol when it is adsorbed at the interfacial layer. In the same time, the *p*-nitrophenol in its protonated state is stabilised by the surrounding water molecules, forming hydrogen bonds with both surfactant molecules and *p*-nitrophenol. In aqueous-organic solvent mixtures, the same effect can be observed,

probably also due to the presence of hydrogen bond donors. If this explanation is also valid for the study at hand, the effect should be much stronger when using surfactants with increasing number of ethylene glycol groups $j$, as they will be able to form increasing number of hydrogen-bonds with the surrounding water molecules.

To investigate this we can use data from the isosbestic points determined for the analysis of the kinetic studies in Section 3.2. For accurate data treatment, the isosbestic point of each system had to be determined by taking spectra at pH 7, 8 and 9 from microemulsions containing $p$-nitrophenol and prepared at $\gamma_{Reaction}$ (see Section 6.5 for details). Thus we can compare the spectra for each pH value for different surfactants, namely with increasing $j = 4$, 4.5, 5 and 5.5, which are shown in Figure 3.4.

Indeed, the results show that with increasing $j$, the amount of $p$-nitrophenolate present in the microemulsion decreases. Whereas at pH 7 the differences are still small, the decrease of $p$-nitrophenolate absorption is clearly to see at pH 8 and pH 9. With the knowledge from the $pK_a$ measurements, it can be expected that the significant decrease of $p$-nitrophenolate formation results in even higher $pK_a$ values if one increases the number of ethylene glycol groups of the head group. From these findings one can conclude that the increased $pK_a$ value of $p$-nitrophenol in microemulsions is mainly caused by to the higher hydrogen bond capacity near the interfacial layer, which is caused by the hydration shell of the surfactant and the nearby organic solvent. Thus, the contribution of a significant local pH change is negligible.
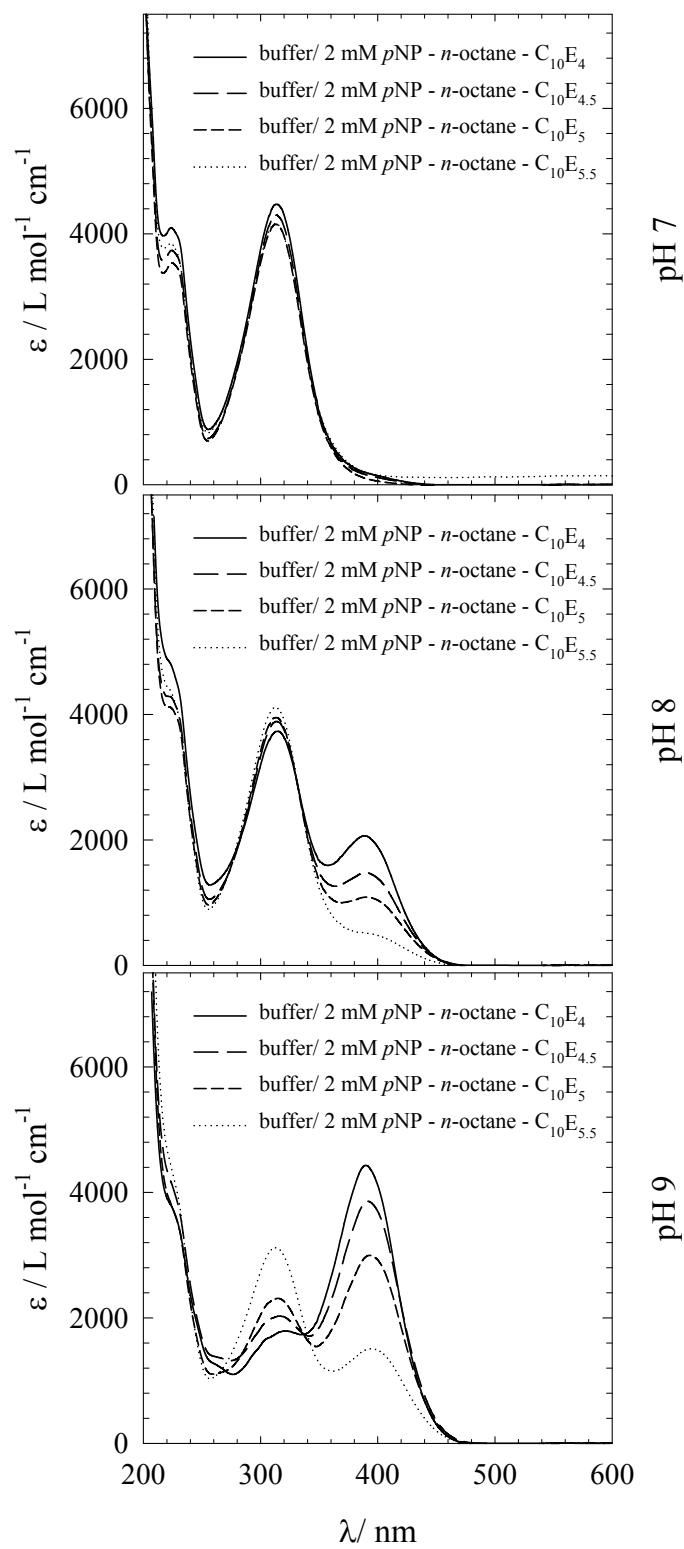
**Figure 3.4**: Spectra of *p*-nitrophenol in microemulsions of the composition buffer/*p*-nitrophenol – *n*-octane – $C_{10}E_j$, with *j* = 4, 4.5, 5, 5.5 at pH 7, 8, and 9 at the respective phase inversion temperatures $\tilde{T}$. The data is corrected with path length and concentration, so that the molar absorptivity ε is plotted instead of the absorbance.

## 3.2 Key Parameters of the CalB Activity

**Effect of pH of the Aqueous Phase on the CalB Activity**

The pH is known to influence largely the properties of enzymes - especially the activity - due to the protonation and deprotonation of amino acids, which is also related to the overall charge of the protein. For lipases, maximum activity is usually reported for pH values between 7-8, but also lower pH values are reported for special conditions, e.g. in o/w-microemulsions.[Valis 1992] To determine the optimum pH value (which refers throughout the work to the pH of the buffer solution used to prepare the microemulsion) for the CalB-catalysed hydrolysis of *p*-nitrophenyl palmitate, a range of pH 4 to pH 8 was investigated. To prepare the buffer solutions, different buffer salts had to be used, namely sodium acetate buffer for pH 4-5, MES buffer for pH 5-7, and TRIS buffer for pH 7-8.

Figure 3.5 shows a bell-shaped relationship between the catalytic activity of CalB in bicontinuous microemulsions and the pH-value of the aqueous solutions. The highest catalytic activity occurs at pH = 5.5 in contrast to aqueous systems, where CalB was found to display its highest activity at pH values around 7.[Anderson 1998] Of particular interest in the study at hand is the sudden increase of activity when the reaction is carried out at pH values above the isoelectric point, which has been determined by isoelectric focusing to be pH 5.2. The isoelectric point is defined as the pH at which the net charge of the enzyme is zero. Possible explanations for the differences in pH optimum found for CalB in aqueous systems and microemulsions could be differences of the local pH at the interfacial layer, differences in adsorption behaviour of differences in the enzyme's conformation. From the studies of the acid-base behaviour of *p*-nitrophenol in bicontinuous microemulsions the main outcome was that the pH value at the interfacial layer differs not significantly from the pH value in the aqueous phase of the microemulsion. Thus, differences in the local pH near the interfacial layer would not explain the found difference. To investigate the adsorption behaviour and the CalB conformation at different pH values, CD

measurements of three-phase systems containing CalB which were prepared with aqueous phases of different pH values were carried out.[Subinya 2015]
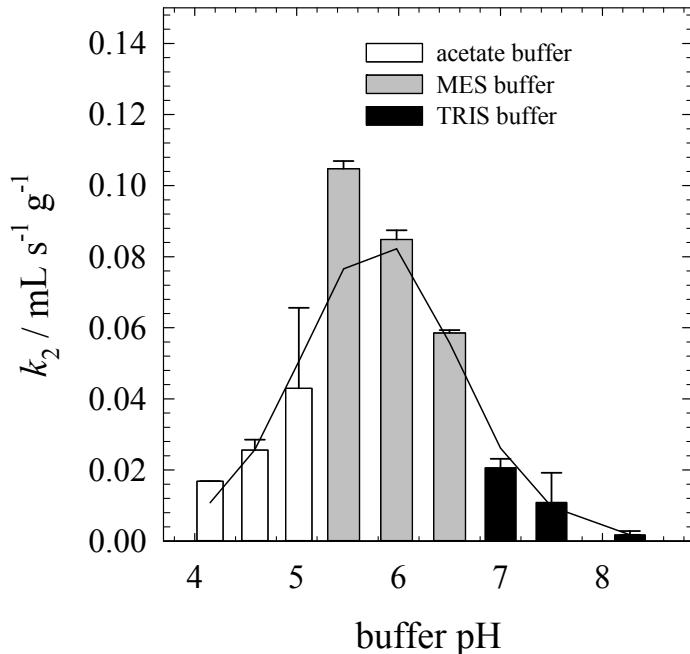


**Figure 3.5**: Observed second order rate constant $k_2$ of the CalB-catalysed hydrolysis of *p*-nitrophenyl palmitate as a function of the pH-value of the aqueous phase. Samples were prepared at $\phi = 0.5$, $\gamma = 0.17$, $\varepsilon_{NaCl} = 0.04$, $c_{substrate} = 5$ mM, $c_{CalB} = 3$ mg mL$^{-1}$ and different pH-values in the aqueous phase from pH 4 to pH 8. The observed second order rate constants are normalised to the values obtained in TRIS buffer (figure taken from [Subinya 2015])

The CD measurements showed a maximum of the α-helix content for the CalB molecules which are adsorbed at the interfacial layer at pH 5.[Subinya 2015] Most probably the pH value of the aqueous phase influences the adsorption behaviour of CalB, which in turn results in different preferred conformation at the interfacial layer. Thus, the observed bell-shaped relationship could be rationalized by (1) the global conformation of CalB, *i.e.* the loss of the α-helix structure[McCabe 2005] and (2) the ionisation state of the ionisable residues on the protein-membrane interface leading to more efficient adsorption at the interfacial monolayer. Because the substrate is water insoluble and resides in the hydrophobic phase, the more efficiently the protein is adsorbed at the interface, the easier it gets access to the substrate. In other words, pH dependent changes in adsorption efficiency could be the reason for the observed

changes of the CalB activity. A higher α-helix content could be caused by higher adsorption of CalB at the interfacial monolayer during which some of the protein loops that are facing the interface get organized. Additionally, at the isoelectric point the protein has no net charge, and usually the maximum adsorption from aqueous solution is observed at such conditions because a net charge leads to electrostatic repulsion that limits the interfacial packing density.[Secundo 2008]

Furthermore, the pH dependent activity data was fitted to a model which takes into account two protonable residues. The data was best fitted with $pK_a$= 6.2 and 5.4 (Figure 3.5) for these residues. The catalytic triad of CalB consists of Serine-Histidine-Aspartate, of which Histidine and Aspartate can be protonated. Based on the published crystal structure of CalB (PDB: 1TCA[Uppenberg 1994]) we have predicted the $pK_a$ values for these catalytic residues using the H++ server.[Anandakrishnan] The predicted $pK_a$ values for catalytic Aspartate (pH < 0) and Histidine (pH >12) indicate that these residues do not change the protonation state in the studied pH range and therefore cannot account for the observed pH dependent activity change. This finding supports again the argument that the bell-shaped dependency between activity and pH-value is mainly due to the change of the interfacial adsorption density which passes a maximum and which is accompanied by a respective change of the α-helix content.[Subinya 2015]

**Effect of Temperature and NaCl Content on the CalB Activity**

Temperature and ionic strength are known to influence enzymatic activities. Kinetic measurements over a range of temperatures or at different salt contents can clarify the enzyme's optimal reaction conditions. To independently study the effect of temperature and NaCl content, ε, on the CalB activity in bicontinuous microemulsions, the hydrophilicity of the surfactant was changed such that different phase inversion temperatures at constant ε, as well as similar phase inversion temperatures at different ε, are accessible.

The influence of the NaCl content, ε, on the CalB activity was studied first. For NaCl contents of ε = 0, ε = 0.04, ε = 0.11 and ε = 0.18 in the aqueous phase of the

microemulsion, the hydrophilicity of the surfactant was increased stepwise by so that phase inversion temperatures around 36 °C were obtained (see Table 3.1). Phase diagrams of microemulsions which consisted of buffer/NaCl – *n*-octane/5 mM *p*-nitrophenyl palmitate – $C_{10}E_j$ were measured and then the CalB activity in the respective microemulsion was determined. The γ used for the reactions was $\gamma_{Reaction} = \tilde{\gamma} + 0.02$ for $\tilde{\gamma}$. The CalB activities are given as observed second order rate constants $k_2$, which were calculated from the slope of the initial reaction rate after 20 minutes of reaction. The results are summarized in Table 3.1, where the *X*-point of the phase diagrams are given for each NaCl content, together with the observed second order rate constants $k_2$.

**Table 3.1**: *X*-points ($\tilde{\gamma}$, $\tilde{T}$) of systems consisting of buffer/NaCl – *n*-octane/5 mM *p*-nitrophenyl palmitate – $C_{10}E_j$. For each system, the salt content ε and the number of ethylene glycol groups *j* is indicated. The CalB activity in each system is given by the observed second order rate constant $k_2$.

| *j* | ε | $\tilde{\gamma}$ | $\tilde{\gamma}_{Reaction}$ | $\tilde{T}$ / °C | $k_2$/ $10^{-3}$ L s$^{-1}$ g$^{-1}$ |
|-----|------|-------|-------|----|------------------|
| 4.5 | 0    | 0.121 | 0.141 | 34 | 0.0817±0.0064 |
| 5   | 0.04 | 0.128 | 0.148 | 36 | 0.0610±0.0014 |
| 6   | 0.11 | 0.156 | 0.176 | 37 | 0.0074±0.0004 |
| 7   | 0.18 | 0.159 | 0.179 | 35 | 0.0033±0.0002 |

As one can see, the observed second order rate constant $k_2$ decreases significantly with increasing NaCl concentrations and thus the addition of NaCl was avoided wherever possible. One also sees that the γ-values and thus the $\gamma_{Reaction}$-values shift towards slightly higher values with increasing NaCl concentration. To test whether changes of the surfactant mass fraction γ influence the CalB activity we run reactions in a range from $\gamma_{Reaction} = \tilde{\gamma} + 0.01$ to $\gamma_{Reaction} = \tilde{\gamma} + 0.05$. Since we found no differences in the activity we can readily say that the $k_2$ values reflect the dependence on the NaCl concentration.

To study the effect of temperature on the CalB activity, all samples were prepared without NaCl ($\varepsilon = 0$). The studied systems consisted of buffer – $n$-octane/5 mM $p$-nitrophenyl palmitate – $C_{10}E_j$ with $j = 4$, 4.5, 5 and 5.5 ($j = 4.5$ means a 1:1 mixture of $C_{10}E_4$ and $C_{10}E_5$). The respective phase diagrams are presented in Figure 3.6 (left), where the surfactant mass fractions used for the reaction $\gamma_{Reaction}$ are also indicated. The phase diagrams are shifted such that measurements at $T = 23$ °C, 34 °C, 44 °C and 51 °C could be carried out. As mentioned above the slight changes of $\tilde{\gamma}$ do not influence the activity.
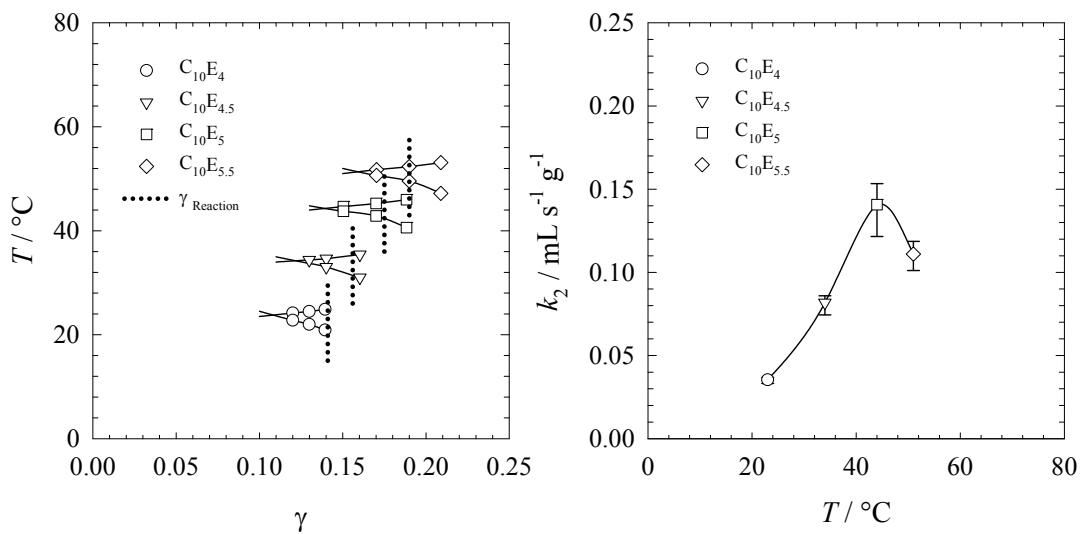


**Figure 3.6:** (left) Phase diagrams of microemulsions consisting of buffer – $n$-octane/5 mM $p$-nitrophenyl palmitate – $C_{10}E_j$ with $j = 4$; 4.5; 5; 5.5. The oil to water ratio was kept constant at $\phi = 0.5$. The phase inversion temperature $\tilde{T}$ and the surfactant mass fraction $\gamma_{Reaction} = \tilde{\gamma} + 0.02$ were used for the kinetic measurements. (right) Influence of the temperature on the CalB activity measured in the respective microemulsions (figure taken from [Steudle 2015]).

In Figure 3.6 (right), the observed second order rate constants $k_2$ for each temperature are shown. The CalB activity shows a bell-shaped dependence from the temperature which is well known from enzyme-catalysed reactions. This shape is explained by the increase of the reaction rate with temperature as described by Arrhenius, which is counteracted by the thermal deactivation of the enzyme at higher temperatures. The maximum CalB activity was found in the microemulsion prepared with buffer – $n$-octane/5 mM $p$-nitrophenyl palmitate – $C_{10}E_5$ at $\tilde{T} = 44$°C and $\gamma_{Reaction} = 0.175$.

Consequently this system was chosen to be the model system for the following studies wherever possible and feasible.

It can be concluded that CalB activity in bicontinuous microemulsions is affected by both NaCl content and temperature. The addition of NaCl decreases the enzymatic activity because it changes the ionic interaction. These changes could decrease the adsorbed amount of CalB molecules at the interfacial layer or affect the CalB conformation. The decrease of the amount of adsorbed lipase molecules at interfaces by increasing the NaCl content has been reported for different systems, such as a membrane reactor system[Pronk 1992] and a two-phase system.[de Souza 2010] In order to investigate if the NaCl content is influencing the activity of CalB in a two-phase system, we carried out a reaction in a two-phase system containing a stock solution of substrate in *n*-octane and a buffer solution with either 0 wt%, 4 wt% or 18 wt% NaCl. The results clearly showed a decrease of the obtained yields when analysed after 24 h, as illustrates Figure 3.7 (left). Due to the fact that in the two-phase system the only possible contact between enzyme and substrate is at the macroscopic interface, desorption of CalB from this macroscopic interface could explain the observed trend. As regards the influence of the NaCl content on the conformation of CalB, CD measurements in aqueous solutions showed no changes of the secondary conformation of CalB, as shown in Figure 3.7 (right). Nevertheless, it is possible that the conformation of the CalB molecules, which are adsorbed at the interfacial layer, are more sensitive to unfavourable ionic interactions.

The relation between temperature and CalB activity revealed a maximum CalB activity at 44 °C, which is higher than in conventional reaction media. For instance, in aqueous solution the maximum activity of a mixture of CalA and CalB is at 35 °C.[Adamczak 2003] An enhancement of the thermostability of lipases was previously reported for lecithin reverse micelles and was explained with a different water activity.[Chen 1993] This finding is supported by studies which showed that in systems containing organic solvents and only small amounts of water good lipase activity was observed at temperatures up to 100 °C.[Zaks 1984] The reason for the enhanced thermostability was explained by the increased rigidity of the enzyme due to the lack of water molecules. Similarly, reduced water content in the surrounding of CalB

adsorbed at the interfacial layer of the bicontinuous microemulsion could explain the slightly higher optimum temperature.
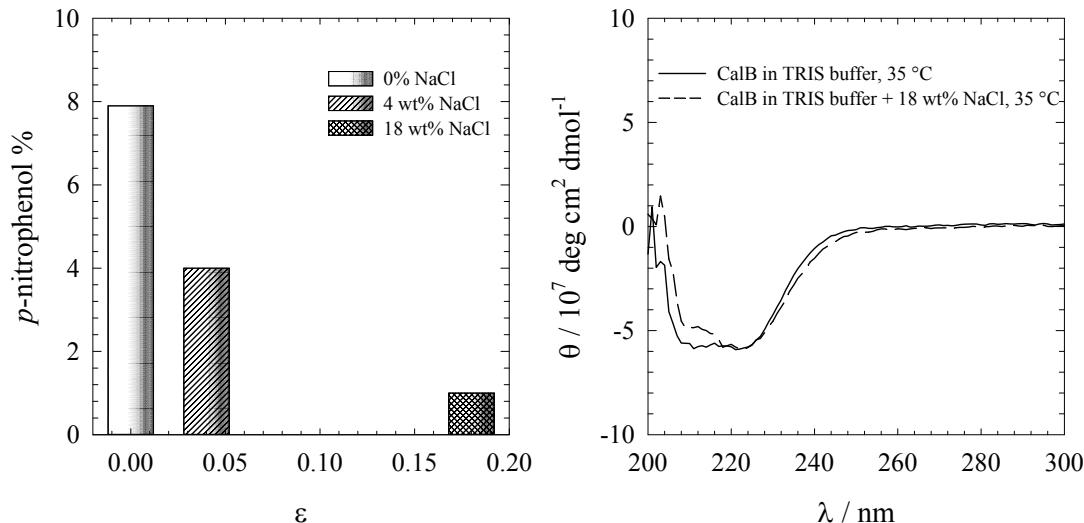


**Figure 3.7**: (left) Hydrolysis of *p*-nitrophenyl palmitate in a two-phase system containing buffer and 5 mM *p*-nitrophenyl palmitate in *n*-octane. The CalB concentration was 6 mg mL⁻¹. The two phases were separated after 24 h and the aqueous phase was analysed by UV/Vis measurements to give the final yield after 24 h. (right) CD spectra of CalB-containing solutions with either 0 wt % or 18 wt% NaCl in the buffer solution (figure taken from [Steudle 2015]).

**Influence of the Substrate's Chain Length and Concentration on the CalB Activity**

In order to find out whether the length of the alkyl chain and the concentration of the substrate influence the CalB activity, the hydrolysis of substrates with different chain lengths were investigated. Moreover, the concentration dependence was studied for one of them. Three substrates were tested, namely *p*-nitrophenyl palmitate, *p*-nitrophenyl laurate, and *p*-nitrophenyl caprylate and *p*-nitrophenyl laurate was used to study the CalB activity at different substrate concentrations. The reactions were carried out in microemulsions at 44 °C which consisted of buffer – *n*-octane/substrate – $C_{10}E_5$ ($\gamma_{Reaction}$ = 0.175) which we have identified to be the most promising system regarding the activity of CalB. Phase diagrams containing 5 mM of the different substrates did not show any differences, as can be seen in Figure 3.8 (left). Figure 3.8 (right) shows the amount of *p*-nitrophenol formed over time for each substrate.

The reactions were followed until completion to detect any inhibitory effects that could be caused by substrates or products. The yield obtained after 10 h showed a clear dependency on the substrate chain length, with 75% for *p*-nitrophenyl caprylate, 80% for *p*-nitrophenyl laurate and 90% for *p*-nitrophenyl palmitate. However, the observed second order rate constants $k_2$ were found to be similar, namely $0.14 \cdot 10^{-3}$ L s$^{-1}$ g$^{-1}$ for *p*-nitrophenyl caprylate, $0.17 \cdot 10^{-3}$ L s$^{-1}$ g$^{-1}$ for *p*-nitrophenyl laurate, and $0.13 \cdot 10^{-3}$ L s$^{-1}$ g$^{-1}$ for *p*-nitrophenyl palmitate. The observed second order rate constants $k_2$ were calculated from the initial rates obtained during the first 20 minutes of the reaction, for details see Section 6.5. Thus any inhibition which occurs at a later stage of the reaction (at $t \gg 20$ min) is not reflected by the observed second order rate constant $k_2$.
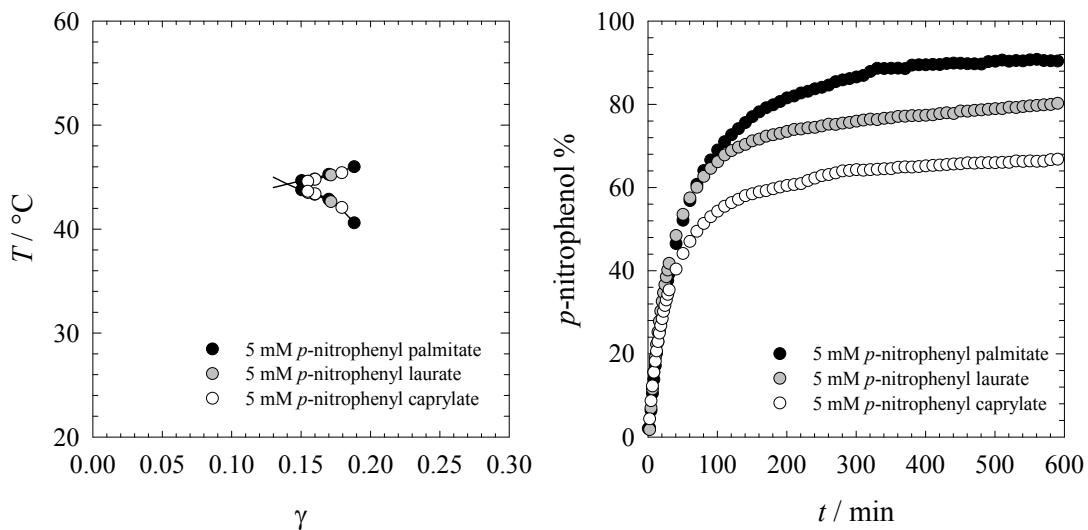


**Figure 3.8**: (left) Phase diagrams of microemulsions consisting of buffer – *n*-octane/5 mM substrate – C$_{10}$E$_5$. The oil to water ratio was kept constant at $\phi = 0.5$. (right) The CalB-catalysed hydrolysis of *p*-nitrophenyl palmitate, -laurate and -caprylate in a bicontinuous microemulsion liberates *p*-nitrophenol the formation of which is plotted as a function of time. The microemulsions consisted of buffer – *n*-octane/5 mM substrate – C$_{10}$E$_5$. The enzyme concentration was 3 mg mL$^{-1}$ in the aqueous phase and the microemulsion was prepared at $\phi = 0.5$, $\gamma = 0.175$ and $T = 44$ °C (figure taken from [Steudle 2015]).

To investigate the CalB activity with increasing substrate concentrations, *p*-nitrophenyl laurate had to be used instead of *p*-nitrophenyl palmitate due to solubilisation problems of the latter in *n*-octane. The microemulsions used were of the same composition as before with the only difference that the amount of substrate

in the oil phase was varied. The resulting phase diagrams can be seen in Figure 3.9 (left). As can be seen, the phase inversion temperature decreases with increasing substrate concentration which is why the reaction temperatures were slightly different, or, more precisely, between 44 °C and 41°C. Figure 3.9 (right) shows the obtained initial reaction rates for the hydrolysis of *p*-nitrophenyl laurate in a concentration range of 5-60 mM. The CalB activity was found to be a linear function of the substrate concentration. In order to find out whether the small temperature differences influence the initial reaction rate three substrate concentrations were measured at two temperatures, namely 20 mM at 44 °C and 43 °C, 40 mM at 43 °C and 42 °C and 60 mM at 42 °C and 41 °C. The obtained $k_2$-values are also plotted in Figure 3.9 and it is obvious that temperature differences of ±1 °C have only a very small effect on the CalB activity.
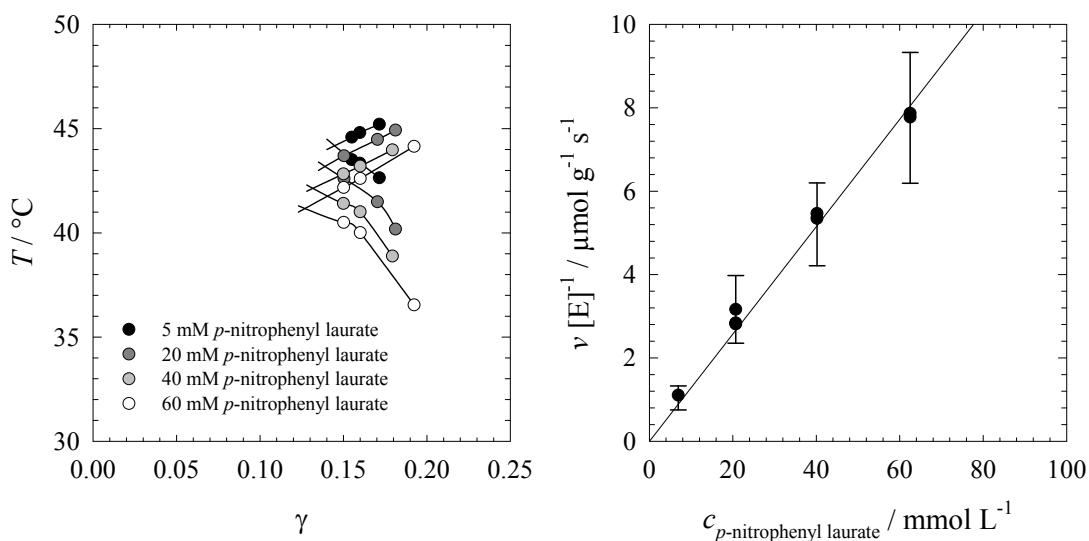


**Figure 3.9**: (left) Phase diagrams of microemulsions consisting of buffer – *n*-octane/*p*-nitrophenyl laurate – $C_{10}E_5$ with increasing *p*-nitrophenyl laurate concentrations from 5-60 mM. (right) Initial reaction rates *v* normalised by the enzyme concentration [E] of the CalB-catalysed hydrolysis of *p*-nitrophenyl laurate in the microemulsion as a function of the substrate concentration. The microemulsions were prepared at $\phi = 0.5$ and $\gamma = 0.175$ and at temperatures between $T = 44$ °C and $T = 41$ °C according to the location of the *X*-point at the respective *p*-nitrophenyl laurate concentration (figure taken from [Steudle 2015]).

The dependence of the CalB activity on the alkyl chain length of the substrate revealed two interesting points. First, all the substrates are dissolved in the oil phase of the microemulsion. Therefore, and in contrast to what happens in conventional

reaction media, no solubility problems are observed. This is why the differences between the initial rates are small. The slightly higher CalB activity towards the *p*-nitrophenyl laurate can be explained by the fact that the active site of CalB fits exactly for 13 C atoms[Pleiss 1998] and that therefore the binding of *p*-nitrophenyl laurate is the most favourable one. The second interesting point concerns the obtained yield after 10 h. The results show that the longer the alkyl chain of the substrate, the higher is the obtained yield, which can be explained with the inhibition of CalB by short-chain fatty acids. Inhibition of CalB and other lipases by alcohols and fatty acids are well known from esterification reactions, also for octanoic acid and lauric acid, which are formed as products in this study.[Lopresto 2014]

It is also very interesting to note that a linear relationship between the substrate concentration and the CalB activity was found. The results suggest that the investigated substrate concentration range falls into the region $[S] \ll K_m$, at which a linear relationship between reaction rate and substrate concentration is observed, as described in Section 2.2.1. This means that either the substrate concentrations were chosen too small, or that the $K_m$ is relatively high for the investigated system. The latter reason would be supported by the fact that higher $K_m$ values were already reported in w/o-microemulsions, compared to the ones found in aqueous systems.[Schomaecker 1988; Valis 1992] In the present study, we did not further increase the substrate concentration due to the large differences in the resulting *X*-points which would have made a comparison of the data very difficult.

**Influence of the Concentration of CalB on its Activity**

Previous kinetic studies of lipase-catalysed reactions performed in w/o-microemulsions reported the presence of lag times[Stark 1990] which are explained by the use of the injection method, i.e. injecting an enzyme solution into an already formed microemulsion. Delays or lag times are observed when the adsorption of the enzyme is slower than the reaction kinetics.[Avramiotis 1996] Possibly the significant curvature of such systems can result in the difficulty of inserting interfacial additives, which is additionally influenced by the packing parameter of the additive. Nevertheless, as we also used the injection method we studied possible delays in the reaction kinetics.

For this purpose, the adsorption of CalB at a bulk buffer – *n*-octane interface was followed by interfacial tension measurements and then compared with reaction kinetics measured at different CalB concentrations focussing on very small CalB concentrations. Given that the bicontinuous microemulsions have zero mean curvature, modelling its interface as a planar bulk one should be appropriate for studying adsorption kinetics. Figure 3.10 (left) shows the interfacial tension measurements between *n*-octane and buffer solutions containing 0.025, 0.075, 0.25, 0.4, 0.5, 1 and 3 mg mL$^{-1}$ CalB which were carried out at room temperature. In Figure 3.10 (right) the corresponding CalB activities in the microemulsions are presented.
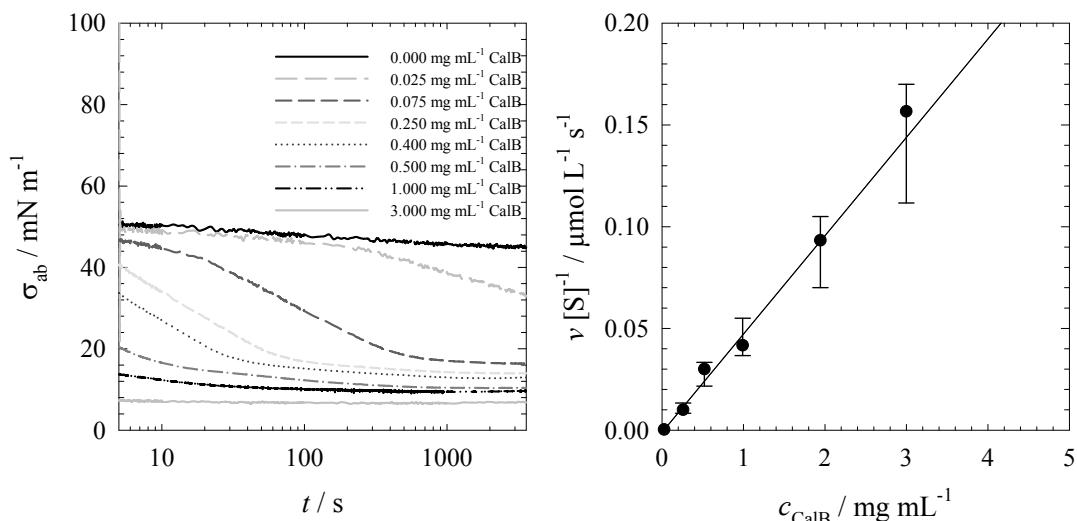


**Figure 3.10**: (left) Interfacial tension $\sigma_{ab}$ between buffer and *n*-octane as a function of time. The samples contained either no or up to 3 mg mL$^{-1}$ CalB in the aqueous phase. (right) Initial reaction rates of the CalB-catalysed hydrolysis of *p*-nitrophenyl palmitate in a microemulsion consisting of buffer – *n*-octane/5mM *p*-nitrophenyl palmitate – C$_{10}$E$_4$ at 23˚C as a function of the initial CalB concentration $c_{CalB}$. The sample was prepared at $\gamma = 0.141$ and $\phi = 0.5$ (figure taken from [Steudle 2015])

The curves seen in Figure 3.10 (left) are typical for interfacial tension measurements with proteins.[Miller 2000] At low CalB concentrations, the induction time can be observed, i.e. the time it takes for CalB to adsorb without significantly reducing the interfacial tension $\sigma_{ab}$. Once a sufficient amount of CalB is adsorbed, the interfacial tension $\sigma_{ab}$ drops sharply, until an equilibrium interfacial tension is reached. At high

CalB concentrations, the induction time and sometimes even the time period in which $\sigma_{ab}$ drops down to the equilibrium value is out of the detectable time range. At the highest CalB concentration of 3 mg mL$^{-1}$ only the equilibrium interfacial tension value could be detected.

Having seen that even small concentrations of CalB adsorb quite fast at the planar buffer – $n$-octane interface, the CalB activity in the microemulsion was measured. By way of an example, for 0.25 mg mL$^{-1}$ CalB the equilibrium value is reached after 100 s. As interfacial tension measurements and adsorption times are sensitive to temperature, we could not use our model system since the phase inversion temperature of the model system is $\tilde{T} = 44$ °C, while the interfacial tension study was carried out at room temperature. Thus the microemulsion consisting of buffer – $n$-octane/5 mM $p$-nitrophenyl palmitate – $C_{10}E_4$ ($\gamma_{Reaction} = 0.141$) was used for the kinetic measurements since it has a phase inversion temperature close to room temperature ($\tilde{T} = 23$ °C) so that interfacial tension and initial reaction rates can be compared directly. Figure 3.10 (right) shows the initial reaction rates plotted against the CalB concentration. Since no lag time was observed during the measurements, we conclude that the reaction immediately started at all studied CalB concentrations (resolution limit was a lag time of less than one minute). As can be seen in Figure 3.10 (right), the CalB activity was found to be a linear function of the CalB concentration. The adsorption of the CalB at the interfacial layer of the microemulsion and the rearrangement of the microemulsion system after the perturbation of adding the CalB solution was therefore fast enough to not cause any lag time in the detectable time range.

Studying the CalB adsorption at an oil-water interface we found that at most CalB concentrations the interfacial tension needs about 100 s to reach the equilibrium value. This relatively fast adsorption time (compared to other proteins) correlates well with the kinetics measured at different CalB concentrations, where no lag time was observed. The conclusion from these findings is that CalB adsorption at the oil-water interface is relatively fast and that the reaction rate directly depends on the

91

CalB concentration. The observed reaction rate therefore depends on both enzyme and substrate concentration, and no retarding effects are observed.

**Co-Surfactants**

The addition of co-surfactants to the system can help to understand how the composition of the interfacial layer is influencing the CalB activity. Two different co-surfactants were chosen, namely the hydrophobic phospholipid 1,2-dioleoyl-sn-glycero-3-phosphocholine (DOPC) and the hydrophilic sugar surfactant $n$-decyl-β-D-glucopyranoside (β-$C_{10}G_1$). Due to different properties, they could not be used at the same co-surfactant mass fraction δ. Phospholipids on the one hand are strongly amphiphilic and form very efficient microemulsions, but also tend to stabilize liquid crystalline phases. To keep the formation of liquid crystalline phases at a minimum, a maximum co-surfactant mass fraction of only δ (DOPC) = 0.05 could be used. Sugar surfactants, on the other hand, have a strongly hydrated head group at nearly all temperatures and the maximum possible co-surfactant mass fraction, without losing the temperature-sensitivity of the microemulsions, was δ (β-$C_{10}G_1$) = 0.50. Due to very high phase inversion temperatures in the presence of the sugar surfactant, it was necessary to add 18 wt% NaCl to the aqueous phase of these microemulsions to decrease the phase inversion temperature so that the system can be compared with the other systems of the present study. As the CalB activity has been proven to be quite temperature dependent, the influence of the co-surfactants was tested over the same temperature range as for the $C_{10}E_j$ microemulsions. The samples were prepared as explained previously by using different $C_{10}E_j$ surfactants to obtain phase inversion temperatures in the range of 20-50 °C, as shown in Figure 3.11.

The resulting systems were buffer – $n$-octane/5 mM $p$-nitrophenyl palmitate – $C_{10}E_j$/DOPC and buffer/18 wt% NaCl – $n$-octane/5 mM $p$-nitrophenyl palmitate – $C_{10}E_j$/β-$C_{10}G_1$. Each of these systems was then used to measure the CalB activity towards the hydrolysis of $p$-nitrophenyl palmitate at the respective phase inversion temperature $\tilde{T}$ and the surfactant mass fraction $\gamma_{Reaction}$ determined from the phase diagrams.
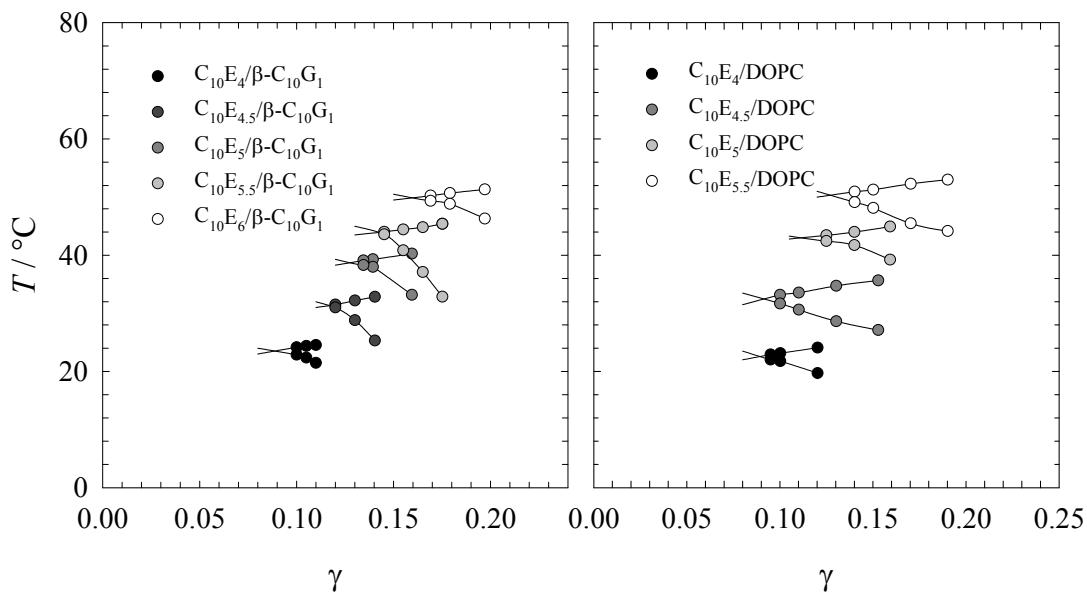
**Figure 3.11**: (left) Phase diagrams of microemulsions consisting of buffer/18 wt% NaCl – *n*-octane/5 mM *p*-nitrophenyl palmitate – $C_{10}E_j/\beta$-$C_{10}G_1$ with $j$ = 4; 4.5; 5; 5.5; 6. The oil to water ratio was kept constant at $\phi$ = 0.5. (right) Phase diagrams of microemulsions consisting of buffer – *n*-octane/5 mM *p*-nitrophenyl palmitate – $C_{10}E_j$/DOPC with $j$ = 4; 4.5; 5; 5.5. The oil to water ratio was kept constant at $\phi$ = 0.5 (figure taken from [Steudle 2015]).

Figure 3.12 shows the resulting CalB activities expressed in observed second order rate constants $k_2$ plotted against the temperature. The system containing only a $C_{10}E_j$ surfactant without co-surfactants is plotted again for comparison. In the observed temperature range, CalB was active in all investigated systems. The maximum activity was found at temperatures of 40-45 °C regardless of the composition of the interfacial layer. The absolute values for the observed second order rate constants $k_2$ vary with the composition of the interfacial layer. The co-surfactant DOPC was found to negatively influence the CalB activity, i.e. lower CalB activities were observed compared to values obtained in the DOPC-free $C_{10}E_j$ systems. On the other hand, the co-surfactant $\beta$-$C_{10}G_1$ enhanced the CalB activity, i.e. higher CalB activities than those observed for the $C_{10}E_j$ systems were found.

The composition of the interfacial layer influences the reaction rate of CalB-catalysed hydrolysis of *p*-nitrophenyl palmitate. Compared to the CalB activity observed in microemulsions formulated with $C_{10}E_j$ alone, the addition of the co-

surfactant DOPC led to lower CalB activities, while the addition of the sugar surfactant $\beta$-$C_{10}G_1$ enhanced the CalB activity.
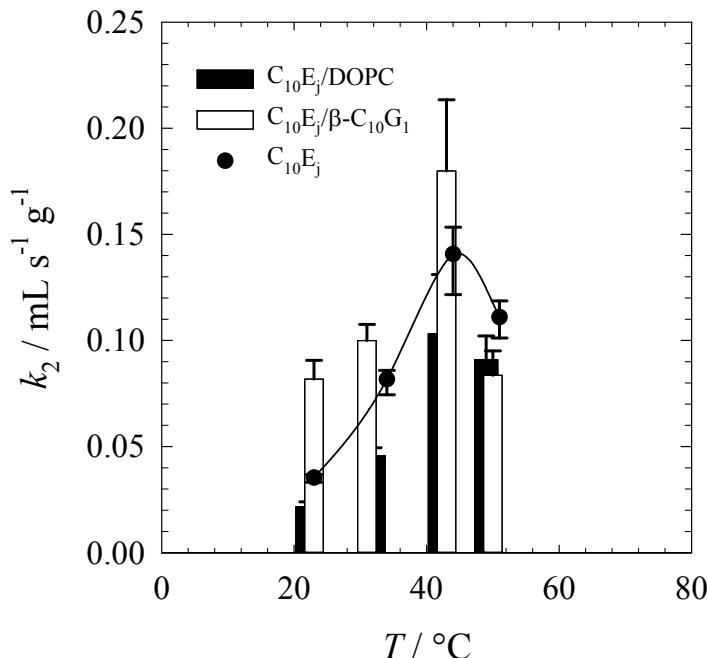


**Figure 3.12**: Influence of the temperature on the observed second order rate constants $k_2$ of the CalB-catalysed hydrolysis of *p*-nitrophenyl palmitate. The samples consisted of buffer – *n*-octane/5 mM *p*-nitrophenyl palmitate – $C_{10}E_j$/DOPC ($\delta = 0.05$) and buffer/18 wt% NaCl – *n*-octane/5 mM *p*-nitrophenyl palmitate – $C_{10}E_j$/$\beta$-$C_{10}G_1$ ($\delta = 0.50$). The different temperatures were realised by changing *j* in the $C_{10}E_j$ surfactants. The samples were prepared at $\phi = 0.5$ and $\gamma_{Reaction} = \tilde{\gamma} + 0.02$. The temperature-dependence of the $k_2$ values obtained for the microemulsion containing only $C_{10}E_j$ surfactants is plotted for comparison (figure taken from [Steudle 2015]).

These results can be explained by the hydrophilicity of the surfactant head group and its hydration level. The results showed that the CalB activity increases with the hydrophilicity of the surfactant. For instance, in the microemulsions prepared with sugar surfactant as co-surfactants, which is more hydrophilic than $C_{10}E_5$ the activity of CalB was higher compared to the $\beta$-$C_{10}G_1$-free system. These results are in agreement with studies performed in w/o-microemulsions which identified hydrophilic surfactants with large head groups as promising surfactants for lipase catalysed reactions.[Das 2005; Das 2003] The strong hydration of the sugar surfactant head group can also play an important role in providing water molecules especially at the interface and in stabilising the CalB even at high (18 wt%) NaCl contents. As a

consequence, the strongly hydrated sugar surfactant head group might also prevent desorption of CalB from the interface, which was assumed to be the reason for the low CalB activity in microemulsions prepared with $C_{10}E_j$ at high ε. Additionally, one should note that the different $\gamma_{Reaction}$ of the systems cannot cause the differences in activities since it holds $\gamma_{Reaction}$ ($C_{10}E_5$/DOPC) < $\gamma_{Reaction}$ ($C_{10}E_5$/β-$C_{10}G_1$) < $\gamma_{Reaction}$ ($C_{10}E_5$) while the activity follows $k_2$ ($C_{10}E_5$/DOPC) < $k_2$ ($C_{10}E_5$) < $k_2$ ($C_{10}E_5$/β-$C_{10}G_1$).

**Reaction Dynamics**

Reaction dynamics describe a chemical reaction from the moment when the reactants get in contact until the product is formed. During the transition from reactant to product, a so-called activated complex, which is a potential energy maximum, is formed. The energy barrier which has to be passed can be expressed as the free energy of activation, $\Delta^{\ddagger}G$. This energy can be lowered by the use of a catalyst, e.g. an enzyme. The reduction of $\Delta^{\ddagger}G$ can be enormous, e.g. the half-time for a glycine decarboxylation in neutral solutions is one billion years.[Wolfenden 2001] Even the hydrolysis of a carboxylic ester (as studied in this work) has a half-time of one year in neutral solution.

Reaction dynamics can be described by thermodynamic parameters. In Table 3.2, the resulting values of apparent free energy $\Delta^{\ddagger}G$, apparent enthalpy $\Delta^{\ddagger}H$, and apparent entropy $\Delta^{\ddagger}S$ of activation are presented. They were calculated from the observed second order rate constants $k_2$ (see Eyring equation [2.19]). Note that in our case the observed second order rate constant is given in units of L $g^{-1}$ $s^{-1}$ as the reaction depends on both enzyme and substrate concentrations and the enzyme concentration is given in mg $mL^{-1}$. However, for the calculations of $\Delta^{\ddagger}G$, $\Delta^{\ddagger}H$ and $\Delta^{\ddagger}S$ the observed second order rate constant $k_2$ was multiplied by the molecular mass of CalB (33 kDa) to obtain the unit L $mol^{-1}$ $s^{-1}$. As can be seen from the values of the observed second order rate constant $k_2$, the reaction is clearly reaction-controlled (for diffusion-controlled reactions one typically observes second order rate constants in the range of $10^9$ L $mol^{-1}$ $s^{-1}$).

**Table 3.2**: Apparent enthalpy, entropy and free energy of activation for the CalB-catalysed hydrolysis of *p*-nitrophenyl palmitate in a bicontinuous microemulsion consisting of buffer – *n*-octane/*p*-nitrophenyl palmitate – surfactant(s). The parameters are $c_{substrate}$ = 5 mM, $\phi$ = 0.5 and for the system with the surfactant mixture $C_{10}E_i/\beta$-$C_{10}G_1$ $\varepsilon$ = 0.18.

| $C_{10}E_i/\beta$-$C_{10}G_1$ | $T$ / °C | $k_2$/ L mol$^{-1}$ s$^{-1}$ | $\Delta^{\ddagger}H$/ J mol$^{-1}$ | $\Delta^{\ddagger}S$/ J mol$^{-1}$ | $\Delta^{\ddagger}G$/ J mol$^{-1}$ |
|---|---|---|---|---|---|
| | 23 | 2.70 | 29 956 | -136 | 70 219 |
| | 31 | 3.14 | 29 890 | -136 | 71 308 |
| | 38 | 4.55 | 29 831 | -136 | 72 262 |
| | 43 | 6.20 | 29 790 | -137 | 72 945 |
| | 50 | 2.93 | 29 732 | -137 | 73 901 |
| $C_{10}E_i$ | $T$ / °C | $k_2$/ L mol$^{-1}$ s$^{-1}$ | $\Delta^{\ddagger}H$/ J mol$^{-1}$ | $\Delta^{\ddagger}S$/ J mol$^{-1}$ | $\Delta^{\ddagger}G$/ J mol$^{-1}$ |
| | 23 | 1.12 | 48 023 | -81 | 72 105 |
| | 34 | 2.62 | 47 932 | -82 | 73 002 |
| | 44 | 4.36 | 47 849 | -82 | 73 820 |
| | 51 | 3.60 | 47 791 | -82 | 74 394 |
| $C_{10}E_i$/DOPC | $T$ / °C | $k_2$/ L mol$^{-1}$ s$^{-1}$ | $\Delta^{\ddagger}H$/ J mol$^{-1}$ | $\Delta^{\ddagger}S$/ J mol$^{-1}$ | $\Delta^{\ddagger}G$/ J mol$^{-1}$ |
| | 22 | 0.72 | 57 734 | -52 | 73 088 |
| | 32 | 1.51 | 57 651 | -52 | 73 610 |
| | 42 | 3.40 | 57 568 | -53 | 74 135 |
| | 49 | 3.00 | 57 510 | -53 | 74 503 |

The information gained from the obtained values is that (1) all the parameters are relatively temperature independent, (2) the apparent enthalpy of activation increases distinctly when going from the system prepared with $C_{10}E_i/\beta$-$C_{10}G_1$ to the systems prepared with $C_{10}E_i$ and $C_{10}E_i$/DOPC and (3) the apparent entropy of activation

becomes less negative in the same order. It is not surprising that the values for the apparent free energy of activation $\Delta^{\ddagger}G$ do not differ much - as it is the same reaction, it is to be expected that the energy barrier is nearly the same in all cases.

The apparent activation enthalpy $\Delta^{\ddagger}H$ was found to be 30 kJ mol$^{-1}$ for the $C_{10}E_i/\beta$-$C_{10}G_1$ system, 48 kJ mol$^{-1}$ for the co-surfactant-free $C_{10}E_i$ system and 58 kJ mol$^{-1}$ for the $C_{10}E_i$/DOPC system. The lowest apparent activation enthalpy $\Delta^{\ddagger}H$ was found for the microemulsion prepared with $C_{10}E_i/\beta$-$C_{10}G_1$ and it is comparable to the activation energies $E_a$ of 20-31 kJ mol$^{-1}$ which were reported for lipase-catalyzed reactions in droplet microemulsions.[Chen 1993; Prazeres 1992] Note that $E_a$ values just slightly differ from $\Delta^{\ddagger}H$ values ($E_a = \Delta^{\ddagger}H + RT$), as explained in Section 2.2.1 (see equation [2.24]). Comparing the data reported in literature, also the length of the alkyl chain of the substrate seems to influence the activation energy. Indeed, the activation energy for the hydrolysis of the esters increases with increasing chain length of the ester, namely from 20 kJ mol$^{-1}$ for *p*-nitrophenyl butyrate to 44 kJ mol$^{-1}$ for *p*-nitrophenyl caprylate.[Crooks 1995]

Low activation enthalpies lead to more temperature insensitive reactions, as was shown for enzymes which were extracted from either cold-blooded species or mammals.[Low 1973] In the same study it was observed that the low activation enthalpy compensates the strongly negative entropy of activation. The same can be observed for the system prepared with $C_{10}E_i/\beta$-$C_{10}G_1$ in the study at hand. The apparent entropy of activation $\Delta^{\ddagger}S$ is strongly negative, but is compensated by the low activation enthalpy $\Delta^{\ddagger}H$. Strongly negative entropies as found in this work (-52 J mol$^{-1}$ to -137 J mol$^{-1}$) are known to occur for enzymatic reactions due to the highly ordered transition state.[Atkins 2005] It is possible that especially the sugar surfactant increases the structural order of water molecules near the active site due to the strong hydrogen bonding, which, in turn, reduces the entropy. However, the lowest apparent enthalpy of activation, together with the most negative apparent entropy of activation, is found in the system which shows the fastest conversion. This fits to previously published results which showed that rate enhancements due to enzyme catalysis are always connected with a significant reduction of the enthalpy of

activation, whereas entropic effects were rarely dominating. This tendency was found to be true especially for hydrolysis reactions or single substrate conversions.[Wolfenden 2001] Thus, the faster reaction rate observed in microemulsions prepared with $C_{10}E_i/\beta$-$C_{10}G_1$ can be explained by the lower activation enthalpy rather than by entropic effects.

Nevertheless, the obtained values should be considered carefully. Throughout the text, only "observed" second order rate constants and "apparent" enthalpies/entropies were reported. The reason is the complexity of the reaction medium, and the difficulties of defining or measuring the exact reaction path. The catalytic turnover of an interfacial active enzyme is shown in Scheme 3.1.[Berg 2003] Prior to forming the enzyme-substrate complex, both enzyme and substrate must adsorb at the interfacial layer of the microemulsion. The adsorption at the interface and desorption into the aqueous phase of the enzyme is described by the rate constants $k_{on}$ and $k_{off}$. Similarly $k'_{on}$ and $k'_{off}$ describe adsorption at the interface and desorption into the oil phase of the substrate. In Scheme 3.1 one can see that additionally to the rate constants $k_1$, $k_{-1}$ and $k_{cat}$ (the back reaction is commonly neglected as it is assumed to be negligible) the rate constants of the adsorption of enzyme and substrate also play a role in the "observed" second order rate constant as measured in this thesis.
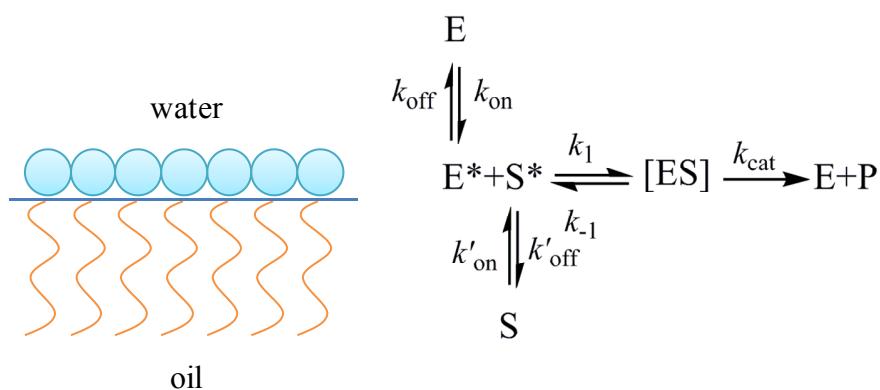


**Scheme 3.1**: The catalytic turnover cycle of an interfacial active enzyme on an oil-water interface, e.g. in a bicontinuous microemulsion. Prior to the formation of the enzyme-substrate complex, both enzyme and substrate must be adsorbed at the interfacial layer (adsorbed species are marked with an asterisk).

As the rate constants are used to calculate the Eyring parameters, they can just be given as "apparent" enthalpies and entropies, as the influence of $k_{off}$, $k_{on}$, $k'_{off}$ and $k'_{on}$ obviously should not be reflected in the activation parameters. However, we have seen that the adsorption of enzyme at the interface is relatively fast, so we would not expect $k_{on}$ and $k_{off}$ to significantly affect the overall rate and hence the determined "apparent" enthalpies and entropies.

# 3.3 Conclusions

The first part of this section showed how important basic investigations are when complex reaction media such as bicontinuous microemulsions are used. Each of the additives to the microemulsions, namely enzyme, substrate and products has their individual influence on the phase behaviour of the microemulsion. At the same time, we found that, although the phase behaviour is shifted by the additives, the main characteristic properties of the microemulsion remain unchanged. Partitioning studies of the substrate carried out in a three-phase system showed that the substrate is preferentially located in the oil domain of the microemulsion, as expected. This is exactly what we wanted to achieve since the conversion of hydrophobic substrates is difficult to realise in aqueous buffer solutions. The product *p*-nitrophenol is the most important compound for the analysis of the reaction, as its formation is followed photometrically and thus, from this data, the second order rate constants are determined. Its acid-base behaviour in bicontinuous microemulsions was investigated in detail, the conclusion being that the higher the hydrogen-bonding capacities of the surfactant, the more the $pK_a$ of *p*-nitrophenol in the respective microemulsion will be increased. The reason for this was seen in the intense hydrogen bonding between surfactant and water molecules, which hinders the deprotonation of *p*-nitrophenol and stabilises the protonated form. To explain this shift with a local pH change seems less likely. In contrast to the substrate, the *p*-nitrophenol prefers to be adsorbed at the interfacial layer of the microemulsion, as was shown in our partitioning studies.

The second part dealt with the CalB activity in bicontinuous microemulsions. Several parameters were investigated, such as pH, temperature and salt content. In summary,

CalB showed optimum activity at a relatively low pH around 5.5 and at a rather high temperature around 44 °C. Furthermore, the presence of salt (NaCl) in the aqueous phase of the microemulsion turned out to decrease the activity significantly. However, the addition of NaCl was tolerated when a surfactant mixture containing sugar surfactant was used to prepare the microemulsion, which we postulated was due to the strong hydration of the sugar surfactant head group which provides enough water molecules near the interface and thus helps stabilising the CalB even at such high NaCl contents.

Interfacial tension measurements between CalB solutions and $n$-octane revealed fast adsorption at nearly all concentrations, which supports our previous results, i.e. that CalB is preferably located at the interface. The CalB activity was found to be a linear function of both enzyme and substrate concentration. The interfacial composition of the microemulsion also had a strong influence on the CalB activity. The results revealed that the addition of the sugar surfactant $\beta$-$C_{10}G_1$ enhanced the reaction rates, but the addition of the phospholipid DOPC decreased the reaction rate (both compared to the reaction rate obtained from microemulsions prepared with only alkyl polyethylene glycol ether). However, it is worth mentioning that the optimum temperature of around 44 °C did not change, i.e. it is independent of the composition of the interfacial layer. The calculation of the apparent enthalpy, entropy, and free energy of activation showed that the superiority of the system containing $\beta$-$C_{10}G_1$ can be explained by a decrease in activation enthalpy rather than being caused by entropic effects. In summary, this section showed that interfacial active enzymes as lipases work well in such complex reaction media and that a bicontinuous microemulsion is indeed a suitable reaction medium for enzymatic hydrolysis of hydrophobic substrates.

# 4 Activity of Aac SHC in Bicontinuous Microemulsions

Squalene-hopene cyclases (SHC) synthesise in just one step cyclic triterpenoic compounds like hopanoids and sterols from linear precursors such as squalene. Hopanoids have a condensing effect on biological membranes due to their rigid ring structures which help to stabilise the membranes once the hopanoids are integrated in the membrane.[Siedenburg 2011] The aim of this part of the thesis is to clarify whether cyclases can be used as biocatalysts in bicontinuous microemulsions, i.e. to investigate the stability and activity of cyclases in this reaction medium. As a model reaction the natural substrate squalene was converted by squalene-hopene cyclases to hopene and hopanol (see Scheme 1.2). In this study, first we investigated the influence of the cyclase from *Alicyclobacillus acidocaldarius* (Aac SHC) on the phase behaviour of bicontinuous microemulsions, as well as the influence of the substrate squalene. Second, we studied the activity of Aac SHC with different enzyme and substrate concentrations. Furthermore, the composition of the interfacial layer was modified, and its influence on the activity and conformation of Aac SHC was determined. Third, the influence of the oil used in the microemulsion on the activity of Aac SHC was investigated. Finally, also the temperature dependence of Aac SHC in bicontinuous microemulsions was studied.

## 4.1 Activity of Aac SHC towards Squalene

To learn about the Aac SHC's properties and activity in the microemulsion, surface tension measurements were carried out and the phase diagrams of the respective microemulsions were determined. Next, the enzymatic activity of Aac SHC towards its natural substrate squalene was determined. For this purpose, both enzyme and substrate concentration were varied. As a last step, the kinetics for one of the substrate concentrations was studied. As a model system, a microemulsion containing a mixture of $C_{10}E_5$ and $\beta$-$C_{10}G_1$ as surfactants was used, as it has been the most suitable reaction medium for the lipase-catalysed reactions (see Section 3). The first investigations with squalene-hopene cyclases were carried out in a

microemulsion consisting of buffer/15 wt% NaCl − *n*-octane/squalene − $C_{10}E_5$/β-$C_{10}G_1$. In this case "buffer" is the abbreviation for a 60 mM citrate buffer with pH = 6 containing 2 mM $MgCl_2$.

**Phase Behaviour**

Prior to carrying out reactions in a bicontinuous microemulsion, the phase behaviour of the respective microemulsions containing substrate and enzyme has to be known. By way of an example, the influence of Aac SHC and the influence of squalene on the phase behaviour were studied. Figure 4.1 (left) illustrates the phase behaviour of a microemulsion containing either no or 2.6 mg $mL^{-1}$ Aac SHC (the maximum Aac SHC concentration used in this section). Upon adding Aac SHC, no difference can be observed. This observation suggests that the Aac SHC is not adsorbed at the interfacial layer and that it also does not have a strong influence as an additive in the aqueous phase of the microemulsion. To get more insight into the surface activity of Aac SHC, surface tension measurements using a pendant drop tensiometer were carried out. The respective curves are shown in Figure 4.1 (right).
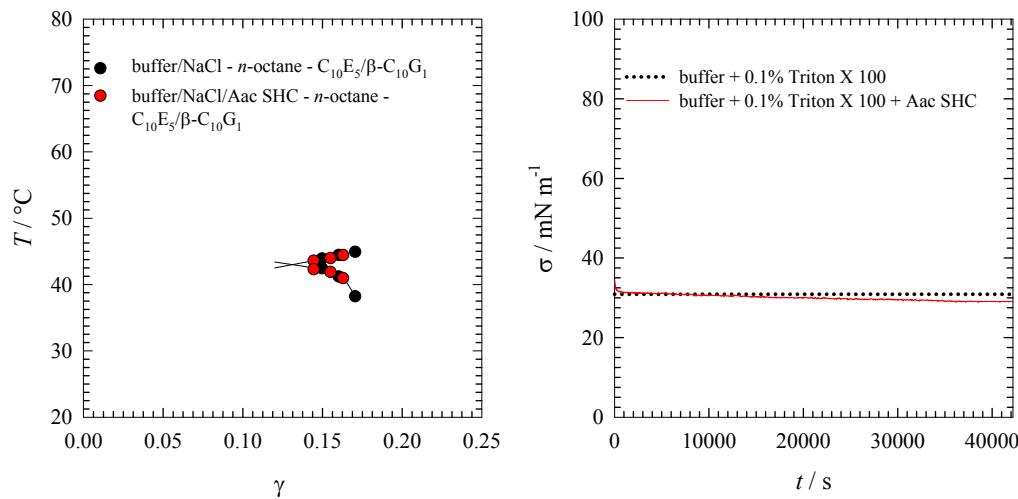


**Figure 4.1**: (left) Influence of Aac SHC on the phase behaviour of a microemulsion consisting of buffer pH 6/15 wt% NaCl/2.6 mg $mL^{-1}$ Aac SHC − *n*-octane − $C_{10}E_5$/β-$C_{10}G_1$ (φ = 0.5). (right) Surface tension measurements of buffer solutions containing either no or 2.6 mg $mL^{-1}$ Aac SHC. Note that due to the isolation procedure small amounts of Triton X 100 are always present in the Aac SHC solution and thus the same amount of Triton X 100 had to be used in the Aac SHC-free solution.

One can see that Aac SHC does not show much surface activity - the surface tension curve of the solution containing 2.6 mg mL$^{-1}$ Aac SHC is only slightly decreased in comparison with the reference without Aac SHC. Especially when comparing these results with the interfacial tension curves of CalB (see Figure 3.10), the differences are remarkable. Thus Aac SHC is not surface active, i.e. it is located in the water phase of the microemulsion rather than being adsorbed at the interfacial layer of the microemulsion. This result explains why the microemulsions' phase behaviour is not altered by adding Aac SHC to the aqueous phase, which is in line with the observations made for other water-soluble enzymes in microemulsions: no interaction between the enzyme diisopropyl fluorophosphatase (DFPase) and the interfacial layer could be observed by means of SANS measurements.[Stehle 2014]

The next step was to measure the phase behaviour of a microemulsion containing squalene which can be dissolved in the oil phase of the microemulsion, i.e. in $n$-octane. In Figure 4.2 the phase diagrams of microemulsions consisting of buffer/15 wt% NaCl – $n$-octane/squalene – $C_{10}E_5$/β-$C_{10}G_1$ are presented.
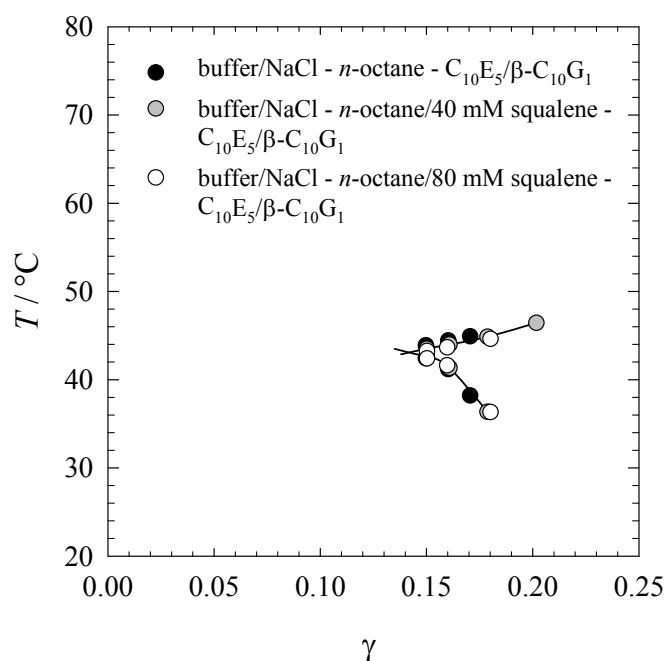


**Figure 4.2**: Phase behaviour of a microemulsion consisting of buffer pH 6/15 wt% NaCl – $n$-octane/squalene – $C_{10}E_5$/β-$C_{10}G_1$ ($\phi = 0.5$). The squalene concentrations were 0 mM, 40 mM and 80 mM.

In the oil phase, either no, 40 mM or 80 mM squalene is dissolved. One can readily see that the influence of the squalene on the microemulsion phase behaviour is rather weak, especially compared to the influence of the additives used in Section 3. Note that squalene, a triterpene, is a non-saturated carbohydrate without any functional groups. Due to the conjugated system it might be slightly more polar than alkanes, thus slightly more polar than *n*-octane. At the same time, the effective carbon number of squalene is obviously much higher than the one from *n*-octane, which leads to a higher hydrophobicity of the former. Although these properties are difficult to determine quantitatively, it can be concluded from the measurements that the influence of squalene on the phase behaviour in this concentration range can be neglected.

**Aac SHC Activity**

The main aim of this chapter is to learn about the activity of Aac SHC in bicontinuous microemulsions. Knowing the influence of the substrate and the enzyme on the microemulsions' phase behaviour, one can prepare the samples at the surfactant mass fraction $\gamma_{\text{Reaction}}$ ($\gamma_{\text{Reaction}} = \tilde{\gamma} + 0.025$). The sample now contains the enzyme in the aqueous phase and the substrate in the oil phase. The temperature was set according to the phase inversion temperature $\tilde{T}$ of the microemulsion. The first step in carrying out enzymatic reactions is to find out suitable concentrations of both enzyme and substrate. Thus reactions were carried out with increasing enzyme and substrate concentration, respectively. As reaction media, the microemulsions described above were used and the reactions run for 7 days at 42.5 °C. The samples were then extracted twice with *n*-octane and analysed by gas chromatography (for details see the Section 6.9). According to Scheme 1.2, two products can be formed, namely hopene and hopanol.

First, the enzyme concentration was varied from 0.65 mg mL$^{-1}$ to 2.6 mg mL$^{-1}$ Aac SHC, while the squalene concentration in the oil phase was kept constant at $c_{\text{Squalene}} = 80$ mM. The results can be seen in Figure 4.3 (left) and show that the yield of hopene and also the absolute concentration of hopene (red plot), respectively, increase with increasing enzyme concentration. Usually an excess of hopene is reported in the

literature and ratios of hopene to hopanol = 5:1 are found.[Hoshino 2002; Seitz 2013] In the study at hand, ratios of 30:1 or more were reached, meaning that hopene is formed in great excess and the amount of hopanol is negligible. For this reason, only the formed hopene will be considered in the following. Although Aac SHC stays solely in the aqueous phase, the reaction rate depends directly on the enzyme concentration, which means that the huge interfacial layer allows for close contact between enzyme and substrate. However, even at the highest Aac SHC concentration of 2.6 mg mL$^{-1}$ only 20 % of squalene was converted, which is why 2.6 mg mL$^{-1}$ of Aac SHC was used throughout this work. An explanation for the rather low yields could be either the poor water solubility of squalene, if one assumes that the reaction takes place in the aqueous phase. If the reaction takes place at the interface, both enzyme and substrate must be present in the interfacial layer which is also not very favourable for both compounds. Thus the effective substrate concentration, which is available for conversion by Aac SHC, is very low in the aqueous phase and at the interface, respectively.[Gäb 2010]

Second, the influence of the squalene concentration on the Aac SHC activity was studied (Figure 4.3 (right)). At a constant enzyme concentration of $c_{Aac\ SHC}$ = 2.6 mg mL$^{-1}$, the squalene concentrations 2 mM, 5 mM, 10 mM, 20 mM, 40 mM and 80 mM were studied. In this case, it is advantageous that squalene did not change the phase behaviour, so that the squalene concentrations could be chosen freely in the desired range without having to consider any changes in surfactant mass fraction or phase inversion temperature $\tilde{T}$. The results show that the observed yield decreases with increasing substrate concentration. Even at the lowest squalene concentration of 2 mM, just 50 % of yield is reached after 7 days. Additionally, the absolute concentrations of the formed hopene are plotted against the substrate concentration. One can see (in the red plot) that the more substrate is available, the more hopene is formed until a plateau is reached around 40 mM squalene. The plateau corresponds to a hopene concentration of about 10 mM, which could be taken as the maximum amount of hopene that can be formed in this particular microemulsion after 7 days of Aac SHC catalysis. This observation could be explained with a saturation of the enzyme molecules once the substrate concentration is too high, which would mean that for this substrate concentrations $v_{max}$ is reached (for details see Section 2.2.1).

However, one has to consider that in the present case not reaction rates, but the conversion after 7 days is plotted and thus any interpretation regarding Michaelis-Menten kinetics is very difficult. In aqueous solution, the Aac SHC catalysed conversion of squalene gives relatively small $K_m$ values of about 16.7 μM which are nearly independent of temperature.[Hoshino 2002] Even with keeping in mind that $K_m$ values are usually much higher in w/o-microemulsions compared to conventional reaction media,[Schomaecker 1988; Valis 1992] to reach $v_{max}$ at substrate concentrations around 40 mM does not seem to be unlikely.
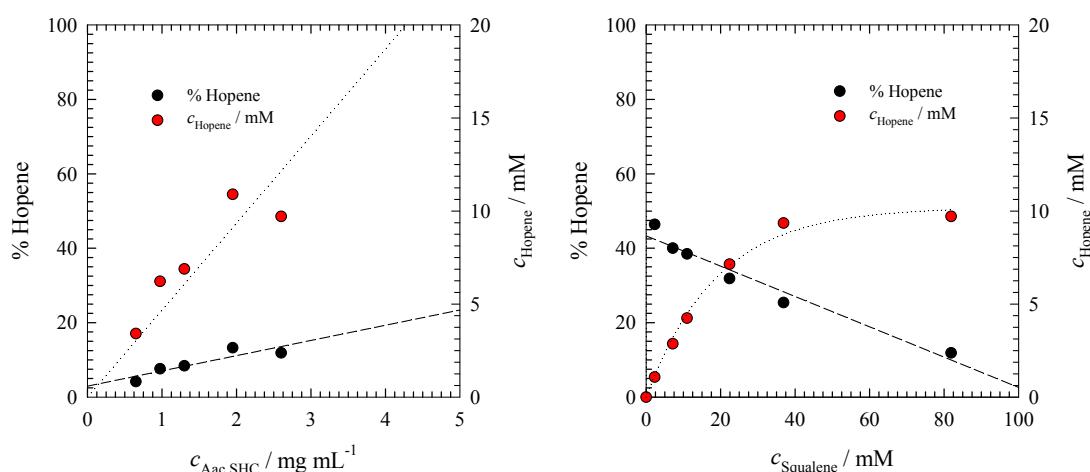


**Figure 4.3**: Aac SHC activity in terms of obtained yield after 7 days for the conversion of squalene to hopene at 42.5 °C in a microemulsion consisting of buffer pH 6/15 wt% NaCl/Aac SHC – *n*-octane/squalene – $C_{10}E_5$/β-$C_{10}G_1$ (ϕ = 0.5). (left) Increasing concentration of Aac SHC up to 2.6 mg mL$^{-1}$ with $c_{Squalene}$ = 80 mM. (right) Increasing concentration of squalene up to 80 mM with $c_{Aac\ SHC}$ = 2.6 mg mL$^{-1}$. In both graphs, additionally to the observed yield, also the product concentration ($c_{Hopene}$) is plotted in red against the enzyme/ substrate concentration.

To investigate in more detail the kinetics of the squalene-hopene conversion, the reaction was monitored for 35 days. For this purpose, several samples were simultaneously prepared with $c_{Aac\ SHC}$ = 2.6 mg mL$^{-1}$ and $c_{Squalene}$ = 10 mM. The microemulsions were extracted and analysed after 0, 4, 7, 10, 22 and 35 days and the obtained data points were fitted by non-linear regression as shown in Figure 4.4 (left). As expected, a hyperbolic curve is observed when plotting the yield of hopene as a function of reaction time. In the first couple of days, the concentration of hopene increases linearly until a plateau is reached after about 10 days of reaction.

According to the non-linear regression, the maximum yield that can be obtained is ~ 74 %. Although this is not a complete conversion, it shows that the Aac SHC is stable and active in the microemulsion for at least 20 days.
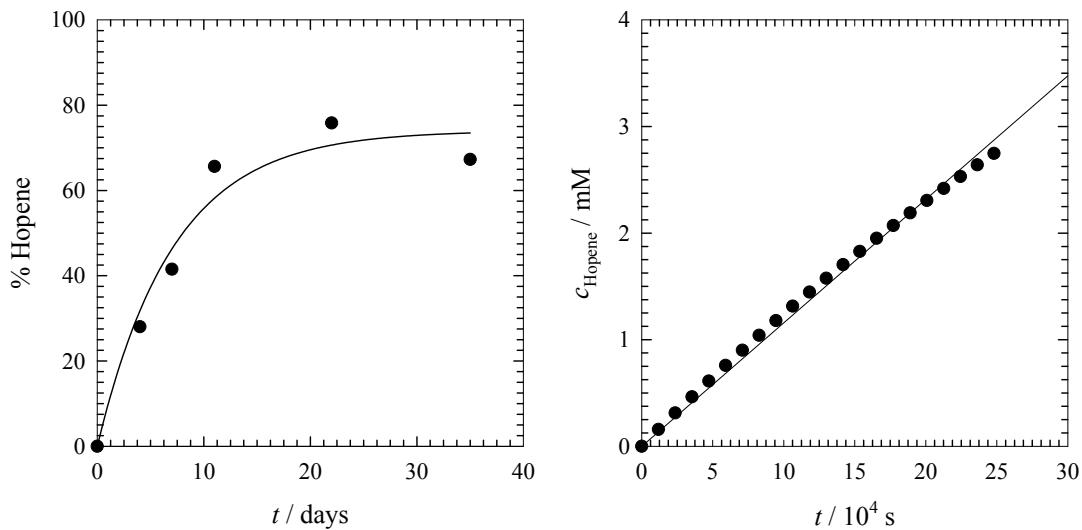


**Figure 4.4**: (left) The obtained yield of hopene as a function of the reaction time. The reaction was carried out in microemulsions consisting of buffer pH 6/ 15 wt% NaCl/ Aac SHC – $n$-octane/ 10 mM squalene – $C_{10}E_5$/β-$C_{10}G_1$ (φ = 0.5). The reaction was performed at 42.5 °C with $c_{Aac\ SHC}$ = 2.6 mg mL$^{-1}$. (right) The determination of the reaction rate from the fitted data, given as the slope of the initial increase of hopene concentration which is plotted against the time.

Looking once again at Figure 4.3 we must now treat the results very carefully since the yield obtained after 7 days is not the maximum yield. A quantitative comparison is only possible if the experimental conditions are the same. However, since we did not study the influence of $c_{Aac\ SHC}$ and $c_{Squalene}$, respectively, on the reaction rate we cannot say anything about the state of the reactions after 7 days compared to all other reactions. The curves may look different if one plotted the maximum yield for all reactions. The fitted data can be used to calculate the reaction rate which is the initial slope as shown in Figure 4.4 (right). The calculated value is 11.6 nmol L$^{-1}$ s$^{-1}$ at a reaction temperature of 42.5 °C. This value is in accordance with literature where a reaction rate of 50.3 nmol L$^{-1}$ s$^{-1}$ is reported for 45 °C in an aqueous system. Note that this value strongly depends on temperature which is reflected in the following data: reaction rate at 30 °C = 6.4 nmol L$^{-1}$ s$^{-1}$ and at 60 °C = 288.3 nmol L$^{-1}$ s$^{-1}$.[Hoshino 2002] Thus, it can be concluded that the reaction rate observed in the bicontinuous

microemulsion is in the same range as the reaction rates observed in aqueous environments. Moreover, it should be stressed that in the bicontinuous microemulsion hopene is formed more selectively compared to aqueous systems. As a reminder, we found a ratio of hopene to hopanol of 30:1 in the microemulsion compared to 5:1 in traditional aqueous environment. [Christianson 2006] Obviously the microemulsion provides an environment in which the reaction is more selective for one of the two products, the reason for which is not known yet.

## 4.2  Influence of Additives and Temperature

In the following, we will investigate how the composition of the microemulsion's interfacial layer influences the activity of the enzyme. For this purpose, the activity is measured for different surfactant mixtures. In addition, the conformation of Aac SHC in the respective microemulsions is studied by circular dichroism spectroscopy. Moreover, the influence of using squalene as the oil phase in the microemulsion and last but not least, the influence of the reaction temperature on the Aac SHC activity in bicontinuous microemulsions is studied.

**Influence of the Composition of the Interfacial Layer on Aac SHC Activity**

In Section 3 we have learned that for the interfacially-active CalB, the composition of the interface is a crucial parameter for the enzymatic activity. In case of Aac SHC, although the enzyme is not interfacially-active, a contact between enzyme and substrate must be created somewhere in the microemulsion when converting the substrate. Bicontinuous microemulsions contain very dynamic networks, which could lead to an enzyme-substrate contact near or at the interface. The fluctuating interfacial film is moving constantly and thus allows species from the oil and water domains to get in contact. If this is the case, the composition of the interfacial layer could also play a role for the Aac SHC activity, for instance the flexibility of the interfacial layer could be important.

To clarify this, reactions were carried out in microemulsions containing only $C_{10}E_5$ as the surfactant or a mixture of $C_{10}E_5$ and DOPC with $\delta = 0.05$. The phase

behaviour of the three systems (the one prepared with the $C_{10}E_5/\beta\text{-}C_{10}G_1$ mixture is shown again for comparison) is shown in Figure 4.5 (left). In all systems, squalene is dissolved at a concentration of 40 mM in *n*-octane, the oil phase of the microemulsion. Each of the co-surfactants leads to distinctive properties. The mixture with 50 wt% sugar surfactant makes the lower phase boundary much steeper compared to the lower phase boundary in the system containing only $C_{10}E_5$. The mixture with 5 wt% of DOPC leads to a more efficient system at a slightly lower phase inversion temperature $\tilde{T}$, and the phase boundaries widen but the shape stays similar to that without DOPC. In summary, the phase inversion temperatures $\tilde{T}$ and surfactant mass fractions $\tilde{\gamma}$ of the *X*-point are in the same range, so that no big differences due to these parameters are expected for the enzymatic activity of Aac SHC.
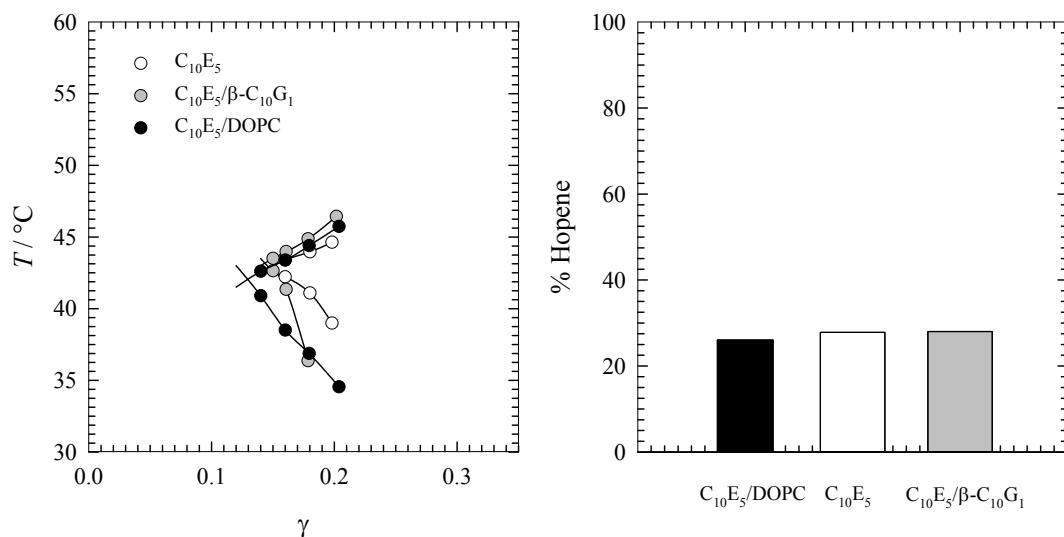


**Figure 4.5**: (left) Phase behaviour of microemulsions containing 40 mM squalene in the oil phase and different surfactant (mixtures) as indicated in the legend. The microemulsion composition is buffer – *n*-octane/40 mM squalene – surfactant (mixture) with $\phi = 0.5$. The amount of added co-surfactant $\beta\text{-}C_{10}G_1$ is 50 wt% and DOPC 5 wt%. Note that for $C_{10}E_5/\beta\text{-}C_{10}G_1$ 15 wt% of NaCl had to be added to the aqueous phase. (right) The obtained yield of Aac SHC catalysed conversion of squalene to hopene in microemulsions of different compositions of the interfacial layer after 4 days.

The reactions were carried out with $c_{\text{Aac SHC}} = 2.6$ mg mL$^{-1}$ and $c_{\text{Squalene}} = 40$ mM. The temperature was set according to the phase inversion temperatures $\tilde{T}$, namely 42.5 °C for the microemulsion prepared with $C_{10}E_5$ and $C_{10}E_5/\beta\text{-}C_{10}G_1$ and 42 °C for

the microemulsion prepared with $C_{10}E_5$/DOPC. The yield obtained after 4 days is shown in Figure 4.5 (right). The results reveal quite similar yields for all systems, from which it can be concluded that the composition of the interfacial layer is not a crucial parameter for the conversion of squalene to hopene catalysed by Aac SHC. Note that again the conversion to hopene is highly selective.

To conclude one can say that the strong influence of the composition of the interfacial layer observed for CalB in the previous section was not found for Aac SHC. From this, we could speculate that the interfacial layer is less involved in the reaction than for interfacial active enzymes. However, the question how and where the enzyme-substrate contact is created in the bicontinuous microemulsion is not answered yet. Stehle et al. consider a dependence of enzyme activity on the transport mechanism of the oil-soluble substrate which has to cross the interfacial layer to reach the aqueous phase of the microemulsion, where the enzyme is located and thus active.[Stehle 2014] The details of this physical transport of the substrate are of increasing importance the more hydrophobic the substrate.[Wellert 2011] Given that squalene is a quite hydrophobic substrate, it is a rather surprising result that the transport of squalene through the interfacial layer is independent of its composition. It could also mean that in our system the transport of the substrate is not the rate-determining step.

**Conformation of Aac SHC in Bicontinuous Microemulsions**

The conformation of an enzyme can change according to its environment. Thus, especially in such special reaction media as microemulsions, one has to consider possible changes in conformation that may lead to a reduced enzymatic activity. To investigate the conformation of Aac SHC in the different regions of a microemulsion, three-phase systems consisting of a microemulsion (middle-phase), and oil excess phase and a water excess phase were used. In such three-phase systems one generally considers that the aqueous and the oil excess phases have the same composition as the aqueous and oil domains in the bicontinuous middle-phase microemulsion since each component has the same chemical potential in each phase. For our study, we prepared three samples with the compositions buffer – *n*-octane – $C_{10}E_5$, buffer – *n*-octane – $C_{10}E_5$/DOPC and buffer/15 wt% NaCl – *n*-octane – $C_{10}E_5$/β-$C_{10}G_1$, each

containing 2.6 mg mL$^{-1}$ Aac SHC in the aqueous phase at $\phi = 0.5$ and $\gamma = 0.08$. The samples were equilibrated at their phase inversion temperature $\tilde{T}$ for 24 h, before the three phases were separated with a syringe. Circular dichroism (CD) spectra were taken from each of the individual phases, again at the respective phase inversion temperatures $\tilde{T}$. Figure 4.6 shows the results.

In Figure 4.6 top, the water excess phases are shown together with the spectrum of the stock solution of Aac SHC, which was used to prepare the samples. The latter shows two negative bands at 222 nm and 208 nm, which are characteristic for the $\alpha$-helical structure. As explained in the theoretical part in Section 2.2.2, these bands are due to $n{\rightarrow}\pi*$ and $\pi{\rightarrow}\pi*$ transitions of the polypeptide backbone of the protein. The expected positive peak at 192 nm due to the $\pi{\rightarrow}\pi*$ transition in $\alpha$-helices cannot be resolved in our case due to the strong absorbance of buffer salts around 190-200 nm. Because of this absorbance, no reproducible data was obtained below 200 nm. The spectra of the water excess phases from the samples prepared with $C_{10}E_5$ or $C_{10}E_5$/DOPC show the same bands with similar or slightly smaller intensities, respectively. Thus, for these two systems, the conformation of Aac SHC has not changed - at least not in the water phase of the microemulsion compared to the initial stock solution. However, for the water excess phase taken from the sample prepared with $C_{10}E_5$/$\beta$-$C_{10}G_1$ a large decrease in intensity can be observed. But, as can be seen with help of the dotted lines at 208 nm and 222 nm, the bands still appear at the same wavelengths. Note that in this sample, the aqueous phase contains 15 wt% NaCl, which could be a reason for the change in the CD spectrum. Another plausible explanation for the decreased intensity of the bands is an unfolding of Aac SHC.

In the middle of Figure 4.6, the spectra of the middle-phase microemulsions are shown for the three systems. Again for the samples prepared with $C_{10}E_5$ and $C_{10}E_5$/DOPC bands appear in the same intensity at the wavelengths 208 nm and 222 nm. Thus, in the middle-phase microemulsions, the Aac SHC is folded mostly in an $\alpha$-helical structure like it is in the aqueous excess phase. A closer look reveals that the signal is much weaker than the one observed in the water excess phase. This is partly due to the fact that the bicontinuous microemulsion contains equal volumes of
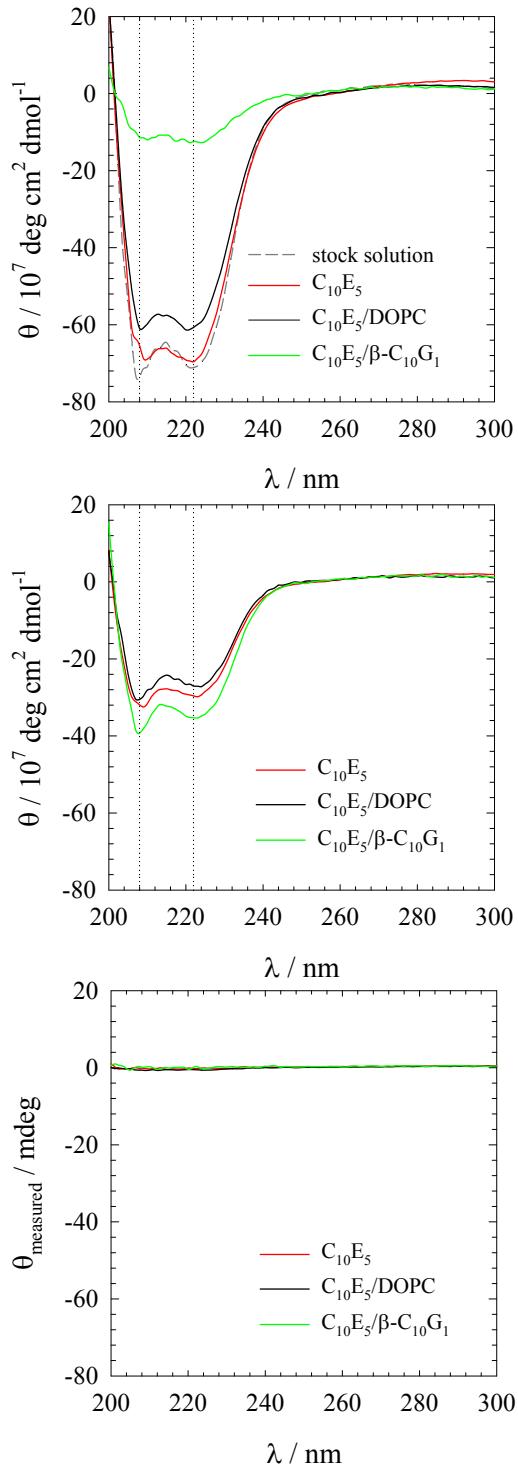
**Figure 4.6**: Circular dichroism spectra of the individual phases of three-phase samples which contained Aac SHC. The samples were formulated with either $C_{10}E_5$, $C_{10}E_5$/DOPC or $C_{10}E_5/\beta$-$C_{10}G_1$ as amphiphilic compound and the composition was buffer – $n$-octane/40 mM squalene – surfactant (mixture) with $\phi = 0.5$. (top) Water excess phases as well as a stock solution for comparison, (middle) middle-phase microemulsion and (bottom) oil excess phases. Note that except of the oil excess phases, the spectra are normalised by the cuvette path length ($d = 0.1$) and the enzyme concentration ($c_{Aac\,SHC} = 2.6$ mg mL$^{-1}$).

both oil and water, but the signal decreases by more than 50 % compared to the water excess phase. This could be caused by the different optical properties of the mixture compared to the aqueous solutions. Alternatively, it may reflect that the Aac SHC is depleted from the more structured aqueous region adjacent to the interfacial layer. Interestingly, the spectrum taken from the middle-phase microemulsion which contains $C_{10}E_5/\beta\text{-}C_{10}G_1$ as surfactant mixture shows bands with more intensity compared to the other two middle-phase microemulsions. The bands appear again at 222 nm and 208 nm, so that the conformation seems to be unchanged. Thus, either the concentration of Aac SHC in the middle-phase microemulsion is higher or less of the enzyme is unfolded. Possibly, the Aac SHC is stabilised by the presence of the hydroxyl groups of the sugar surfactant, with which it can form many hydrogen bonds, so that Aac SHC is preferentially located near the interface. It can be concluded that in the $C_{10}E_5/\beta\text{-}C_{10}G_1$ system, Aac SHC prefers the bicontinuous microstructure rather than the aqueous excess phase, where some unfolding processes might occur. For a more detailed discussion, a detailed partitioning study and further investigations of the interaction between Aac SHC and the involved surfactants would be needed.

On the bottom, the spectra of the oil phases are presented. No signal could be detected in any of the oil excess phases, so it can be concluded that negligible amounts of Aac SHC are present in the oil phase of the microemulsion.

The amount of Aac SHC which is detected in the middle-phase microemulsion would be expected to be the crucial part for the enzymatic activity. The fact that in the 15 wt% NaCl containing microemulsion prepared with $C_{10}E_5/\beta\text{-}C_{10}G_1$ exactly the same yield is reached as with the other two systems, despite the CD spectra showing slightly increased amounts of Aac SHC present in/or close to the interfacial region, would support this explanation. This may reflect that in all three systems there is always sufficient quantity of Aac SHC present to not be the limiting factor in the reaction rate. It should also be mentioned that the differences in the intensity of the middle-phase microemulsions are rather small. Thus comparing the data of the water excess phase with the data of the middle-phase microemulsions, and considering the results of the activity measurements, one can argue that the CD spectra of the

middle-phase microemulsions monitor the enzyme molecules involved in the conversion of squalene in the one-phase microemulsion. Moreover, the results show that the secondary structure of Aac SHC is not changing in the microemulsion regardless of the environment, e.g. the presence of surfactant and the vicinity of the organic solvent. This can be extracted from the spectra showing a dominating α-helical structure in both aqueous excess phase and middle-phase microemulsion. The high α-helix content of the structure fits very well with the crystal structure of Aac SHC,[Wendt 1997] which shows that it contains indeed mainly α-helical structures.

**Influence of the Oil Phase**

Due to the difficulties arising from significantly shifted phase diagrams for the substrates used in Section 3, we decided initially to use only small concentrations of squalene dissolved in *n*-octane. Note that Aac SHC is known to tolerate the presence of detergents which are necessary for the isolation of the membrane protein from the cells. However, the interactions of Aac SHC with organic solvents are still to be investigated, as until now the reactions have usually been carried out in aqueous systems. These thoughts are important because in the microemulsion, Aac SHC can get in contact with an organic solvent, namely *n*-octane. To study whether *n*-octane influences the activity of Aac SHC (that it is not influencing the conformation was reported above) all the *n*-octane was replaced by squalene to create a solvent-free oil phase or microemulsion, respectively. Figure 4.7 (left) shows the obtained phase diagram of the buffer – squalene – $C_{10}E_5$ system together with the initially used phase diagram of the system buffer – *n*-octane/40 mM squalene – $C_{10}E_5$. In this case, to reduce unknown parameters, the microemulsion was prepared only with $C_{10}E_5$ because the phase behaviour and properties of the microemulsions containing alkyl polyethylene glycol ether - type surfactants are well-known. One can see that the phase behaviour is significantly shifted when all the *n*-octane is replaced by squalene. The phase inversion temperature $\tilde{T}$ is increased by more than 10 °C and about 15 wt% more surfactant is needed to solubilise squalene and buffer compared with *n*-octane and buffer. The loss of efficiency and the shift to higher temperatures of $\tilde{T}$ is explained by the fact that squalene is more hydrophobic than *n*-octane.

Indeed, Burauer et al. studied the microemulsion phase behaviour of several microemulsion systems consisting of water – *n*-alkane – $C_iE_j$. Their results showed that changing the oil phase from *n*-octane to *n*-tetradecane shifted the *X*-point to higher temperatures and the system becomes less efficient.[Burauer 1999] The results of the reaction run in the microemulsion with only squalene as oil phase are given in Figure 4.7 (right) again in comparison with the result obtained in the microemulsion with 40 mM squalene dissolved in *n*-octane (in both reactions the enzyme concentration was $c_{\text{Aac SHC}} = 2.6$ mg mL$^{-1}$). The amount of hopene produced after four days is lower for the reaction in the microemulsion prepared solely with squalene as oil phase compared to the amount produced in the microemulsion prepared with *n*-octane/squalene mixture as oil phase.
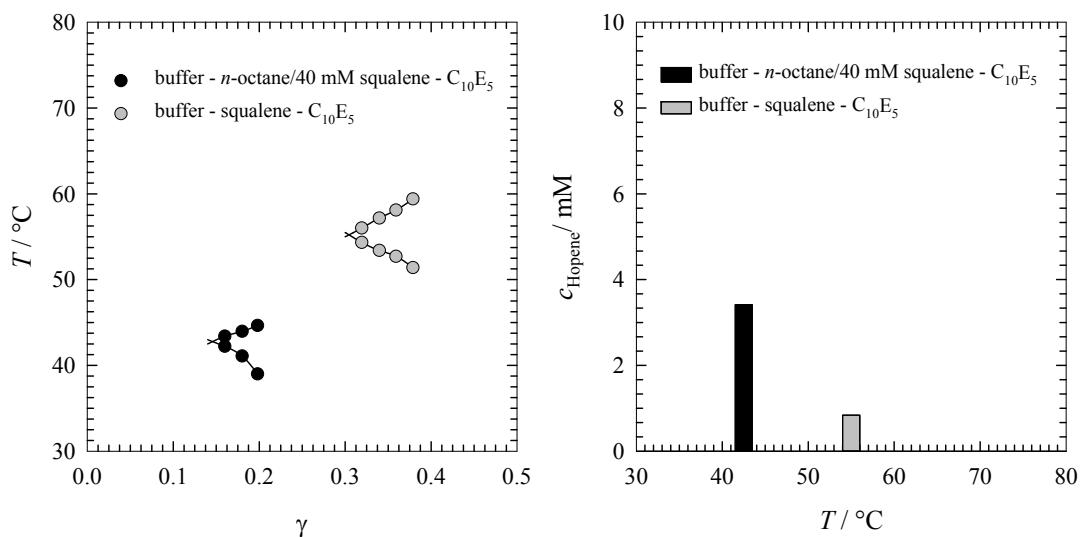


**Figure 4.7**: (left) Phase diagrams of two microemulsions, one containing 40 mM squalene in *n*-octane while in the other one only squalene is used as oil phase. The reactions were carried out at the appropriate phase inversion temperatures $\tilde{T}$ taken from the phase diagrams (42.5 °C and 55 °C for 40 mM squalene dissolved in *n*-octane, and squalene as oil phase, respectively). (right) The amount of formed hopene is plotted against the temperature.

The results suggest two conclusions. First, *n*-octane does not have a negative influence on the Aac SHC activity, or the contact between enzyme and *n*-octane is sufficiently minimised by the interfacial layer. Second, the reaction could be inhibited by the substrate. A possible explanation for the latter is the SHC's catalytic behaviour in vivo. SHC's convert their substrate squalene directly from the inner side

of the membrane, from where it enters the channel to the active site.[Wendt 1997] This mechanism ensures in nature that an equilibrium between substrate and product can be achieved. Especially for the substrate squalene and its product hopene, which helps stabilising the membrane, it is important to control the hopene concentration in a way that the membrane has the desired stiffness, i.e. not too rigid but also not too flexible. Thus, SHC's are not made for large and fast conversion of bulk squalene, which could be an explanation of the saturation of the enzyme already at intermediate substrate concentrations. However, more experiments would be necessary to clarify whether the substrate inhibits the reaction, and if so at which concentrations.

Another reason for the decreased Aac SHC activity could be the much higher amount of surfactant needed in the microemulsion formulated with only squalene as oil phase. Such high concentration could lead to a deactivation of the Aac SHC. Less probable is the difference in temperature as a reason for the decreased enzymatic activity, as Aac SHC is known to work very well for temperatures up to 60 °C. The stability of Aac SHC in the aqueous stock solution up to 60 °C has been shown by CD spectroscopy by taking spectra from 30 °C to 70 °C, which are shown in Section 6.8. Between 40 °C and 70 °C, no difference in conformation is observed, thus no unfolding occurs due to high temperatures.

**Temperature Dependence**

To clarify if differences in temperature could lead to the observed difference in Aac SHC activity, microemulsions with different phase inversion temperatures $\tilde{T}$ were prepared. The composition was buffer – squalene – $C_{12}E_j$ with $j = 4, 5, 6$ to increase the temperature in a stepwise manner. The aim of using surfactants with a longer hydrophobic chain ($i = 12$ instead of $i = 10$) was to increase the efficiency of the systems, which was very low in the system containing only squalene as oil phase and $C_{10}E_5$. As can be seen in Figure 4.8 (left) this has worked out well with values for $\tilde{\gamma}$ between 0.15 - 0.20. The phase inversion temperatures $\tilde{T}$ are 27 °C, 47 °C and 57 °C for $C_{12}E_4$, $C_{12}E_5$ and $C_{12}E_6$, respectively. The increase of the phase inversion temperature $\tilde{T}$ is expected and due to the increasing hydrophilic head group of the

surfactant. The reactions were carried out with $c_{\text{Aac SHC}} = 2.6$ mg mL$^{-1}$ and were run for four days. The observed yield of hopene is plotted as function of temperature in Figure 4.8 (right).
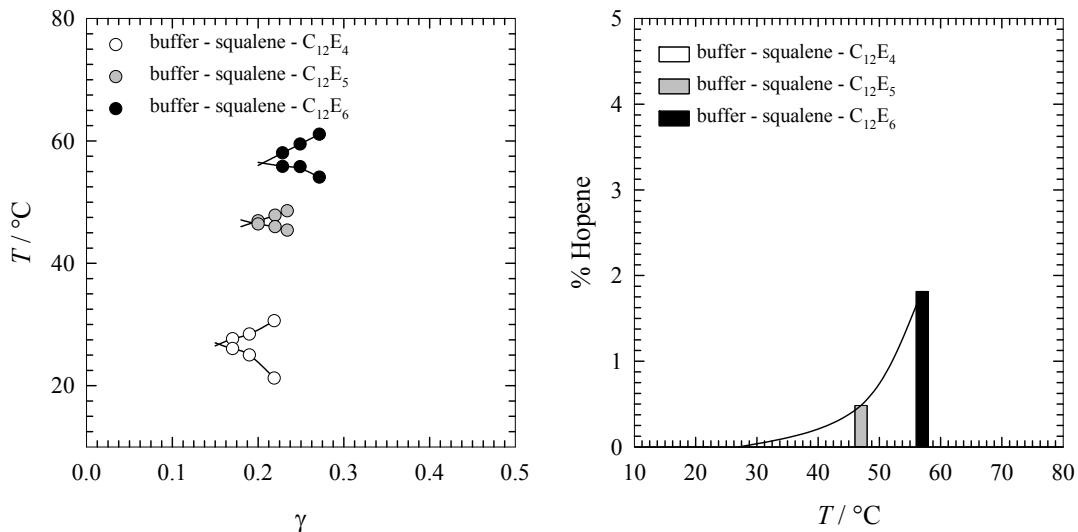


**Figure 4.8**: Phase diagrams (left) of microemulsions containing only squalene as oil phase and surfactants with increasing hydrophilic head groups. The increase of the phase inversion temperature $\tilde{T}$ is used to study the Aac SHC activity at different temperatures. The observed yield of hopene is plotted against the temperature (right).

Although in total the yield remains very low, a clear trend is observed, from no conversion at 27 °C and the highest conversion at 57 °C. Thus, the optimum reaction temperature in bicontinuous microemulsions will be expected to be similar to that observed in aqueous systems, namely around 60 °C.[Sato 1999]

## 4.3  Conclusions

To conclude, one can say that Aac SHC is active in bicontinuous microemulsions, although the yields could be improved. From a microemulsions' point of view, neither the enzyme nor the substrate disturbed the phase behaviour, which facilitates the execution of the reactions. A suitable Aac SHC concentration was found, whereas the influence of the substrate concentration seems to be more complex. With increasing substrate concentration, the enzyme was saturated relatively fast; however one has to keep in mind the natural environment of the squalene hopene cyclases,

where no excess of substrate is to be expected, as the substrate diffuses from the inner of the membrane into the active site of the enzyme, which is just partially penetrating the membrane. Moreover, the reaction catalysed by Aac SHC is one of the most complex reactions catalysed by enzymes in which nine stereocenters have to be formed. This is one of the reasons why also different side-products can be formed, e.g. hopanol. In this study, it is remarkable that in the bicontinuous microemulsion significantly less hopanol was formed than observed in conventional reaction media. In our case, the formation of hopanol can be nearly neglected compared to the hopene formation. This might be a direct effect of the new reaction media. The CD spectra show that Aac SHC is stable in microemulsions, especially in the middle-phase microemulsion with bicontinuous microstructure. Solely in the aqueous phase containing 15 wt% NaCl, Aac SHC gave only a weak signal. Upon replacing all the *n*-octane used as oil phase of the microemulsion by squalene to create a solvent-free system, the before mentioned trend seen with increasing substrate concentration was continued. The substrate concentration was too high, and may have caused an inhibition of the enzyme, as the reaction velocity was decreased when solely squalene was used as the oil phase in the microemulsion. The investigation of different reaction temperatures showed that the optimum temperature seems to be similar to the one observed in aqueous systems, namely around 60 °C. In summary, one can say that bicontinuous microemulsions can be used as reaction media for enzymatic reactions without having a negative influence on the enzyme conformation, but yields are not necessarily improved by the nanostructured environment. Hence the main driving force for the use of microemulsions as reaction media for enzymatic reactions would be to obtain significantly different selectivities.

# 5 Conclusion and Outlook

In Sections 3 and 4, two different enzymes were used to investigate a bicontinuous microemulsion as a reaction medium for enzymatic catalysis. The lipase B from *Candida antarctica* (CalB) shows interfacial activation at an oil-water interface,[Gruber 2012] which is characteristic of lipases. The results show that a bicontinuous microemulsion with its large interfacial area is a suitable reaction medium for lipase-catalysed reactions. In addition, the membrane-associated squalene-hopene cyclase from *Alicyclobacillus acidocaldarius* (Aac SHC) was tested in a bicontinuous microemulsion. Cyclases have recently been detected to have a high potential as general Brønsted acid catalysts for multiple substrates containing different functional groups.[Hammer 2013] Although the only reaction media cyclases have been employed in to-date are aqueous solutions, Aac SHC exhibited considerable stability and activity in bicontinuous microemulsions. What is remarkable about Aac SHC is its higher selectivity when conducting the reaction in a microemulsion.

## 5.1 Lipase B from *C. antarctica*

The focus of the investigations with CalB was the general behaviour of interfacially-active enzymes in a bicontinuous microemulsion and to gain some insight into which parameters influence the activity. The parameters studied can be divided into three groups. First, parameters like pH, temperature and ionic strength were investigated, which are commonly known to influence enzymatic activity in conventional aqueous reaction media. The maximum CalB activity was found at temperatures of around 44 °C and at pH values of around 5.5. The best results were obtained when no additional NaCl was dissolved in the aqueous buffer. Second, parameters that are known to influence the enzyme kinetics like enzyme and substrate concentration were investigated. It was found that the CalB activity is a linear function of both enzyme and substrate concentration. Therefore, no saturation typical for Michaelis-Menten kinetics was detected in the investigated substrate concentration range, with the conclusion that the substrate concentrations used where much smaller than $K_m$. A relatively high $K_m$ (above 40 mM *p*-nitrophenyl laurate) would support this

conclusion, and as higher Michaelis-Menten constants $K_m$ in w/o-microemulsions compared to aqueous systems have already been reported elsewhere, this explanation is likely in our study, too. Suitable enzyme concentrations were identified and they correlated with adsorption studies. For example, for CalB concentrations at which fast activities were found, the enzyme adsorbed at the oil-water interface either immediately (3 mg mL$^{-1}$) or in less than 10 seconds (1 mg mL$^{-1}$). It is assumed that such a fast adsorption also occurs in the microemulsion, and thus no lag times are observed in this reaction medium. Third, the influence of a specific parameter of the microemulsions, namely the composition of the interfacial layer, was studied. The composition of the interfacial layer was modified by adding different co-surfactants, namely a sugar surfactant ($\beta$-C$_{10}$G$_1$) and a phospholipid (DOPC). We found that the highest CalB activity was displayed in the system containing sugar surfactant, thus increasing the hydrophilicity of the interfacial layer is favourable for CalB activity. The assumption is that the intense hydrogen-bonding capacities of the hydroxyl groups of the sugar surfactant head group have a positive influence on the CalB activity. An investigation of the reaction dynamics of the three systems revealed that the enthalpy of activation $\Delta^{\ddagger}H$ was the lowest for the system containing sugar surfactants. Thus the ability of this system to considerably lower the enthalpy of activation $\Delta^{\ddagger}H$ leads to the higher CalB activity in this system. Additionally, it was found that entropic effects are not dominating.

Scheme 5.1 shows a drawing which summarises the catalytic turnover of CalB in bicontinuous microemulsions. Most of the enzyme is adsorbed at the interfacial layer, where the substrate which is dissolved in the oil phase can also adsorb. Consequently the enzyme-substrate complex is formed at the interfacial layer and thus the product is generated. In the study at hand, we found the product *p*-nitrophenol to be preferably adsorbed at the interfacial layer, too.

An important step towards possible applications for CalB-catalysed reactions in bicontinuous microemulsions on an industrial scale is to optimise the formulation of the microemulsion. First, cheaper surfactants should be used, e.g. technical sugar surfactants could reduce costs. Then, the formulation of a non-toxic microemulsion should be encouraged, so as to fully exploit the potential of the biocatalysts to create

more "green" processes. By way of an example, in the system prepared with $C_{10}E_5/\beta$-$C_{10}G_1$, in which the highest CalB activity was observed, one could exchange the $C_{10}E_5$ by a suitable non-toxic co-surfactant, e.g. an alkane-1,2-diol.[Kahlweit 1995] The advantage of alkane-1,2-diols is that by varying the number of carbon atoms, their properties as co-surfactant can be easily adjusted. Remember that sugar surfactants are completely biodegradable and non-toxic, but without any co-surfactant they cannot form a microemulsion. Oil phases that could possibly be used instead of alkanes include biological oils, e.g. triglycerides.[Kahlweit 1995] However, one has to make a point of choosing components that do not act as substrate for the respective enzyme. Hence triglycerides would obviously not be suitable to replace the oil phase for a lipase-catalysed reaction, as triglycerides are the natural substrates of lipases. In this case, the oil phase could be replaced e.g. by limonene, a non-toxic and biodegradable oil.
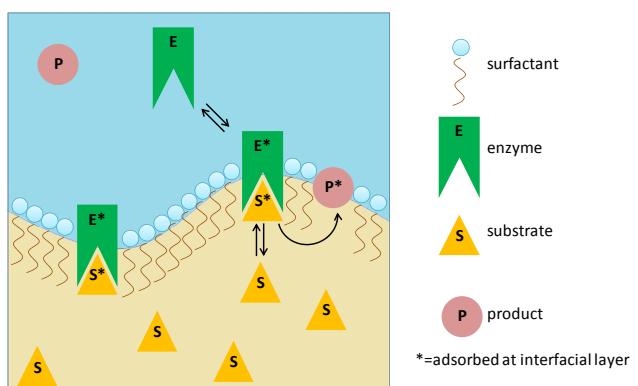


**Scheme 5.1**: Schematic drawing of the catalytic turnover of an interfacial active enzyme, e.g. CalB, at the interfacial layer of bicontinuous microemulsion. The oil-water interface is saturated with surfactant molecules. Enzyme and substrate must adsorb at this interface to form the enzyme-substrate complex.

Once the formulation is optimised, one has to search for suitable reactions, for which the potential of the bicontinuous microemulsion potential could be fully exploited. These reactions should employ a rather hydrophobic substrate, to use the advantage of being able to solubilise substrates in the oil phase of the microemulsion. In the ideal case, one would find a reaction which is chemically not only difficult to execute, but is also not in the desired stereoselectivity. Thus the high stereoselectivity of CalB could facilitate the production of highly valuable and

demanding fine chemicals, e.g. pharmaceuticals. CalB could also replace other, less robust and more difficult to handle biocatalysts, for cheaper or faster production of already available chemicals. An example for such an application is shown in Section 7.2, although this reaction would still need optimisation in the bicontinuous microemulsion. The application range is wide, as CalB accepts many substrates, and thus offers many possibilities, once suitable reactions are found.

## 5.2  Squalene-Hopene Cyclase from *A. acidocaldarius*

The aim of Section 4 was to find out the potential the bicontinuous microemulsion has as a reaction medium for enzymes that are not interfacially-active, and whether these would be active in an environment containing surfactants and organic solvents. We investigated the conversion of the natural substrate squalene to hopene by the squalene-hopene cyclase from *Alicyclobacillus acidocaldarius* (Aac SHC). Studying the phase behaviour of microemulsions containing Aac SHC revealed that Aac SHC is not interfacially-active. In vivo, Aac SHCs penetrate partly the membrane, in which the squalene is incorporated. Thus, the substrate accesses the active site of the enzyme directly from inside the membrane. Obviously, the interfacial layer of a microemulsion is too different from a cell membrane, hence Aac SHC is dissolved in the aqueous domain of the microemulsion instead of adsorbed at the interfacial layer. The substrate squalene was found not to influence the phase behaviour of microemulsions prepared with *n*-octane as the majority oil phase, and thus it is unlikely to be adsorbed at the interfacial layer. The probability of an enzyme-substrate contact is thus reduced. Two possibilities for the catalytic turnover can be considered, which are illustrated in Scheme 5.2. In the middle of Scheme 5.2 one can see the situation which is suggested by the microemulsion's phase behaviour studies. The enzyme is dissolved in the aqueous phase, the substrate is dissolved in the oil phase and they are separated by the interfacial layer. Two options arise: either the substrate dissolves into the aqueous phase (left) or the enzyme-substrate contact is created at the interfacial layer (right) similar to an interfacially-active enzyme, although with probably much less enzyme molecules adsorbed at the interface compared to the amount of enzyme molecules in the aqueous phase.
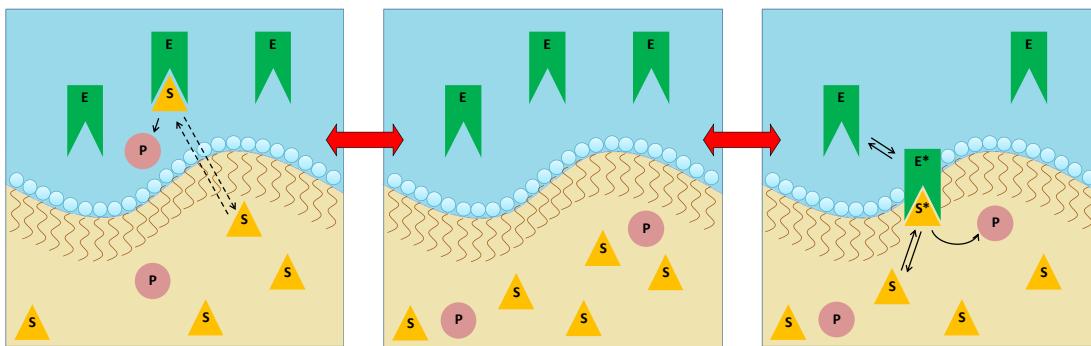
**Scheme 5.2**: Schematic drawing of two possibilities of the catalytic turnover of a water soluble enzyme, e.g. Aac SHC, in a bicontinuous microemulsion. Either the oil-soluble substrate must dissolve in the aqueous phase of the microemulsion (left), or enzyme and substrate must adsorb at the interfacial layer to form the enzyme-substrate complex (right), as described for interfacial active enzymes. For the legend see Figure 5.1.

The study of the activity of Aac SHC in bicontinuous microemulsions was started by determining the influence of enzyme and substrate concentration. It was found that the Aac SHC activity is a linear function of the enzyme concentration, which was indeed expected. However, with increasing substrate concentrations we identified a saturation level. For substrate concentrations above 20 mM, a maximum of 10 mM of hopene was formed, regardless of the employed substrate concentration. The reaction rate was determined for one substrate and enzyme concentration and was found to be similar to literature values.[Hoshino 2002] The fact that the enzyme-substrate contact is hindered in the microemulsion, as illustrated in Scheme 5.2, could be a reason for the substrate-independent reaction rate. To find out more about the role of the interfacial layer, its composition was modified. Surprisingly, no difference in Aac SHC activity was found when preparing systems with either $C_{10}E_5$ alone or with the mixtures $C_{10}E_5/\beta$-$C_{10}G_1$ or $C_{10}E_5/DOPC$. Investigating the enzyme conformation in the three systems, no difference was found in the middle-phase microemulsions, except a higher intensity of the signal from the system prepared with $C_{10}E_5/\beta$-$C_{10}G_1$. Another aspect was the mostly unknown tolerance of Aac SHC towards organic solvents, unlike lipases which are known to work well even in pure organic solvents.[Carrea 2000] To date, Aac SHC-catalysed reactions have mostly been conducted in aqueous buffer solutions. Thus the advantage of being able to change the oil phase of a microemulsion was taken and squalene, assumed to have no negative influence

on the enzyme, was used as oil phase. The main conclusion of this study is that *n*-octane did not have a negative influence on the Aac SHC activity, which could partly be due to the interfacial layer protecting the Aac SHC in the aqueous phase from the oil phase. Finally, the optimum temperature for Aac SHC-catalysed conversion of squalene was investigated and was found to be around 60 °C, which is in agreement with literature data.[Sato 1999] Maybe the most important result is an observation which was made for all the reactions conducted in bicontinuous microemulsions. The hopene to hopanol ratio was found to be 30:1 or even higher. Compared to a commonly observed ratio of 5:1, the selectivity towards hopene is obviously increased significantly in all microemulsions of this study. The difference between the formation of the two products is that in the last step either the terminal methyl group is deprotonated to form hopene (elimination), or the nucleophilic attack by a water molecule forms hopanol (addition). The two options are illustrated in Scheme 5.3.
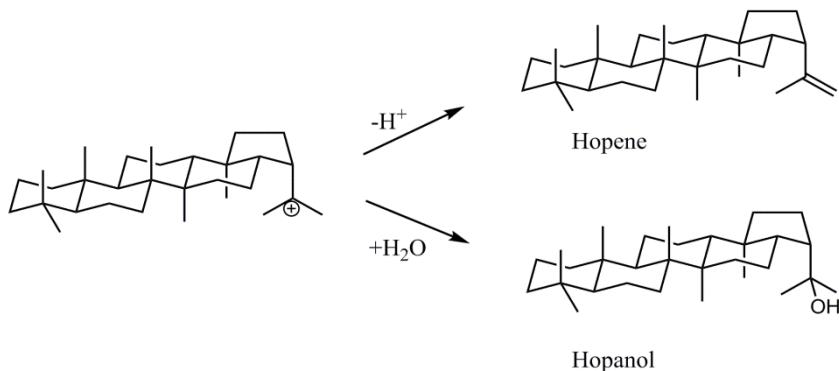


**Scheme 5.3**: Elimination or addition as the last step of the reaction mechanism of squalene conversion to either hopene or hopanol.

In the active centre of Aac SHC several amino acids have been identified to be responsible for the initial protonation, substrate binding, carbocation stabilisation and stereocontrol.[Hoshino 2002] The last deprotonation step is probably catalysed by a polarised water molecule, which is stabilised by a hydrogen bonding network of glutamine, glutamic acid and arginine.[Wendt 1997] Thus, also the formation of the side product hopanol can be explained. However, as this last reaction step takes place in the bottom of the active centre of the enzyme it should not be influenced by the

reaction medium. Generally, eliminations are favoured if steric hindrance plays a role, and additions are favoured in protic solvents. Of course, one could argue that the different environment in the bicontinuous microemulsions leads to small conformational changes that can influence the active centre in such a way that the elimination becomes the favoured process. To clarify this, further experiments, e.g. simulations, would be useful to get more insight how the reaction medium influences the active site residues and thus the selectivity of the enzyme.

Another interesting point to study would be to investigate the selectivity of Aac SHC when converting substrates other than squalene. It has been shown that Aac SHC catalyses many reactions with substrates containing different functional groups.[Hammer 2013] A challenge of these complicated and demanding reactions is that usually two or more products are generated, especially when other than the natural substrates are used. To improve space-time yields, it is essential to generate the products as selectively as possible. Microemulsions seem to be suitable reaction media to improve selectivity due to the nanostructured environment, as shown in Section 4. Thus substrates other than squalene could be tested in the microemulsion to see whether the selectivity of Aac SHC is improved also for other substrates. If so, microemulsions could open up an arena for improved selectivities. These experiments could additionally help to clarify the different selectivity of Aac SHC in bicontinuous microemulsions, if a similar pattern could be identified for different substrates which would give an idea which products are preferably formed and why.

In summary, it could be shown that bicontinuous microemulsions offer a suitable environment for the biocatalysts CalB and Aac SHC. For the lipase the focus was to study the bicontinuous microemulsion itself as a reaction medium, to learn about which parameters are crucial for successful lipase-catalysed reactions. The fact that the lipase was active in this reaction medium was expected, as it has been shown already that lipases are robust enzymes that work in multiple reaction media, such as organic solvents or w/o microemulsions.[Klibanov 2001; Stamatis 1999] Once an overview about the influence of the different parameters in general was gained, the aim was to focus on how generally applicable these results are. For this purpose, Aac SHC was chosen as an enzyme which has not been previously applied in non-conventional

reaction media. It was thus interesting to see how the parameters that were crucial for lipase activity, e.g. the composition of the interfacial layer, did not play a role for Aac SHC activity. Still, e.g. the temperature, had a great influence on both enzymes, as known from conventional reaction media. The differences of how the enzymes were influenced by the employed reaction conditions could finally be explained by their physico-chemical properties. While the lipase adsorbs at the interfacial layer of the microemulsion due to its interfacial activity, the cyclase is a water-soluble enzyme which partitions at most to only a small extent to the interfacial layer. The affinity for the substrates was also different for both enzymes, whereas in both cases the influence of the bicontinuous microemulsion could lead to different availabilities of the substrate due to partitioning effects in the subdomains of the microemulsion. To conclude one can say that the aim of this work, the conversion of hydrophobic substrates which are difficult to dissolve in the natural aqueous environment of enzymes, has been effectively feasible for both CalB and Aac SHC. Especially for the interfacially-active CalB, good turnover rates were achieved due to the enhanced enzyme-substrate contact at the interfacial layer. However, for the water-soluble Aac SHC it could be shown that, although no faster reaction rate can be reported, the selectivity of the enzyme is enhanced. A ratio of 30:1 or more was reached for the formation of hopene to hopanol. Finally, bicontinuous microemulsions were found to influence the properties of both interfacial active enzymes as well as water-soluble enzymes in a positive way, which is why they are interesting in terms of reaction medium engineering to optimise biocatalytic processes. Enzymes that were not yet employed in non-conventional reaction media, such as Aac SHC, shows the advantage of using bicontinuous microemulsions, even for enzymes which are sensitive towards organic solvents. To reveal the full potential of the bicontinuous microemulsion as a reaction medium for biocatalysis, more varied enzymes have to be studied, of course, in these complex reaction medium. This will ultimately establish how generally applicable bicontinuous microemulsions are for reactions involving enzymes or biocatalysts in general.

# 6 Experimental Section

## 6.1 Preparation of the Microemulsions

For the measurements of the phase behaviour, microemulsions were prepared in thin glass vials, having a diameter of 13 mm and a length of 10 cm. The vials were cleaned at least three times alternating with distilled water and acetone, using a brush, to remove both oily and aqueous contaminations. Subsequently, the vials were flushed with bi-distilled water and dried in an oven. The masses of surfactant, aqueous phase and oil phase needed for the specific phase diagram was calculated according to equations 2.1, 2.2 and 2.3. The volumes of oil and water were equal ($\phi$ = 0.5) and were chosen to be 0.3 mL each. The components were weighed to an accuracy of 0.5 mg using micropipettes (Eppendorf, Reference) and an analytical balance (Sartorius, CPA). The surfactant was always weighed in first, as it was the most expensive component and possible errors in weighing in could still be corrected. The next component which was weighed in was the oil phase, as the aqueous phase could form complex structures with the surfactant molecules which might not be easy to destroy after they have been formed and thus would falsify the measured data. Consequently, the aqueous phase was always the last component which was weighed in. After all the components were in the vial, the vial was closed with a plastic stopper and sealed with laboratory film. Before placing the vial in a water basin for the determination of the phase boundaries, it was shaken vigorously to avoid any inhomogeneities.

The water basin used for the determination of the phase boundaries was equipped with a thermostat (Thermo scientific, SC150), a magnetic stirrer below the sample holder, a digital thermometer with an accuracy of 0.01 °C to measure the temperature next to the sample, a lamp and crossed polarisers. An example of such an equipment is shown in Figure 6.1. The sample was usually prepared at a surfactant mass fraction $\gamma$ clearly above $\tilde{\gamma}$, which could be approximated from phase diagrams of similar composition. At $\gamma > \tilde{\gamma}$, the phase boundaries $\underline{2} \to 1$ and $1 \to \overline{2}$ were passed when the temperature was increased. If present, liquid crystalline phases occurred in the one-

127

phase region. As a first step, a fast screening from low to high temperatures was done to see if the above mentioned phases could be identified to ensure that the chosen γ was the right one.



**Figure 6.1**: Water basin used to determine the phase boundaries of a microemulsion. It is equipped with a thermostat with attached tap water cooling, a magnetic stirrer, a sample holder, a digital thermometer, a lamp and crossed polarisers.

Then, the measurement of the phase boundary 2 → 1 was started. For this purpose, a temperature was set where the microemulsion was clearly in the one-phase region. Once the temperature was held constant, the stirrer was turned off. The temperature and the respective phase was noted. The next step was to decrease significantly the temperature such that the two-phase region is reached. It was important to always stir the sample when the temperature was changed to avoid temperature inhomogeneities in the sample. Once the temperature was stable and the sample in the two-phase region, the stirrer was stopped, and again phase and temperature was noted. This procedure was now repeated several times, whereas each time the temperature interval was decreased to get closer to the phase boundary. Once the temperature difference between 2 and 1 was only 0.1 °C, the average was taken as the temperature of the phase boundary. Note that the last phase transition was measured

from 2 to 1 to avoid that kinetic hindrance of the formation of 2 would have caused wrong results (creation of an interface requires work and hence give rise to an energy barrier that constitutes the kinetic hindrance). For the upper phase boundary, i.e. the transition $1 \rightarrow \overline{2}$, exactly the same procedure was followed, this time with a transition from $\overline{2}$ to 1 being the last one.

Further, the surfactant mass fraction $\gamma$ of the sample was decreased by adding oil and water in appropriate amounts and the phase boundaries of the sample were measured. This was done for so many surfactant mass fractions $\gamma$ until the gap between the upper and lower phase boundary was not more than 1 °C, so that they were extrapolated to give the $X$-point of the respective microemulsion.

## 6.2  Preparation of the Buffer Solutions

Throughout this work, buffer solutions were used as aqueous phases in the microemulsion to ensure a stable pH for the enzymes. Different buffer salts had to be used to prepare buffer solutions of different pH values, as no single buffer salt can cover all the pH range. Thus, for the experiments done with CalB, the buffer solutions contained either sodium acetate (pH 4-5), MES (pH 5-7) or TRIS HCl (pH 7-8). The abbreviation MES stands for 2-(N-morpholino)ethanesulfonic acid and TRIS stands for 2-amino-2-hydroxy-methyl-propane-1,3-diol. However, for most of the experiments TRIS HCl buffer pH 7 was used. For the experiments done with Aac SHC, only Citrate buffer pH 6 was used. The concentration of the buffer salts was 100 mM for each of the buffers. Two solutions of 100 mM of the buffer salt were prepared, with one of them made acidic (e.g. for TRIS buffer with HCl). Afterwards, the two solutions could be used to prepare the buffer solution with the pH of choice, by mixing the two solutions accordingly. For this purpose, one of the solutions was stirred with a magnetic stirrer and the pH was measured simultaneously using a pH-meter. The second solution was added slowly, until the desired pH value was reached. The final pH value, e.g. after adding the appropriate amount of NaCl, was always double-checked to ensure it did not differ significantly from the initial buffer solution.

## 6.3  Localisation of Compounds in a Three-Phase System

A three-phase system was used to investigate the localisation of the compounds which were solubilised in the microemulsions. The advantage of the use of a three-phase system is that the middle-phase microemulsion has a bicontinuous microstructure and that the oil excess phase and the water excess phase are commonly assumed to have the same composition as the water or oil domains in the bicontinuous microemulsion because each component must have the same chemical potential in each phase at equilibrium. Thus, one can investigate the individual phases to learn about the distribution of compounds in the microemulsion. The three-phase system was prepared at a surfactant mass fraction $\gamma \ll \tilde{\gamma}$, i.e. in the present study $\gamma = 0.08$ was used. The volumes of the oil phase and the aqueous phase were 0.5 mL each to generate a sample with enough volume to facilitate the separation process. The samples were prepared in GC vials and sealed with laboratory film. The three-phase system was equilibrated at the phase inversion temperature taken from the respective phase diagram for 24 h. It was checked carefully if the phases were completely separated, before they were removed one by one with a syringe and needle through the septum. First, the oil excess phase was taken out, then the middle-phase microemulsion and finally the water excess phase. To remove a maximum of each phase, the tip of the needle was cut flat using pliers. The respective phases were then investigated by UV/Vis spectroscopy, where the temperature was set to the phase inversion temperature $\tilde{T}$ to get the middle-phase microemulsion clear and homogeneous. For the UV/Vis spectra, a Cary 100 spectrophotometer with a Peltier thermostated multi-cell holder was used.

## 6.4  Measurement of the pK$_a$

The pK$_a$ value of *p*-nitrophenol was determined in an aqueous solution and in the microemulsion. For this purpose, several solutions of 2 mM *p*-nitrophenol were prepared at pH values from 4-9. Furthermore, the same solutions containing additionally 4 wt % NaCl were prepared. UV/Vis spectra were collected from each solution, the maximum wavelength of the *p*-nitrophenolate peak was identified, and

the respective absorption values were plotted as function of the pH value. The pK$_a$ is then the inflexion point of the curve. It was calculated by fitting the data to the equation

$$A_{obs} = \frac{A_{min} \cdot 10^{-pH} + K_a \cdot A_{max}}{10^{-pH} + K_a} \qquad [6.1]$$

from which the pK$_a$ can be easily derived as the negative common logarithm of $K_a$. To determine the pK$_a$ of *p*-nitrophenol in microemulsions, three-phase systems were prepared with the composition buffer/4 wt% NaCl/2 mM *p*-nitrophenol – *n*-octane – C$_{10}$E$_5$, with pH values from 4-9. The samples were equilibrated and the phases separated as described in Section 6.3. UV/Vis spectra were measured for each of the phases at each pH value, and the spectra of the middle-phase microemulsions were used to determine the pK$_a$ of *p*-nitrophenol in microemulsions. For this purpose, the wavelength of the maximum absorbance of the *p*-nitrophenolate peak was determined and the absorbances at this wavelength were plotted against the pH value of the initial water phase to determine the inflexion point with Equation 6.1.

## 6.5  Measurement of Reaction Kinetics by UV/Vis Spectroscopy

The reaction rate was determined according to the Michaelis-Menten kinetics. To calculate the reaction velocity, the absorbance of *p*-nitrophenol is followed at the isosbestic wavelength of *p*-nitrophenol to avoid that any irregularities in pH would influence the obtained reaction velocity. Thus the first step was to determine the isosbestic wavelength of *p*-nitrophenol in the respective microemulsion. For this purpose, 2 mM of *p*-nitrophenol was dissolved in buffer solutions of different pH values, which were used to prepare the microemulsions. Then, the UV/Vis spectra of these microemulsions were measured. By way of an example are shown in Figure 6.2 (left) spectra from which the isosbestic point can be clearly identified. The second step was to determine the molar absorptivity ε of *p*-nitrophenol at the isosbestic

wavelength to be able to calculate the concentration from the absorbance values. As illustrated in Figure 6.2 (right), spectra of microemulsions containing different concentrations of *p*-nitrophenol were used to calculate the molar absorptivity ε. The absorbance values are plotted as function of the concentration *c* multiplied by the cuvette path length *d*, which gives the molar absorptivity ε as slope. The isosbestic wavelengths and molar absorptivities of all investigated systems in this work are summarized in Section 7.3.
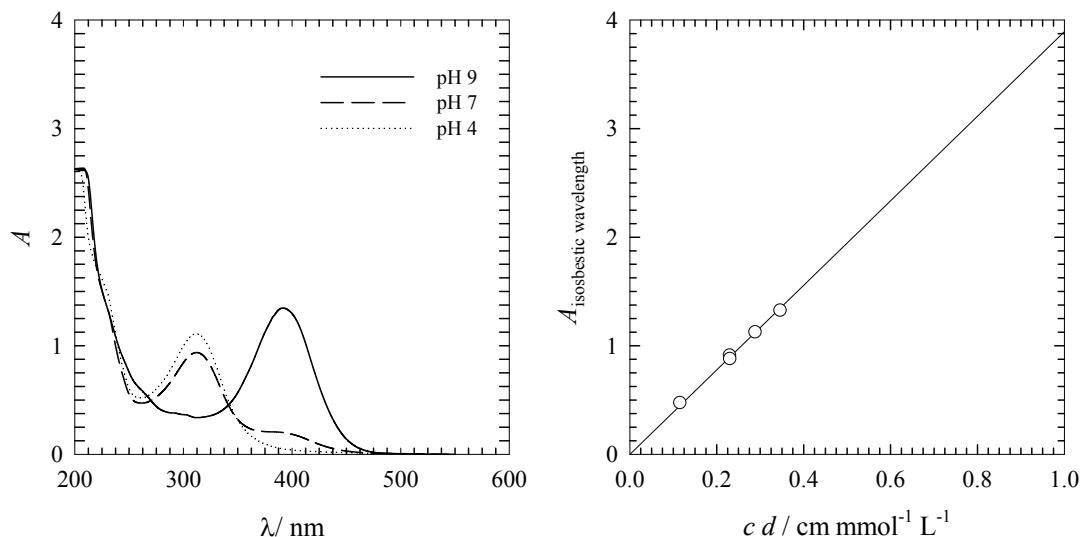


**Figure 6.2**: (left) UV/Vis spectra of *p*-nitrophenol in a microemulsion consisting of buffer/NaCl/*p*-nitrophenol – *n*-octane – $C_{10}E_5$. The buffer solutions had pH values of 4, 7, and 9 to determine the isosbestic point of *p*-nitrophenol in the respective microemulsion. (right) Absorbance values at the isosbestic wavelength of microemulsions containing increasing amount of *p*-nitrophenol plotted as function of the concentration *c* multiplied by the cuvette path length *d*. The molar absorptivity ε can be taken from the slope of the linear regression obtained from the data points.

Knowing these two parameters, the kinetic measurements could be started. They were carried out in Quartz Suprasil (Hellma) cuvettes of 0.1 cm path length which were closed with a round plastic stopper. The procedure to prepare the microemulsions was the following. The microemulsions' parameters were calculated for total volume of water and oil of 150 µL. But, for the aqueous phase and the oil phase, 12.5 µL less were weighed in (the aqueous and oil volumes had been calculated as mass as explained above). Once the sample was thermostated in the spectrophotometer, the missing oil phase was added. The sample might then become

turbid, as it has not yet the right composition to form the one-phase microemulsion. To start the reaction, the missing 12.5 µL of the aqueous phase were added, which consisted of a concentrated CalB solution, which after being diluted in the sample would give the desired concentration of CalB. Note that both CalB and substrate concentrations were calculated as the respective concentrations in the oil phase or the aqueous phase, and not in the total mixture.

The measurement started once the CalB solution was added, then the sample was shaken thoroughly and the first spectrum was measured after one minute. The spectra were collected from 600 to 200 nm. As in the region from 600 to 400 nm no signal was expected, this region was used to check if the microemulsion stays clear throughout the measurement. Any occurring turbidity would have been detected, as the light beam cannot fully pass through a turbid sample and the absorbance would increase. To record the kinetics, spectra of the reaction mixture were taken at least every 2 minutes.

An example is shown in Figure 6.3 (left). It is easy to distinguish two characteristic peaks, one around 266 nm which is due to absorbance of the substrate, and one around 316 nm which is due to absorbance of the *p*-nitrophenol. The vertical line is drawn at the isosbestic wavelength of *p*-nitrophenol in microemulsions prepared only with $C_{10}E_5$, at 342 nm. The absorbance values taken at this wavelength were used to calculate the reaction rate, by determining the concentration of *p*-nitrophenol from the absorbance values. One has to consider that the substrate also absorbs to a very small extend at this wavelength. The absorbance at a specific wavelength is described as

$$A = d \cdot \sum_i \varepsilon_i c_i \qquad [6.2]$$

so that we can write for the concentration of *p*-nitrophenol at a time *x* during the reaction

$$c_{p\text{NP, t=x}} = \frac{\left( \dfrac{A_{\lambda(\text{isosb.})}}{d} - \varepsilon_{\text{substrate}} \cdot c_{\text{substrate,t=0}} \right)}{(\varepsilon_{p\text{NP}} - \varepsilon_{\text{substrate}})} \cdot \qquad [6.3]$$

Thus the concentration of *p*-nitrophenol is known and can be plotted as function of the time, as illustrated in Figure 6.3 (right).

The initial reaction velocity can be calculated by determining the slope from the concentration-time plot during the first 20 minutes. At the beginning of the reaction, enough substrate is available and thus the initial formation of product is a linear function of the time and its slope can be used to determine the initial reaction velocity. After a certain time, the reaction velocity slows down due to lower concentration of the substrate, and the plot shows a hyperbolic curve.
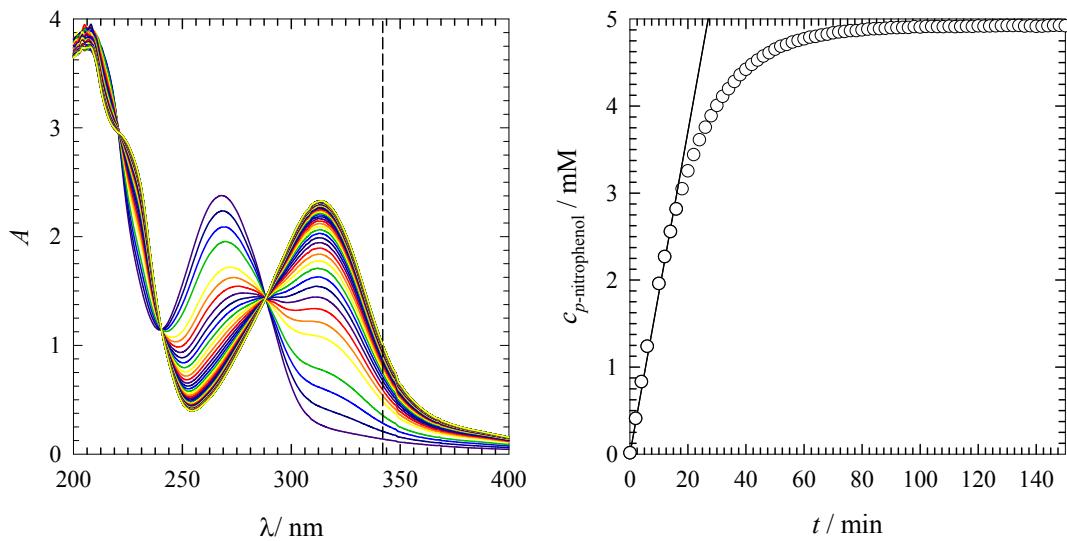


**Figure 6.3**: (left) Spectra of the reaction mixture taken every two minutes. The substrate peak at 266 nm is disappearing, while the *p*-nitrophenol peak at 316 nm is appearing. The vertical line indicates the isosbestic wavelength of *p*-nitrophenol (exemplarily for the system prepared with only $C_{10}E_5$). (right) The absorbance values taken along the vertical line were taken to calculate the concentration of *p*-nitrophenol, which was plotted against the time. The initial reaction rate was given by the slope obtained from the data points taken during the first 20 minutes of the measurement.

The measurements were carried out using a Cary 100 spectrophotometer with a Peltier thermostated cell holder. After the measurements the sample was checked again to be in the one-phase region.

## 6.6  Surface and Interfacial Tension Measurements

Surface and interfacial tension measurements were carried out with a Profile Analysis Tensiometer (Sinterface, PAT-1), which measures surface or interfacial tensions in a range of 1-1000 mN m$^{-1}$. The physical principle for the determination of the surface or interfacial tension is to evaluate the shape of a pendant drop. The apparatus, equipped with a CCD-camera, registers the shape of a pendant drop, which is surrounded by a second phase, e.g. oil or air for an aqueous drop. The shape of the drop is described by the Gauss- Laplace equation

$$\sigma_{ab}\left(\frac{1}{R_1}+\frac{1}{R_2}\right)=\Delta P_0 + \Delta\rho gz \qquad\qquad [6.4]$$

in which $\sigma_{ab}$ is the surface or interfacial tension, $R_1$ and $R_2$ are the main radii of curvature, $\Delta P_0$ is the pressure difference in a reference plane, $\Delta\rho$ is the density difference, $g$ the acceleration due to gravity and $z$ is the vertical height of the drop. For data analysis, the shape of the drop obtained by the video images is fitted with the Gauss- Laplace equation using $\sigma_{ab}$ as the fitting parameter. The best fit gives then the surface or interfacial tension $\sigma_{ab}$. The only requirement is the knowledge of the densities of the used liquids for the case of interfacial tension measurements, which were determined with a density meter from Anton Paar (DMA 5000 M).

Dynamic interfacial tension measurements were done in the same way, but the surface or interfacial tensions were measured continuously over an appropriate time scale. The adsorption process of surfactants can be very fast, sometimes in the timescale of milliseconds.[Eastoe 2000] In contrast, enzymes absorb much slower; they can need several hours or even several days to adsorb.[Miller 2000]

## 6.7  Isolation of Aac SHC

Aac SHC was isolated from expressed and disrupted cells. A citrate buffer pH 6 containing 1 % Triton X 100 was used to solubilise the cells, which were shaken overnight in a cold room. The next day the cells were heated up to 50 °C and were incubated for 30 minutes at this temperature (heatshock). All insoluble cell components were separated from the Aac SHC containing solution by centrifuging for 30 minutes at 4000 rpm.

The concentration of Aac SHC in the supernatant buffer solution was determined by the Bradford Ultra test from Expedeon. It is a colorimetric protein assay in which an absorbance shift of the dye Coomassie Brilliant Blue G-250 from brown to blue occurs when the dye binds to a protein.[Compton 1985] The bound (blue) form of the dye absorbs at 595 nm, so that the absorbance at this wavelength is proportional to the amount of protein present in the sample. As a reference, bovine serum albumin (BSA) was used as a standard protein to determine a calibration curve. It is important to note that depending on the initial Aac SHC concentration always some Triton X 100 is still present in the enzyme solution. The Bradford Ultra test tolerates detergents up to 1 %.

## 6.8  Circular Dichroism Spectroscopy

Circular dichroism spectroscopy was carried out to measure the enzyme conformation either in aqueous solutions or microemulsions. The circular dichroism spectra were obtained using a JASCO-185 spectrometer which is equipped with a $N_2$ purge and a Peltier system (PTC-4235) to control the temperature. The spectra were recorded from 200 to 300 nm. In order to improve the signal-to-noise level, 8 spectra were acquired and averaged for each sample. The measurements were carried out with the following parameters: the scan speed was set to 100 nm min$^{-1}$, the response time was 1 s and the bandwidth was 1 nm. Cells made of Quartz Suprasil (Hellma) with a path length of 0.1 mm up to 10 mm were used to record the spectra, depending

on the enzyme concentration. The intensity of the CD spectra were normalized as follows

$$\theta_M = \frac{100 \cdot \theta_{measured}}{c_{enzyme} \cdot d}$$  [6.5]

with $\theta_{measured}$ being the measured ellipticity in mdeg, $d$ the cuvette path length in cm and $c_{enzyme}$ as the concentration of enzyme in mol $L^{-1}$ (which was obtained by dividing $c_{enzyme}$ given in mg $mL^{-1}$ by the molecular weight of the enzyme).

CD spectroscopy is a useful technique to determine an enzyme's stability at different temperatures. Unfolding due to thermal effects was studied for both enzymes investigated in this work, CalB and Aac SHC, by recording spectra at different temperatures, after equilibrating at least 20 minutes at this temperature. The spectra of both enzymes are shown in Figure 6.4.

For CalB, large differences were detected between the spectra taken at 20 °C – 40 °C, which show the typical α-helical structure, and the spectra taken at 50 °C and 60 °C, which show that CalB has unfolded. The unfolding profile was created by plotting the molar ellipticity values at 222 nm as function of temperature. The graph shows that above 40 °C, CalB had lost most of its α-helical structure.

For the Aac SHC the same procedure was used. However, as Aac SHC is known to be very stable even at high temperatures, the investigated temperature range was chosen to 30 °C – 70 °C. One can see that the spectra nearly overlap, only the spectra taken at 30 °C is slightly different. The unfolding profile shows that the conformation of Aac SHC is stable over the investigated temperature range. Thus, no unfolding at high temperatures occurs in the case of Aac SHC, as expected. The small amount of Triton X 100 in the Aac SHC solutions did not give any signal in reference measurements and thus its influence can be neglected.
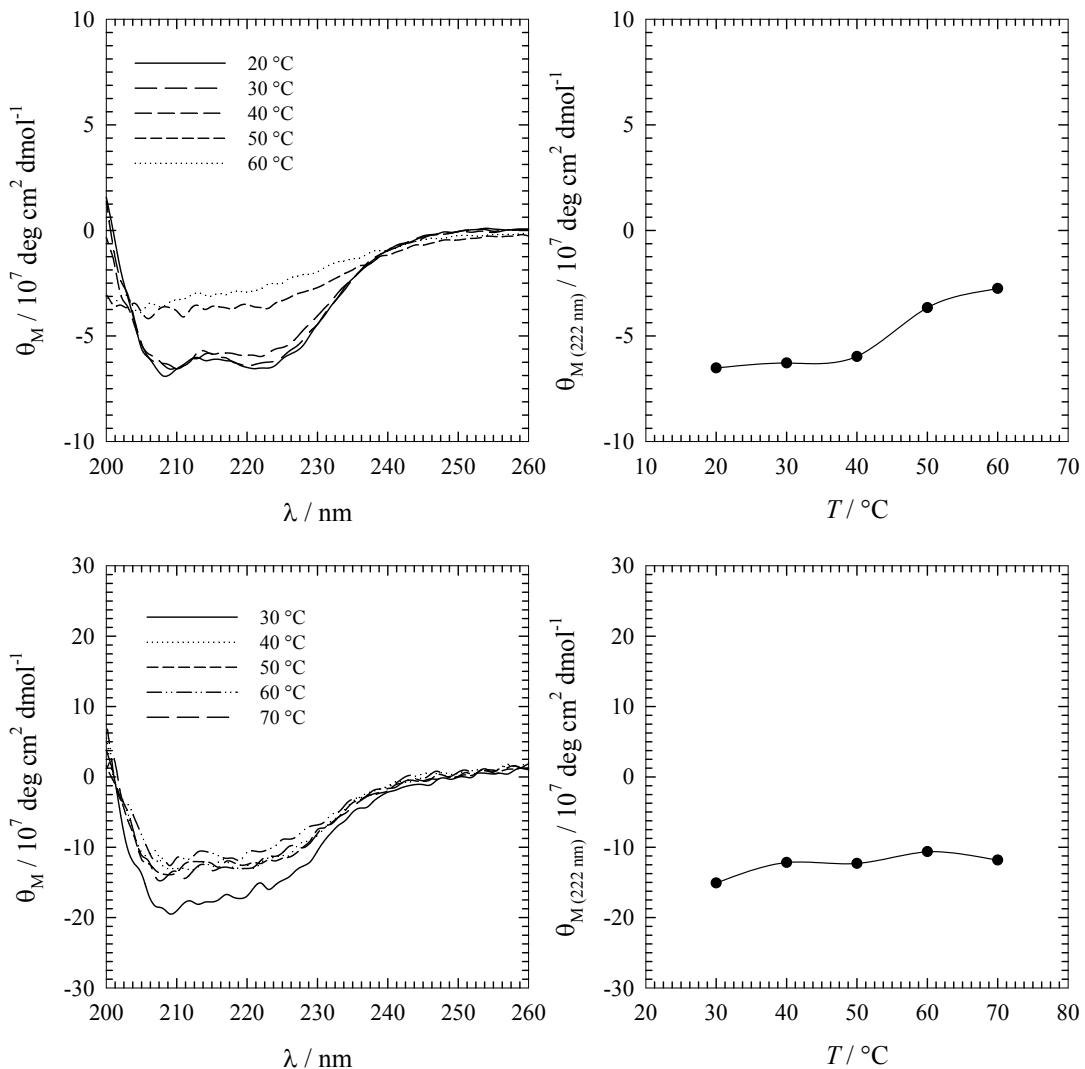
**Figure 6.4**: (top, left) CD spectra of a 10 mg mL$^{-1}$ CalB solution in TRIS HCl buffer pH 7 at temperatures between 20 °C – 60 °C. (top, right) The unfolding of CalB at temperatures above 40 °C can be seen by plotting the molar ellipticity at 222 nm as function of temperature. (bottom, left) CD spectra taken of a 0.18 mg mL$^{-1}$ Aac SHC solution in citrate buffer pH 6 at temperatures between 30 °C – 70 °C. (bottom, right) A stable Aac SHC conformation at all temperatures is shown by plotting the molar ellipticity at 222 nm as function of the temperature. Note that Aac SHC is known to be stable at high temperatures.

## 6.9 Gas Chromatography

For the Aac SHC catalysed conversion of squalene, the monitoring of the reaction in situ by UV/ Vis spectroscopy was not possible, as for the involved molecules no clear difference was observed between substrate and product absorbance. Therefore gas chromatography was chosen to analyse the reaction mixture, as the reactants of

138

the Aac SHC-catalysed reaction, namely squalene, hopene and hopanol, are substances which are easily volatile. The GC-FID analysis was carried out with a Shimadzu GC2010 equipped with an AOC-20i auto injector by using $H_2$ as carrier gas (linear velocity 30 cm/sec). A 5 % phenyl-polysil-phenylene-siloxane phase column (CS-Chromatographie, Langerwehe, Germany, 30 m, 0.25 mm, 0.25 μm) was used. The gas chromatograph was equipped with a flame ionisation detector (FID).

The reaction was carried out in a glass vial identical to the one used to measure the phase diagrams (see Section 6.1). Both oil and aqueous phase were calculated to be 0.5 mL each to give a total volume of at least 1 mL which facilitates the handling of the samples. The oil phase contained the respective concentration of squalene and the aqueous phase contained the Aac SHC in the respective concentration. The sample was shaken thoroughly and set in the pre-heated water basin. The reaction was run for 4 to 35 days.

For analysis, the internal standard (1-decanol) was added to the reaction mixture which was extracted twice with 750 μL of *n*-octane by mixing with a vortex mixer and subsequent centrifugation with 12 000 rpm for 60 minutes each. The combined organic phases were then analysed by gas chromatography. To analyse the chromatograms, first the peaks were assigned qualitatively to the substances present in the mixture. From literature values, the retention times for the internal standard 1-decanol, squalene, hopene and hopanol were known.[Seitz 2013] To confirm these and to identify the peak of the surfactants, gas chromatograms were recorded of solutions of 1-decanol in *n*-octane, $C_{10}E_5$ in *n*-octane and squalene in *n*-octane. Note that only alkyl polyethlylene glycol ethers are supposed to be in the organic phase due to their very good solubility in *n*-alkanes. The two co-surfactants DOPC and β-$C_{10}G_1$ would either stay in the aqueous phase or not be able to enter the column as they are not volatile. The found retention times are listed in Table 6.1.

**Table 6.1**: Retention times for all substances present in the organic phases after extraction of the reaction mixture.

| Substance | Retention time/ min |
|-----------|---------------------|
| 1-decanol | 4.8 |
| $C_iE_j$ | ~9.0 |
| Squalene | 10.2 |
| Hopene | 16.6 |
| Hopanol | 20.4 |

For a quantitative analysis, the use of an internal standard is useful. To relate the concentration of the internal standard with the area of the peak in the chromatogram, first a calibration with solutions of different concentrations of 1-decanol in *n*-octane was carried out. Being able to calculate the concentration of the internal standard from the peak area, the unknown concentration from the compound *x* can be calculated as follows

$$c_x = \frac{c_{intst} \cdot area_x}{RF \cdot area_{intst}} \qquad [6.6]$$

with $c_x$ and $c_{intst}$ being the concentration of the compound *x* and the internal standard, respectively, $area_x$ and $area_{intst}$ the peak area of the compound *x* and the internal standard, respectively, and RF the relative response factor. The RF value of a compound *x* can be calculated according to

$$RF = \frac{ECN_x}{ECN_{intst}} \, . \tag{6.7}$$

The effective carbon numbers (ECN) of each of the compounds as well as the calculated RF values are summarised in Table 6.2. The ECN concept is used commonly when no pure substances are available for calibration.[Scanlon 1985]

**Table 6.2**: ECN numbers and RF values of the internal standard used in this work, 1-decanol, and the substrate and products of the investigated reaction.

| Compound | ECN | RF |
|----------|-----|-----|
| 1-decanol | 9.50 | 1.00 |
| squalene | 29.40 | 3.09 |
| hopene | 29.90 | 3.15 |
| hopanol | 29.75 | 3.13 |

# 7 Appendix

## 7.1 Materials

**Table 7.1**: List of chemicals used in this project with information about purity and supplier.

| Compound | Purity | Supplier |
|---|---|---|
| $C_{10}E_4$ | ≥97% | Sigma Aldrich |
| $C_{10}E_5$ | ≥97% | Sigma Aldrich |
| $C_{10}E_6$ | ≥99% | Sigma Aldrich |
| $C_{10}E_8$ | ≥98 % | Sigma Aldrich |
| $C_{12}E_4$ | ≥98 % | Sigma Aldrich |
| $C_{12}E_5$ | ≥97 % | Bachem |
| $C_{12}E_6$ | ≥98 % | Sigma Aldrich |
| $\beta$-$C_{10}G_1$ | ≥98 % | Sigma Aldrich |
| DOPC | ≥95 % | Sigma Aldrich |
| *n*-octane | ≥99% | Sigma Aldrich |
| squalene | ≥98 % | Sigma Aldrich |
| *p*-nitrophenol | spectrophotometric grade | Sigma Aldrich |
| *p*-nitrophenyl caprylate | spectrophotometric grade | Sigma Aldrich |
| *p*-nitrophenyl laurate | spectrophotometric grade | Sigma Aldrich |
| *p*-nitrophenyl palmitate | spectrophotometric grade | Sigma Aldrich |
| palmitic acid | ≥99% | Sigma Aldrich |
| Sodium Chloride | ≥99.5% | Sigma Aldrich |

The lipase B from *Candida antarctica* was purified and provided by the Institute of Technical Biochemistry, Stuttgart (Germany). The purification was done by ion-exchange chromatography.[Trodler 2008] The squalene-hopene cyclase from *Alicyclobacillus acidocaldarius* was also provided by the Institute of Technical Biochemistry, Stuttgart (Germany) as expressed and disrupted cells. For the preparation of the microemulsions, bi-distilled water was used.

## 7.2 Kinetic Resolution of Chiral Amines by CalB

As described in Section 2.2.3, lipases are widely used in industry. In synthetic chemistry, the generation of chiral amines is an important application of lipases. These chiral amines can be used as building blocks, chiral auxiliaries or resolving agents in organic synthesis.[Karl 2009] Thus, an attempt was made to carry out a reaction in bicontinuous microemulsions, which is of interest for applications namely the generation of a chiral amine by stereoselective hydrolysis of an amide. Scheme 7.1 illustrates the chosen reaction.
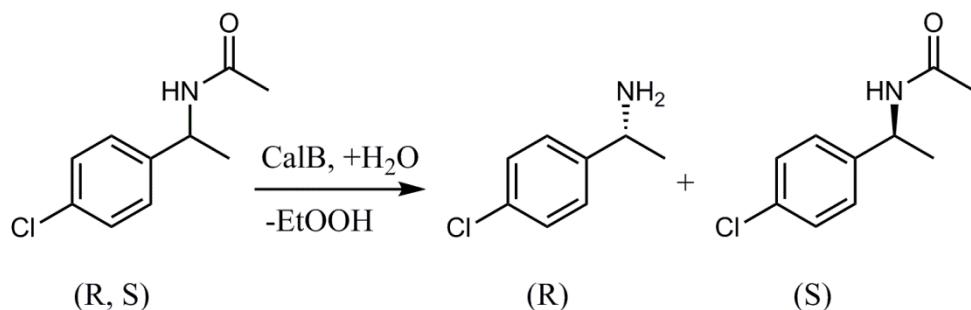


**Scheme 7.1**: CalB-catalysed hydrolysis of racemic N-[1-(4-chloro-phenyl)ethyl]acetamide to give the (R)-1-(4-chloro-phenyl)ethylamine. The (S)-enantiomer is not converted by CalB.

The racemic N-[1-(4-chloro-phenyl)ethyl]acetamide, in the following abbreviated as acetamide, is the substrate for the reaction and was synthesised according to the literature.[Sanz 2007] The amide was obtained as a white powder, which showed poor solubility in both buffer solution and *n*-octane. To measure the phase behaviour of a microemulsion containing the substrate prior to the reaction, it was thus necessary to

solubilise it directly in the microemulsion. The phase behaviour of a microemulsion with the composition buffer – $n$-octane – $C_{10}E_5$ as well as the phase behaviour of a microemulsion in which 30 mM of the substrate was solubilised are shown in Figure 7.1.
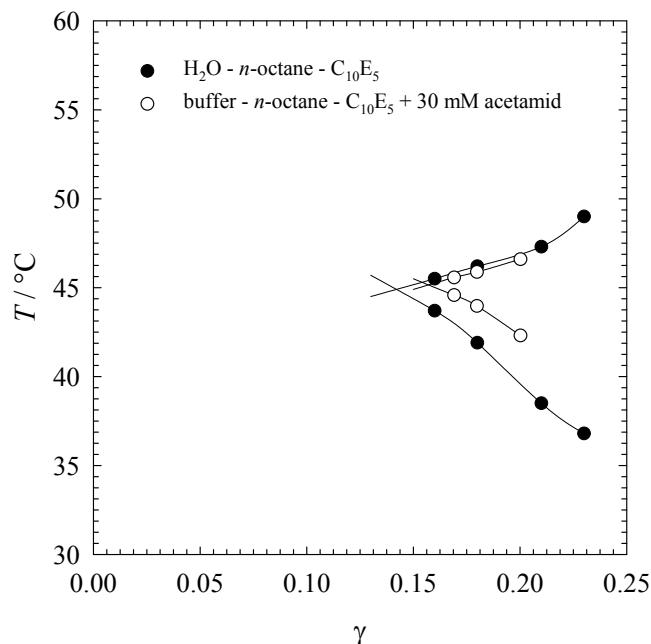


**Figure 7.1**: Phase diagram of a microemulsion consisting of buffer pH 7 – $n$-octane – $C_{10}E_5$, in which 30 mM of acetamide are solubilised. In comparison, the basic phase diagram without acetamide is shown.

As can be seen from the phase behaviour, the phase inversion temperature $\tilde{T}$ is slightly increased from 44.8 °C to 45.1 °C when 30 mM acetamide is added to the microemulsion. Simultaneously, the efficiency is decreased, i.e. $\tilde{\gamma}$ is increased from 0.142 to 0.158. This result can be either explained by the acetamide acting as a co-surfactant, which is less efficient than $C_{10}E_5$ and thus decreases the efficiency (which would be combined with the increasing phase inversion temperature $\tilde{T}$). Another possibility is that the acetamide partitions also in the oil and water domains and influences the phase behaviour by changing the polarity of the respective phases. The product, (R)-1-(4-chloro-phenyl)ethylamine, in the following abbreviated as amine, was not available in an isolated form, thus the phase diagram could not be determined.

To ensure a bicontinuous microemulsion throughout the reaction even without knowing the influence of the product on the phase behaviour, $\gamma_{\text{Reaction}}$ was chosen as $\gamma_{\text{Reaction}} = \tilde{\gamma} + 0.03$. The reaction was run for 15 days, with two CalB concentrations, namely $c_{\text{CalB}} = 5$ mg mL$^{-1}$ and $c_{\text{CalB}} = 20$ mg mL$^{-1}$. For analysis, gas chromatography (GC) was used to determine the obtained yield as well as the enantiomeric excess (ee). Unfortunately, no product peak could be found in the obtained spectra. This can be due to the instability of the formed product, or due to difficulties to extract the product from the microemulsion. Nevertheless, by assuming a selectivity of CalB of > 99%, as reported in literature for this reaction,[Fischer 2001] the yield was calculated out of the ratio of (R) and (S) acetamide after the reaction. The racemic acetamide could be separated by using a CP-Chirasil-DEX CB column from Varian. The amount of disappeared acetamide was thus interpreted as formed amine. The obtained yield for each reaction is given in Table 7.2.

**Table 7.2**: Yields are given for CalB-catalysed chiral resolution of (R)-1-(4-chloro-phenyl)ethylamine. The reaction was run for 15 days and analysed by chiral GC and an assumed ee > 99%.

| $c_{\text{CalB}}$ / mg mL$^{-1}$ | 5 | 20 |
|---|---|---|
| yield / % | 3 | 15 |

As can be seen from the results, the CalB concentration seems to be a crucial parameter for the obtained yield. Whereas at low CalB concentration (5 mg mL$^{-1}$) nearly no product is formed (3 %), at higher CalB concentration (20 mg mL$^{-1}$) at least 15 % of yield are reached. Note that the maximum yield of a kinetic resolution of racemic mixtures is only 50 % due to the fact that only one enantiomer is converted. Also, one should keep in mind that the enantiomeric excess can also differ to that observed in literature, leading to higher yields and accordingly lower ee values.

In aqueous buffer solution, a yield of 25 % with an ee > 99% was observed.[Fischer 2001] The results show that compared to aqueous buffer solutions, the reaction rate is not enhanced by using a bicontinuous microemulsion as a reaction medium. The aim of this project was to improve the yield of the reaction, as well as the reduction of the amount of catalyst needed, which are the main reasons why this reaction is not applied industrially. The accessibility of the substrate is likely to be better in the bicontinuous microemulsion, given that the substrate is neither soluble in buffer nor in $n$-octane, one can assume the substrate can reside near the interfacial layer, where also CalB is adsorbed. However, no enhancement of the reaction rate could be reported. A possible explanation is that the acetamide is not very suitable to be converted by CalB, and thus the enzyme-substrate contact is not the rate determining step.

## 7.3  Isosbestic Wavelengths and Molar Absorptivity Values

**Table 7.3**: Overview of isosbestic wavelength and molar absorptivity $\varepsilon$ of all microemulsions prepared with only $C_{10}E_i$ as surfactant. Note the difference between molar absorptivity $\varepsilon$ in L cm$^{-1}$ mol$^{-1}$ and the salt content $\varepsilon$ without units.

| $j$ | $\lambda_{isosbestic}$ / nm | $\varepsilon$ / L cm$^{-1}$ mol$^{-1}$ |
|---|---|---|
| 4 | 343 | 1856 |
| 4.5 | 343 | 1759 |
| 5 | 344 | 1606 |
| 5.5 | 348 | 1342 |
| 5; $\varepsilon = 0.04$ | 342 | 1881 |
| 6; $\varepsilon = 0.11$ | 346 | 1496 |
| 7; $\varepsilon = 0.18$ | 347 | 1462 |

**Table 7.4**: Overview of isosbestic wavelength and molar absorptivity $\varepsilon$ of all microemulsions prepared with $C_{10}E_i/\beta\text{-}C_{10}G_1$ as surfactant mixture.

| $j$ | $\lambda_{isosbestic}$ / nm | $\varepsilon$ / L cm$^{-1}$ mol$^{-1}$ |
|-----|-----|-----|
| 4 | 338 | 2239 |
| 4.5 | 338 | 2122 |
| 5 | 338 | 2076 |
| 5.5 | 338 | 2001 |
| 6 | 338 | 1996 |

**Table 7.5**: Overview of isosbestic wavelength and molar absorptivity $\varepsilon$ of all microemulsions prepared with $C_{10}E_i/DOPC$ as surfactant mixture.

| $j$ | $\lambda_{isosbestic}$ / nm | $\varepsilon$ / L cm$^{-1}$ mol$^{-1}$ |
|-----|-----|-----|
| 4 | 342 | 3313 |
| 4.5 | 343 | 3256 |
| 5 | 343 | 2875 |
| 5.5 | 344 | 2717 |

# 8 References

Abbaszaadeh, A., Ghobadian, B., Omidkhah, M. R. and Najafi, G. (**2012**). "Current biodiesel production technologies: A comparative review." *Energy Conversion and Management*, *63*, 138-148.

Acharya, P. and Rao, N. M. (**2002**). "Anomalous Ester Hydrolysis in Mixed Micelles of p-Nitrophenyloleateâˆ'Triton X-100 in the Presence of Guanidinium Chloride: Implications in Lipase Assays." *Langmuir*, *18*, 3018-3026.

Adamczak, M. (**2003**). "Synthesis, properties, and application of lipase from Candida antarctica for high yield monoacylglycerol biosynthesis." *Polish journal of food and nutrition sciences*, *12*, 3-8.

Adlercreutz, P. (**2013**). "Immobilisation and application of lipases in organic media." *Chemical Society Reviews*, *42*, 6406-6436.

Anandakrishnan, R., Aguilar, B. and Onufriev, A. V. "H++ 3.0: automating pK prediction and the preparation of biomolecular structures for atomistic molecular modeling and simulations." *Nucleic Acids Research*, *40*, W537-W541.

Anastas, P. and Eghbali, N. (**2009**). "Green chemistry: principles and practice." *Chemical Society Reviews*, *39*, 301-312.

Anderson, E. M., Larsson, K. M. and Kirk, O. (**1998**). "One biocatalyst-many applications: the use of Candida antarctica B-lipase in organic synthesis." *Biocatalysis and Biotransformation*, *16*, 181-204.

Asaad, N. and Engberts, J. B. F. N. (**2003**). "Cytosol-Mimetic Chemistry: Kinetics of the Trypsin-Catalyzed Hydrolysis of p-Nitrophenyl Acetate upon Addition of Polyethylene Glycol and N-tert-Butyl Acetoacetamide." *Journal of the American Chemical Society*, *125*, 6874-6875.

Atkins, P. and de Paula, J. (**2005**). "Elements of Physical Chemistry". Oxford, Oxford University Press.

Avramiotis, S., Lianos, P. and Xenakis, A. (**1996**). "Trypsin In Lecithin Based w/o Microemulsions. Fluorescence and Enzyme Activity Studies." *Biocatalysis and Biotransformation*, *14*, 299-316.

Berg, J. M., Tymoczko, J. L. and Stryer, L. (**2007**). "Biochemistry". New York, W. H. Freeman and Company.

Berg, O. G. and Jain, M. K. (**2003**). "Interfacial enzyme kinetics". Chichester, John Wiley & Sons, Ltd.

Biermann, U., Bornscheuer, U., Meier, M. A., Metzger, J. O. and Schäfer, H. J. (**2011**). "Oils and fats as renewable raw materials in chemistry." *Angewandte Chemie International Edition*, *50*, 3854-3871.

Bornscheuer, U. T., Bessler, C., Srinivas, R. and Hari Krishna, S. (**2002**). "Optimizing lipases and related enzymes for efficient application." *Trends in Biotechnology*, *20*, 433-437.

Bornscheuer, U. T. (**2003**). "Immobilizing Enzymes: How to Create More Suitable Biocatalysts." *Angewandte Chemie International Edition*, *42*, 3336-3337.

Brady, D. and Jordaan, J. (**2009**). "Advances in enzyme immobilisation." *Biotechnology Letters*, *31*, 1639-1650.

Breuer, M., Ditrich, K., Habicher, T., Hauer, B., Keßeler, M., Stürmer, R. and Zelinski, T. (**2004**). "Industrielle Verfahren zur Herstellung von optisch aktiven Zwischenprodukten." *Angewandte Chemie*, *116*, 806-843.

Bru, R., Sanchez-Ferrer, A. and Garcia-Carmona, F. (**1990**). "The effect of substrate partitioning on the kinetics of enzymes acting in reverse micelles." *Biochem. J*, *268*, 679-684.

Burauer, S., Sottmann, T. and Strey, R. (**2000**). "Nonionic microemulsions with cyclic oils." *Tenside, surfactants, detergents*, *37*, 8-16.

Burauer, S., Sachert, T., Sottmann, T. and Strey, R. (**1999**). "On microemulsion phase behavior and the monomeric solubility of surfactant." *Physical Chemistry Chemical Physics*, *1*, 4299-4306.

Carrea, G. and Riva, S. (**2000**). "Properties and Synthetic Applications of Enzymes in Organic Solvents." *Angewandte Chemie International Edition*, *39*, 2226-2254.

Carvalho, C. M. and Cabral, J. (**2000**). "Reverse micelles as reaction media for lipases." *Biochimie*, *82*, 1063-1085.

Chen, J.-P. and Chang, K.-C. (**1993**). "Lipase-catalyzed hydrolysis of milk fat in lecithin reverse micelles." *Journal of Fermentation and Bioengineering*, *76*, 98-104.

Christianson, D. W. (**2006**). "Structural Biology and Chemistry of the Terpenoid Cyclases." *Chemical Reviews*, *106*, 3412-3442.

Clouthier, C. M. and Pelletier, J. N. (**2012**). "Expanding the organic toolbox: a guide to integrating biocatalysis in synthesis." *Chemical Society Reviews*, *41*, 1585-1605.

Compton, S. J. and Jones, C. G. (**1985**). "Mechanism of dye response and interference in the Bradford protein assay." *Analytical Biochemistry*, *151*, 369-374.

Córdova, A., Iversen, T., Hult, K. and Martinelle, M. (**1998**). "Lipase-catalysed formation of macrocycles by ring-opening polymerisation of e-caprolactone." *Polymer*, *39*, 6519-6524.

Crooks, G. E., Rees, G. D., Robinson, B. H., Svensson, M. and Stephenson, G. R. (**1995**). "Comparison of hydrolysis and esterification behavior of Humicola lanuginosa and Rhizomucor miehei lipases in AOT-stabilized water-in-oil microemulsions: II. Effect of temperature on reaction kinetics and general considerations of stability and productivity." *Biotechnol Bioeng*, *48*, 190-6.

Das, D., Roy, S., Mitra, R. N., Dasgupta, A. and Das, P. K. (**2005**). "Head-Group Size or Hydrophilicity of Surfactants: The Major Regulator of Lipase Activity in Cationic Water-in-Oil Microemulsions." *Chemistry-A European Journal*, *11*, 4881-4889.

Das, D. and Das, P. K. (**2003**). "Improving the Lipase Activity Profile in Cationic Water-in-Oil Microemulsions of Hydroxylated Surfactants." *Langmuir*, *19*, 9114-9119.

Davids, T., Schmidt, M., Böttcher, D. and Bornscheuer, U. T. (**2013**). "Strategies for the discovery and engineering of enzymes for biocatalysis." *Current Opinion in Chemical Biology*, *17*, 215-220.

de Souza, R. L., Barbosa, J. M. P., Zanin, G. M., Lobão, M. W. N., Soares, C. M. F. and Lima, Á. S. (**2010**). "Partitioning of porcine pancreatic lipase in a two-phase systems of polyethylene glycol/potassium phosphate aqueous." *Applied biochemistry and biotechnology*, *161*, 288-300.

Drepper, T., Eggert, T., Hummel, W., Leggewie, C., Pohl, M., Rosenau, F., Wilhelm, S. and Jaeger, K.-E. (**2006**). "Novel biocatalysts for white biotechnologie." *Biotechnology Journal*, *1*, 777-786.

Duetz, W. A., Van Beilen, J. B. and Witholt, B. (**2001**). "Using proteins in their natural environment: potential and limitations of microbial whole-cell hydroxylations in applied biocatalysis." *Current opinion in biotechnology*, *12*, 419-425.

Eastoe, J. and Dalton, J. S. (**2000**). "Dynamic surface tension and adsorption mechanisms of surfactants at the air-water interface." *Advances in Colloid and Interface Science*, *85*, 103-144.

Elander, R. P. (**2003**). "Industrial production of b-lactam antibiotics." *Applied Microbiology and Biotechnology*, *61*, 385-392.

Eyring, H. (**1935**). "The activated complex in chemical reactions." *The Journal of Chemical Physics*, *3*, 107-115.

Faiola, C., Erickson, M., Fricaud, V., Jobson, B. and VanReken, T. (**2012**). "Quantification of biogenic volatile organic compounds with a flame ionization detector using the effective carbon number concept." *Atmospheric Measurement Techniques Discussions*, *5*, 2415-2447.

Fernandez, M. S. and Fromherz, P. (**1977**). "Lipoid pH indicators as probes of electrical potential and polarity in micelles." *The Journal of Physical Chemistry*, *81*, 1755-1761.

Fischer, A., Fischer, P., Schmid, R. D., Smidt, H. and Stelzer, U. (**2001**). Process for preparing optically active amines.

Gäb, J., Melzer, M., Kehe, K., Wellert, S., Hellweg, T. and Blum, M.-M. (**2010**). "Monitoring the hydrolysis of toxic organophosphonate nerve agents in aqueous buffer and in bicontinuous microemulsions by use of diisopropyl fluorophosphatase (DFPase) with $^{1}$H-$^{31}$P HSQC NMR spectroscopy." *Analytical and Bioanalytical Chemistry*, *396*, 1213-1221.

Goldberg, K., Schroer, K., Lütz, S. and Liese, A. (**2007**). "Biocatalytic ketone reduction-a powerful tool for the production of chiral alcohols-part I: processes with isolated enzymes." *Applied microbiology and biotechnology*, *76*, 237-248.

Gotor-Fernández, V., Brieva, R. and Gotor, V. (**2006a**). "Lipases: Useful biocatalysts for the preparation of pharmaceuticals." *Journal of Molecular Catalysis B: Enzymatic*, *40*, 111-120.

Gotor-Fernández, V., Busto, E. and Gotor, V. (**2006b**). "Candida antarctica Lipase B: An Ideal Biocatalyst for the Preparation of Nitrogenated Organic Compounds." *Advanced Synthesis & Catalysis*, *348*, 797-812.

Gradzielski, M. (**2008**). "Recent developments in the characterisation of microemulsions." *Current Opinion in Colloid & Interface Science*, *13*, 263-269.

Gruber, C. C. and Pleiss, J. (**2012**). "Lipase B from Candida antarctica binds to hydrophobic substrate–water interfaces via hydrophobic anchors surrounding the active site entrance." *Journal of Molecular Catalysis B: Enzymatic*, *84*, 48-54.

Hammer, S. C., Dominicus, J. M., Syrén, P.-O., Nestl, B. M. and Hauer, B. (**2012**). "Stereoselective Friedel-Crafts alkylation catalyzed by squalene hopene cyclases." *Tetrahedron*, *68*, 7624-7629.

Hammer, S. C., Syrén, P.-O., Seitz, M., Nestl, B. M. and Hauer, B. (**2013**). "Squalene hopene cyclases: highly promiscuous and evolvable catalysts for stereoselective CC and CX bond formation." *Current Opinion in Chemical Biology*, *17*, 293-300.

Hammes, G. G. (**2005**). "Spectroscopy for the Biological Sciences". Hoboken, N.J., Wiley-Interscience.

Hanefeld, U., Gardossi, L. and Magner, E. (**2009**). "Understanding enzyme immobilisation." *Chemical Society Reviews*, *38*, 453-468.

Hasan, F., Shah, A. A., Javed, S. and Hameed, A. (**2013**). "Enzymes used in detergents: lipases." *African Journal of Biotechnology*, *9*, 4836-4844.

Hirose, Y., Kariya, K., Sasaki, I., Kurono, Y., Ebiike, H. and Achiwa, K. (**1992**). "Drastic solvent effect on lipase-catalyzed enantioselective hydrolysis of prochiral 1,4-dihydropyridines." *Tetrahedron Letters*, *33*, 7157-7160.

Hoshino, T. and Sato, T. (**2002**). "Squalene-hopene cyclase: catalytic mechanism and substrate recognition." *Chemical Communications*, 291-301.

Illanes, A., Cauerhff, A., Wilson, L. and Castro, G. R. (**2012**). "Recent trends in biocatalysis engineering." *Bioresour Technol*, *115*, 48-57.

Jaeger, K.-E. and Eggert, T. (**2002**). "Lipases for biotechnology." *Current Opinion in Biotechnology*, *13*, 390-397.

Jaeger, K., Dijkstra, B. and Reetz, M. (**1999**). "Bacterial biocatalysts: molecular biology, three-dimensional structures, and biotechnological applications of lipases." *Annual Reviews in Microbiology*, *53*, 315-351.

Jhoti, H., Cleasby, A., Verdonk, M. and Williams, G. (**2007**). "Fragment-based screening using X-ray crystallography and NMR spectroscopy." *Current Opinion in Chemical Biology*, *11*, 485-493.

Kahlweit, M., Busse, G., Faulhaber, B. and Eibl, H. (**1995**). "Preparing nontoxic microemulsions." *Langmuir*, *11*, 4185-4187.

Kahlweit, M., Strey, R., Firman, P., Haase, D., Jen, J. and Schomäcker, R. (**1988**). "General patterns of the phase behavior of mixtures of water, nonpolar solvents, amphiphiles, and electrolytes. 1." *Langmuir*, *4*, 499-511.

Kahlweit, M., Strey, R. and Busse, G. (**1990**). "Microemulsions: a qualitative thermodynamic approach." *Journal of Physical Chemistry*, *94*, 3881-3894.

Kahlweit, M., Strey, R. and Busse, G. (**1991**). "Effect of alcohols on the phase behavior of microemulsions." *The Journal of Physical Chemistry*, *95*, 5344-5352.

Kahlweit, M. and Strey, R. (**1985**). "Phase Behavior of Ternary Systems of the Type H2O-Oil-Nonionic Amphiphile (Microemulsions)." *Angewandte Chemie International Edition in English*, *24*, 654-668.

Karl, U. and Simon, A. (**2009**). "BASF's ChiPros chiral building blocks: The cornerstones of your API syntheses!" *Chimica Oggi*, *27*,

Kelly, S. M., Jess, T. J. and Price, N. C. (**2005**). "How to study proteins by circular dichroism." *Biochimica et Biophysica Acta (BBA) - Proteins and Proteomics*, *1751*, 119-139.

Kim, J., Grate, J. W. and Wang, P. (**2006**). "Nanostructures for enzyme stabilization." *Chemical Engineering Science*, *61*, 1017-1026.

Klibanov, A. M. (**2001**). "Improving enzymes by using them in organic solvents." *Nature*, *409*, 241-246.

Kobayashi, N., Muranaka, A. and Mack, J. (**2012**). "Circular dichroism and magnetic circular dichroism spectroscopy for organic chemists". Royal Society of Chemistry.

Kourist, R., Dominguez de Maria, P. and Miyamoto, K. (**2011**). "Biocatalytic strategies for the asymmetric synthesis of profens - recent trends and developments." *Green Chemistry*, *13*, 2607-2618.

Kumar, P. and Mittal, K. L. (**1999**). "Handbook of microemulsion science and technology". CRC press.

Lagourette, B., Peyrelasse, J., Boned, C. and Clausse, M. (**1979**). "Percolative conduction in microemulsion type systems."

Larsson, K. M., Adlercreutz, P., Mattiasson, B. and Olsson, U. (**1990**). "Enzymatic catalysis in microemulsions: Enzyme reuse and product recovery." *Biotechnology and bioengineering*, *36*, 135-141.

Larsson, K. M., Adlercreutz, P., Mattiasson, B. and Olsson, U. (**1991**). "Enzyme catalysis in uni- and bi-continuous microemulsions: dependence of kinetics on substrate partitioning." *Journal of the Chemical Society, Faraday Transactions*, *87*, 465-471.

Laupheimer, M., Engelskirchen, S., Tauber, K., Kroutil, W. and Stubenrauch, C. (**2011**). "Bicontinuous Microemulsion as Reaction Medium for ω-Transaminase Catalysed Biotransformations." *Tenside Surfactants Detergents*, *48*, 28-33.

León, R., Fernandes, P., Pinheiro, H. M. and Cabral, J. M. S. (**1998**). "Whole-cell biocatalysis in organic media." *Enzyme and Microbial Technology*, *23*, 483-500.

Lindman, B., Stilbs, P. and Moseley, M. E. (**1981**). "Fourier transform nmr self-diffusion and microemulsion structure." *Journal of Colloid and Interface Science*, *83*, 569-582.

Lopresto, C. G., Calabrò, V., Woodley, J. M. and Tufvesson, P. (**2014**). "Kinetic study on the enzymatic esterification of octanoic acid and hexanol by immobilized Candida antarctica lipase B." *Journal of Molecular Catalysis B: Enzymatic*, *110*, 64-71.

Low, P. S., Bada, J. L. and Somero, G. N. (**1973**). "Temperature Adaptation of Enzymes: Roles of the Free Energy, the Enthalpy, and the Entropy of Activation." *Proceedings of the National Academy of Sciences*, *70*, 430-432.

Magid, L., Butler, P., Payne, K. and Strey, R. (**1988**). "SANS study of ternary nonionic microemulsions." *Journal of Applied Crystallography*, *21*, 832-834.

Martinez, C. A., Hu, S., Dumond, Y., Tao, J., Kelleher, P. and Tully, L. (**2008**). "Development of a Chemoenzymatic Manufacturing Process for Pregabalin." *Organic Process Research & Development*, *12*, 392-398.

Mateo, C., Palomo, J. M., Fernandez-Lorente, G., Guisan, J. M. and Fernandez-Lafuente, R. (**2007**). "Improvement of enzyme activity, stability and selectivity via immobilization techniques." *Enzyme and Microbial Technology*, *40*, 1451-1463.

McCabe, R., Rodger, A. and Taylor, A. (**2005**). "A study of the secondary structure of Candida antarctica lipase B using synchrotron radiation circular dichroism measurements." *Enzyme and Microbial Technology*, *36*, 70-74.

Miller, R., Fainerman, V. B., Makievski, A. V., Krägel, J., Grigoriev, D. O., Kazakov, V. N. and Sinyachenko, O. V. (**2000**). "Dynamics of protein and mixed protein/surfactant adsorption layers at the water/fluid interface." *Advances in Colloid and Interface Science*, *86*, 39-82.

Oldfield, C., Robinson, B. H. and Freedman, R. B. (**1990**). "Acid-base behaviour of 4-nitrophenol and 4-nitrophenyl-2-sulphonate in water-in-oil microemulsions stabilized by aerosol-OT." *Journal of the Chemical Society, Faraday Transactions*, *86*, 833-841.

Olsson, U., Shinoda, K. and Lindman, B. (**1986**). "Change of the structure of microemulsions with the hydrophile-lipophile balance of nonionic surfactant as revealed by NMR self-diffusion studies." *The Journal of Physical Chemistry*, *90*, 4083-4088.

Orlich, B. and Schomäcker, R. (**2001**). "< i> Candida Rugosa</i> lipase reactions in nonionic w/o-microemulsion with a technical surfactant." *Enzyme and microbial technology*, *28*, 42-48.

Ourisson, G., Rohmer, M. and Poralla, K. (**1987**). "Prokaryotic hopanoids and other polyterpenoid sterol surrogates." *Annual Reviews in Microbiology*, *41*, 301-333.

Papadimitriou, V., Xenakis, A., Cazianis, C. T. and Kolisis, F. N. (**1997**). "Structural and catalytic aspects of cutinase in w/o microemulsions." *Colloid and Polymer Science*, *275*, 609-616.

Pelton, J. T. and McLean, L. R. (**2000**). "Spectroscopic Methods for Analysis of Protein Secondary Structure." *Analytical Biochemistry*, *277*, 167-176.

Pleiss, J., Fischer, M. and Schmid, R. D. (**1998**). "Anatomy of lipase binding sites: the scissile fatty acid binding site." *Chemistry and Physics of Lipids*, *93*, 67-80.

Poliakoff, M., Fitzpatrick, J. M., Farren, T. R. and Anastas, P. T. (**2002**). "Green chemistry: science and politics of change." *Science*, *297*, 807-810.

Pollard, D. J. and Woodley, J. M. (**2007**). "Biocatalysis for pharmaceutical intermediates: the future is now." *TRENDS in Biotechnology*, *25*, 66-73.

Prazeres, D., Garcia, F. and Cabral, J. (**1992**). "Kinetics and stability of a chromobacterium viscosum lipase in reversed micellar and aqueous media." *Journal of Chemical Technology and Biotechnology*, *53*, 159-164.

Pronk, W., Boswinkel, G. and van't Riet, K. (**1992**). "Parameters influencing hydrolysis kinetics of lipase in a hydrophilic membrane bioreactor." *Enzyme and Microbial Technology*, *14*, 214-220.

Ran, N., Zhao, L., Chen, Z. and Tao, J. (**2008**). "Recent applications of biocatalysis in developing green chemistry for chemical synthesis at the industrial scale." *Green Chemistry*, *10*, 361-372.

Reis, P., Holmberg, K., Watzke, H., Leser, M. E. and Miller, R. (**2009**). "Lipases at interfaces: A review." *Advances in Colloid and Interface Science*, *147–148*, 237-250.

Rotticci, D., Rotticci-Mulder, J. C., Denman, S., Norin, T. and Hult, K. (**2001**). "Improved enantioselectivity of a lipase by rational protein engineering." *ChemBioChem*, *2*, 766-770.

Ruckenstein, E. and Karpe, P. (**1990**). "Enhanced enzymatic activity in reverse micelles." *Biotechnology Letters*, *12*, 241-246.

Ryan, L. D. and Kaler, E. W. (**2001**). "Alkyl polyglucoside microemulsion phase behavior." *Colloids and Surfaces A: Physicochemical and Engineering Aspects*, *176*, 69-83.

Ryan, L. D. and Kaler, E. W. (**1997**). "Role of Oxygenated Oils in *n*-Alkyl β-D-Monoglucoside Microemulsion Phase Behavior." *Langmuir*, *13*, 5222-5228.

Sáenz, J. P., Sezgin, E., Schwille, P. and Simons, K. (**2012**). "Functional convergence of hopanoids and sterols in membrane ordering." *Proceedings of the National Academy of Sciences*, *109*, 14236-14240.

Santaniello, E., Ferraboschi, P. and Grisenti, P. (**1993**). "Lipase-catalyzed transesterification in organic solvents: Applications to the preparation of enantiomerically pure compounds." *Enzyme and Microbial Technology*, *15*, 367-382.

Sanz, R., Martínez, A., Guilarte, V., Álvarez-Gutiérrez, J. M. and Rodríguez, F. (**2007**). "The Ritter Reaction under Truly Catalytic Brønsted Acid Conditions." *European Journal of Organic Chemistry*, *2007*, 4642-4645.

Sathishkumar, M., Jayabalan, R., Mun, S. and Yun, S. (**2010**). "Role of bicontinuous microemulsion in the rapid enzymatic hydrolysis of ( R, S)-ketoprofen ethyl ester in a micro-reactor." *Bioresource technology*, *101*, 7834-7840.

Sathishkumar, M., Jeong, E. S., Yun, S. E., Mun, S. P. and Rusling, J. F. (**2008**). "Bicontinuous microemulsion as reaction medium for the β-glucosidase-catalyzed synthesis of n-hexyl-β-d-glucopyranoside." *Enzyme and Microbial Technology*, *42*, 252-258.

Sato, T. and Hoshino, T. (**1999**). "Kinetic studies on the function of all the conserved tryptophans involved inside and outside the QW motifs of squalene-hopene cyclase: stabilizing effect of the protein structure against thermal denaturation." *Bioscience, Biotechnology, and Biochemistry*, *63*, 1171-1180.

Scanlon, J. T. and Willis, D. E. (**1985**). "Calculation of Flame Ionization Detector Relative Response Factors Using the Effective Carbon Number Concept." *Journal of Chromatographic Science*, *23*, 333-340.

Schmid, A., Dordick, J. S., Hauer, B., Kiener, A., Wubbolts, M. and Witholt, B. (**2001**). "Industrial biocatalysis today and tomorrow." *Nature*, *409*, 258-268.

Schmid, R. D. and Verger, R. (**1998**). "Lipases: interfacial enzymes with attractive applications." *Angewandte Chemie International Edition*, *37*, 1608-1633.

Schomaecker, R., Robinson, B. H. and Fletcher, P. D. I. (**1988**). "Interaction of enzymes with surfactants in aqueous solution and in water-in-oil microemulsions." *Journal of the Chemical Society, Faraday Transactions 1: Physical Chemistry in Condensed Phases*, *84*, 4203-4212.

Secundo, F., Miehé-Brendlé, J., Chelaru, C., Ferrandi, E. E. and Dumitriu, E. (**2008**). "Adsorption and activities of lipases on synthetic beidellite clays with variable composition." *Microporous and Mesoporous Materials*, *109*, 350-361.

Seifert, A. M. and Wendorff, J. H. (**1992**). "Spinning drop experiments on interfacial phenomena: Theoretical background and experimental evidence." *Colloid and Polymer Science*, *270*, 962-971.

Seitz, M., Syrén, P.-O., Steiner, L., Klebensberger, J., Nestl, B. M. and Hauer, B. (**2013**). "Synthesis of Heterocyclic Terpenoids by Promiscuous Squalene-Hopene Cyclases." *ChemBioChem*, *14*, 436-439.

Shinoda, K., Araki, M., Sadaghiani, A., Khan, A. and Lindman, B. (**1991**). "Lecithin-based microemulsions: phase behavior and microstructure." *The Journal of Physical Chemistry*, *95*, 989-993.

Siedenburg, G. and Jendrossek, D. (**2011**). "Squalene-hopene cyclases." *Applied and Environmental Microbiology*, *77*, 3905-3915.

Siedenburg, G., Jendrossek, D., Breuer, M., Juhl, B., Pleiss, J., Seitz, M., Klebensberger, J. and Hauer, B. (**2012**). "Activation-independent cyclization of monoterpenoids." *Applied and Environmental Microbiology*, *78*, 1055-1062.

Skagerlind, P., Jansson, M. and Hult, K. (**1992**). "Surfactant interference on lipase catalysed reactions in microemulsions." *Journal of Chemical Technology and Biotechnology*, *54*, 277-282.

Sottmann, T. and Stubenrauch, C. (**2009**). "Phase Behaviour, Interfacial Tension and Microstructure of Microemulsions". Microemulsions. Stubenrauch, C. Blackwell Publisher Ltd.

Sottmann, T. and Strey, R. (**2005**). "Microemulsions." *Fundamentals of Interface and Colloid Science*, *5*, 1-96.

Soumanou, M. M., Pérignon, M. and Villeneuve, P. (**2013**). "Lipase-catalyzed interesterification reactions for human milk fat substitutes production: A review." *European Journal of Lipid Science and Technology*, *115*, 270-285.

Stamatis, H., Xenakis, A. and Kolisis, F. N. (**1999**). "Bioorganic reactions in microemulsions: the case of lipases." *Biotechnology advances*, *17*, 293-318.

Stark, M. B., Skagerlind, P., Holmberg, K. and Carlfors, J. (**1990**). "Dependence of the activity of a rhizopus lipase on microemulsion composition." *Colloid and Polymer Science*, *268*, 384-388.

Stehle, R., Schulreich, C., Wellert, S., Gäb, J., Blum, M.-M., Kehe, K., Richardt, A., Lapp, A. and Hellweg, T. (**2014**). "An enzyme containing microemulsion based on skin friendly oil and surfactant as decontamination medium for organo phosphates: Phase behavior, structure, and enzyme activity." *Journal of Colloid and Interface Science*, *413*, 127-132.

Steudle, A. (**2011**). Influence of the surfactant on stereoselective enzyme-catalysed reactions in microemulsions. Institute for Physical Chemistry. Stuttgart, University of Stuttgart. **Diploma:**

Steudle, A. K., Subinya, M., Nestl, B. M. and Stubenrauch, C. (**2015**). "Hydrolysis of Hydrophobic Esters in a Bicontinuous Microemulsion Catalysed by Lipase B from Candida antarctica." *Chemistry – A European Journal*, *21*, 2691-2700.

Strey, R. (**1994**). "Microemulsion microstructure and interfacial curvature." *Colloid and Polymer Science*, *272*, 1005-1019.

Stubenrauch, C. (**2001**). "Sugar surfactants — aggregation, interfacial, and adsorption phenomena." *Current Opinion in Colloid & Interface Science*, *6*, 160-170.

Stubenrauch, C. (**2009**). "Microemulsions : background, new concepts, applications, perspectives". Oxford, Wiley.

Subinya, M., Steudle, A. K., Jurkowski, T. and Stubenrauch, C. (**2015**). "Conformation and Activity of Lipase B from *Candida antarctica* in Bicontinuous microemulsions." *Colloid and Surfaces B: Biointerfaces*, *submitted*,

Subinya, M. (**2014a**). The Lipase B from *Candida antarctica* in Bicontinuous Microemulsions: A Structural Study. Institute of Physical Chemistry. Stuttgart, University Stuttgart. **PhD:** 148.

Subinya, M., Steudle, A. K., Nestl, B., Nebel, B., Hauer, B., Stubenrauch, C. and Engelskirchen, S. (**2014b**). "Physicochemical aspects of lipase B from Candida antarctica in bicontinuous microemulsions." *Langmuir*, *30*, 2993-3000.

Tan, T., Lu, J., Nie, K., Deng, L. and Wang, F. (**2010**). "Biodiesel production with immobilized lipase: a review." *Biotechnology Advances*, *28*, 628-634.

Tischer, W. and Kasche, V. (**1999**). "Immobilized enzymes: crystals or carriers?" *Trends in Biotechnology*, *17*, 326-335.

Torre, O., Alfonso, I. and Gotor, V. (**2004**). "Lipase catalysed Michael addition of secondary amines to acrylonitrile." *Chemical communications*, 1724-1725.

Trodler, P., Nieveler, J., Rusnak, M., Schmid, R. D. and Pleiss, J. (**2008**). "Rational design of a new one-step purification strategy for Candida antarctica lipase B by ion-exchange chromatography." *Journal of chromatography. A, 1179*, 161-167.

Uppenberg, J., Oehrner, N., Norin, M., Hult, K., Kleywegt, G. J., Patkar, S., Waagen, V., Anthonsen, T. and Jones, T. A. (**1995**). "Crystallographic and molecular-modeling studies of lipase B from Candida antarctica reveal a stereospecificity pocket for secondary alcohols." *Biochemistry*, *34*, 16838-16851.

Uppenberg, J., Hansen, M. T., Patkar, S. and Jones, T. A. (**1994**). "The sequence, crystal structure determination and refinement of two crystal forms of lipase B from Candida antarctica." *Structure*, *2*, 293-308.

Valis, T. P., Xenakis, A. and Kolisis, F. N. (**1992**). "Comparative Studies of Lipase from Rhizopus Delemar in Various Microemulsion Systems." *Biocatalysis and Biotransformation*, *6*, 267-279.

Vaze, A., Parizo, M. and Rusling, J. F. (**2004**). "Enhanced rates of electrolytic styrene epoxidation catalyzed by cross-linked myoglobin-poly (L-lysine) films in bicontinuous microemulsions." *Langmuir*, *20*, 10943-10948.

Verger, R. (**1997**). "'Interfacial activation' of lipases: facts and artifacts." *Trends in Biotechnology*, *15*, 32-38.

Verhaert, R. M. D., Hilhorst, R., Vermue, M., Schaafsma, T. J. and Veeger, C. (**1989**). "Description of enzyme kinetics in reversed micelles." *European Journal of Biochemistry*, *187*, 59-72.

von Rybinski, W. and Hill, K. (**1998**). "Alkyl Polyglycosides—Properties and Applications of a new Class of Surfactants." *Angewandte Chemie International Edition*, *37*, 1328-1345.

Wellert, S., Tiersch, B., Koetz, J., Richardt, A., Lapp, A., Holderer, O., Gab, J., Blum, M. M., Schulreich, C., Stehle, R. and Hellweg, T. (**2011**). "The DFPase from Loligo vulgaris in sugar surfactant-based bicontinuous microemulsions: structure, dynamics, and enzyme activity." *Eur Biophys J*, *40*, 761-74.

Wendt, K., Poralla, K. and Schulz, G. (**1997**). "Structure and function of a squalene cyclase." *Science*, *277*, 1811-1815.

Wendt, K. U. (**2005**). "Enzyme Mechanisms for Triterpene Cyclization: New Pieces of the Puzzle." *Angewandte Chemie International Edition*, *44*, 3966-3971.

Winkler, U. K. and Stuckmann, M. (**1979**). "Glycogen, hyaluronate, and some other polysaccharides greatly enhance the formation of exolipase by Serratia marcescens." *Journal of Bacteriology*, *138*, 663-70.

Wolfenden, R. and Snider, M. J. (**2001**). "The Depth of Chemical Time and the Power of Enzymes as Catalysts." *Accounts of Chemical Research*, *34*, 938-945.

Zaks, A. and Klibanov, A. M. (**1984**). "Enzymatic catalysis in organic media at 100 degrees C." *Science*, *224*, 1249-1251.

Zhang, N., Suen, W. C., Windsor, W., Xiao, L., Madison, V. and Zaks, A. (**2003**). "Improving tolerance of Candida antarctica lipase B towards irreversible thermal inactivation through directed evolution." *Protein Engineering*, *16*, 599-605.

**List of publications**

Papers included in this thesis:

Steudle, A. K., Subinya, M., Nestl, B. M. and Stubenrauch, C. (**2015**). "Hydrolysis of Hydrophobic Esters in a Bicontinuous Microemulsion Catalysed by Lipase B from Candida antarctica." *Chemistry – A European Journal*, *21*, 2691-2700.

Subinya, M., Steudle, A. K., Jurkowski, T. and Stubenrauch, C. (**2015**). "Conformation and Activity of Lipase B from *Candida antarctica* in Bicontinuous microemulsions." *Colloid and Surfaces B: Biointerfaces*, *131*, 108-114.

Papers not included in this thesis:

Subinya, M., Steudle, A. K., Nestl, B., Nebel, B., Hauer, B., Stubenrauch, C. and Engelskirchen, S. (**2014b**). "Physicochemical aspects of lipase B from Candida antarctica in bicontinuous microemulsions." *Langmuir*, *30*, 2993-3000.